# PERSISTENCE IN NON-EQUILIBRIUM SYSTEMS : A STUDY ON SPATIAL CORRELATIONS

*Thesis submitted*
*in partial fulfillment of the requirements*
*for the award of the Degree of*
DOCTOR OF PHILOSOPHY

by

G. MANOJ
The Institute of Mathematical Sciences,
Chennai 600 113.

UNIVERSITY OF MADRAS
CHENNAI 600 005

AUGUST 2001

# DECLARATION

I declare that the thesis entitled "**Persistence in Non-equilibrium Systems : A Study on Spatial Correlations**" submitted by me for the Degree of Doctor of Philosophy is the record of work carried out by me during the period from January 1998 to July 2001 under the guidance of Dr. Purusattam Ray and has not formed the basis for the award of any degree, diploma, associateship, fellowship, titles in this or any other University or other similar Institution of Higher Learning.

Chennai
9 August 2001.

G.Manoj

# CERTIFICATE FROM THE SUPERVISOR

I certify that the thesis entitled " Persistence in Non-equilibrium Systems : A Study on Spatial Correlations" submitted for the Degree of Doctor of Philosophy by Mr. G. Manoj is the record of research work carried out by him during the period from January 1998 to July 2001 under my guidance and supervision, and that this work has not formed the basis for the award of any degree, diploma, associateship, fellowship or other titles in this University or any other University or Institution of Higher Learning.

It is further certified that the thesis represents independent work by the candidate and collaboration when existed was necessitated by the nature and scope of the problems dealt with.

Chennai
9 August 2001.

Dr. Purusattam Ray,
Reader, Theoretical Physics,
Institute of Mathematical Sciences,
Chennai 600 113.

# Acknowledgements

*This thesis is the realisation of a long cherished dream for me, and this wouldn't have been possible but for the help and support of a large number of people.*

*Above all, I would like to express my deep sense of gratitude to my thesis advisor Dr. Purusattam Ray. It has been a very nice experience working with him. I remember with gratitude all the freedom and encouragement that he had given me to pursue my own ideas and his excellent guidance in the very important aspect of communication. He allowed me to explore, but at the same time was subtly guiding me towards important problems. At a more personal level, I would like to add that were it not for his helping hand in a difficult situation in my academic life, this thesis perhaps would not have materialised.*

*I consider myself fortunate to have got an opportunity to work with Prof. Mustansir Barma. I have been rather fascinated by his excellent insight and depth of knowledge. His enthusiasm was contagious and the long discussions we had over endless cups of tea is something I would be again looking forward to.*

*I have had the chances to get to know and interact with quite a number of people during my doctoral studies, and I have learned many things from them. Madan introduced me to biological physics, a subject still close to my heart, and which I hope to explore more in coming years. Sunil and Jayajit taught me the basics of computation. I was fortunate to have had the chance to meet and interact with such insightful physicists like Deepak Dhar and Alan Bray. Closer home, it was very nice to have Gautam around, who has helped us out many a time with his suggestions.*

*And, of course, I won't forget soon all the interesting people who made my six years of stay in IMSc rather pleasant and cheerful..Khan, Vinod, Sridhar, Sarasij, Ronojoy, Pushan, Murugesh, Balaji, Naveen and more recently Suresh Rao, Gautam,*

*Sant, Paramita, Tarun and many others. I thank them all for the nice times I've had with them, especially the friday movie club, cricket matches and terrace parties.*

*Among my teachers during my College days, I remember fondly Mr. Premlet, Prof. Lawrence Michael, Prof. Telveenus and the late Prof. Unnithan who have always been supportive, helpful and affectionate towards me. I would also like to thank the Quilon Public Library, where I first saw the Landau volumes.*

*My love, respect and eternal gratitude to my parents, Manju, Raman, and then my little friends Unni, Achu, Ammu and Appu who make all this worthwhile.*

*And BSG, I thank you for being such a wonderful person in my life.*

*G. Manoj*

*Would you tell me, please, which way I ought to go from here?*

*"That depends a good deal on where you want to get to," said the Cat.*

*"I don't much care where–" said Alice.*

*"Then it doesn't matter which way you go," said the Cat.*

*"–so long as I get SOMEWHERE," Alice added as an explanation.*

*"Oh, you're sure to do that," said the Cat, "if you only walk long enough."*

*Lewis Carroll, 'Alice in Wonderland'.*

# Abstract

In this thesis, I study some aspects of coarsening and the associated notion of Persistence in a few well-known Nonequilibrium processes. The thesis is divided into 5 chapters. In the introductory chapter, I briefly discuss some salient features of coarsening systems in general and also list some of the well-known models which we shall come across in the rest of the thesis. Coarsening is a rather well-studied phenomena in general, while the notion of Persistence and the associated Persistence exponent are recent entrants to this field. Persistence and its interplay with the underlying coarsening process are the subjects of Chapters 2 and 3, and also provides the link to Chapter 4, where we study fluctuating interfaces. In Chapter 5, the main results presented in this thesis are summarised.

Accordingly, this thesis may be broadly divided into two parts. In the first part of the thesis, covered by Chapters 2 and 3, we study the time evolution of the spatial structure of the persistent region in several standard models of coarsening in different spatial dimensions. The most important result here is the formation of a scale-invariant pattern in the distribution of persistent regions in space. Chapter 2 deals with a rather detailed study of the problem in $d = 1$ Ising model which coarsens only at $T = 0$. In Chapter 3, we extend our study to higher dimensions and non-zero temperatures and some other relevant models. The universality of the phenomenon is emphasised here. In Chapter 4, we take a clue from Persistence studies and investigate whether a fluctuating interface may be viewed as a coarsening system evolving towards a phase separated steady state. We find that this assertion is indeed true, but the phase separation is found to be different in several ways from that found in more conventional systems.

This thesis is based on the following publications/preprints:

1. *Persistence in one dimensional reaction-diffusion systems,*
   G. Manoj, *IMSc preprint/98/07/44.*

2. *Dynamical scaling in the spatial distribution of persistent sites,*
   G. Manoj and P. Ray, *e-print cond-mat/9901130.*

3. *Reply to comment on 'Dynamical scaling in the spatial distribution of persistent sites'*, G. Manoj and P. Ray, *e-print cond-mat/9902339.*

4. *Scaling and Fractal formation in Persistence,*
   G. Manoj and P. Ray, *J. Phys. A* **33** L109 (2000) (*cond-mat/9912209*).

5. *Spatial distribution of persistent sites,*
   G. Manoj and P. Ray, *J. Phys. A* **33** 5489 (2000)(*cond-mat/0003203*).

6. *Persistence in higher dimensions : A finite size scaling study,*
   G. Manoj and P. Ray, *Phys. Rev. E* **62**, 7455 (2000).
   (*ICTP preprint IC/2000/66, cond-mat/0009189*).

# Contents

# Chapter 1

# Introduction

## 1.1 Overview and Purpose

Stochastic processes in Physics needs no introduction[1]. Any time dependent phenomena in a thermodynamic system, with $\sim 10^{23}$ individual molecules in it, necessarily has some amount of randomness in it. For example, consider a volume of gas with fixed volume and in thermal equilibrium with an external heat bath. Its pressure and temperature fluctuates in time in a random fashion, about a mean value which is determined by the equation of state. Let us consider a fluctuating thermodynamic variable $x(t)$ with zero mean and variance $Q = \sqrt{\langle x^2 \rangle}$. In thermodynamic equilibrium, the two-time correlator $\phi(t,t') = \langle x(t)x(t') \rangle$ has a stationary form (ie., it depends only on the time difference $T = |t - t'|$) and typically decays exponentially at large $T$, $\phi(0,T) \sim Q^2 e^{-\lambda T}$[2]. The time scale $\tau \sim 1/\lambda$ gives the typical duration of a fluctuation.

However, the situation is different in systems far from Equilibrium, and in situations where the variance $Q$ itself diverges with time. To illustrate the latter case, let us consider one of the simplest and well-known examples of a stochastic process, a Brownian particle in a gas[3]. The particle is constantly bombarded by gas molecules from all directions, with varying momenta. The motion of the particle as a result of these bombardments is almost perfectly random. It is well-known that over large enough length and time scales, this random motion is well-represented by

a *random walk*[4, 5], a mathematical model where, at every instant of observation, the position of the particle is incremented by a fixed amount in a randomly chosen direction. For simplicity, let us now consider a 1-dimensional random walker, whose position at time $t$ is denoted by $x(t)$. The equation of motion of such a walker over long time scales may be written as

$$\frac{dx(t)}{dt} = \eta(x,t) \tag{1.1}$$

where $\eta$ on the RHS is a random variable called the *noise*. This term represents the net displacement of the walker between two consecutive observations. From the preceding arguments, it is clear that the mean value of $\eta$ over sufficiently large number of observations would be zero, and its correlator should vanish beyond a certain microscopic time scale. Further, the variance of $\eta$ is determined by the Fluctuation-Dissipation Theorem[1, 6]. We summarize these conditions in the following set of equations.

$$\langle \eta(t) \rangle = 0 \quad ; \quad \langle \eta(t)\eta(t') \rangle = \alpha\delta(|t-t'|) \tag{1.2}$$

From the linearity of the equation of motion, it follows that the mean value of the position of the random walker is time-independent and the RMS variation grows linearly in time, ie., $\langle x(t) \rangle = 0$ and $\langle x^2(t) \rangle \propto t$. It is also straightforward to compute the normalized correlator

$$\phi(t,t') = \frac{\langle x(t)x(t') \rangle}{\sqrt{\langle x^2(t) \rangle \langle x^2(t') \rangle}}$$

for the random walk. It may be shown that in this case, $\phi(t,t') \sim (t/t')^{-\frac{1}{2}}$. In this case, the correlator is not stationary, and does not decay in any finite amount of time. The long-ranged correlation in this case is a measure of the tendency of the variable $x(t)$ to make long excursions from the mean value over large time scales. This may be further quantified by a very simple question: What is the probability that $x(t)$ does not return to the starting point till time $t$ ? In other words, consider $N$ random walkers, all starting from the origin at $t = 0$. What fraction $P(t)$ of walkers remain on one side of the origin till time $t$ ? It is obvious that this fraction

should decay with time, but the important point is that it can be shown to decay only as a *power-law* at large $t$ : $P(t) \sim t^{-1/2}$.

The quantity $P(t)$ is usually called the Persistence probability. The problem of Persistence falls in a certain class of similar problems in stochastic processes, called First Passage problems. One may also generalize the above definition and consider the probability $P(x_0, t)$ that the random walker does not cross a certain (arbitrary) point $x_0$ till time $t$. In this case it may be easily shown that $P(x_0, t) \sim x_0 t^{-1/2}$. We note that the exponent of time does not change from the previous expression. In general, for a given stochastic process $X(t)$, one may consider the probability $P(t)$ that $X(t') > X_0$ throughout a time interval $[0, t]$. In several processes of physical interest, which includes a large class of Non-equilibrium processes, this quantity is found to decay as a power-law in time, ie., $P(t) \sim t^{-\theta}$[7]. The exponent $\theta$ is called the Persistence exponent for the stochastic process under consideration.

The random walk considered above is one among a well studied class of stochastic process called *Markov processes*[4]. A Markov process is defined as follows. Consider a stochastic process $X(t)$ at time $t$. Let $X(t) = X_0$. Now, consider the probability that $X(t + \delta t) = X_1$, where $\delta t$ is the time interval between two consecutive observations. If this probability is a function only of $X_1$ and $X_0$ , and does not depend on the values of $X$ at any previous instants, $X(t)$ is a Markov process.

We next show that for a Markov processes which also has a Gaussian probability distribution at all times, it is possible to have an exact expression for the Persistence exponent $\theta$[7]. To illustrate this case, we note that the random walk defined by Eq.1.1 is Gaussian at all times if the noise $\eta(t)$ has a Gaussian distribution. The two-point correlator of Eq.1.1 is given by $\langle X(t)X(t')\rangle = min(t, t')$. Now let us consider the normalized process $X(t) \equiv \frac{X(t)}{\sqrt{\langle X^2(t)\rangle}}$ and consider a new time variable $T = log(t)$. Then $\langle X(T)X(T')\rangle \equiv f(\tau) = e^{-\frac{\tau}{2}}$ where $\tau = |T - T'|$. We note that with the log-transformation, the correlator depends only on the difference $|T - T'|$, and hence the process has become stationary.

The correlator written above for the random walk is actually a special case of a more general form: $f(T) = e^{-\lambda' T}$, which may be derived from the Langevin equation

for a general stationary Markovian process:

$$\frac{dX}{dT} = -\lambda' X + \eta \tag{1.3}$$

When the noise $\eta$ is taken from a Gaussian probability distribution, the distribution of $X(T)$ also remains Gaussian at all times, in which case $X(T)$ is called a Gaussian process. Let $P_0(T)$ be the probability that the stationary Markov process does not cross its initial starting point $X(0)$ till time $T$. Then it is known exactly that $P_0(T) = \frac{2}{\pi} sin^{-1} f(T)$[8]. To find the late time behaviour, we expand $sin^{-1}(x)$ around $x = 0$. After doing the inverse transformation $T \to t$, we have the final result $P_0(t) \sim t^{-\lambda'}$ at large $t$, so that for this process, $\theta = \lambda'$.

We now consider another example, which is not Markovian. This is the problem of a randomly accelerated particle in one dimension, which is represented by the following equation.

$$\frac{d^2x(t)}{dt^2} = \eta(x,t) \tag{1.4}$$

Unlike the random walk problem studied before, this problem does not fall into the class of Markovian processes (However, it is Gaussian if $\eta$ is Gaussian). The computation of Persistence probability in this problem is non-trivial. The exact solution is $P(t) \sim t^{-1/4}$[9] so that $\theta = \frac{1}{4}$ in this problem. In a later section of this chapter, we will review some approximate analytical methods that has been developed to study similar non-Markovian processes.

The two simple examples we had considered so far in this section dealt with a stochastic variable that only depended on time. At this moment, it is natural to extend our discussion to Persistence in spatially extended many-body systems, where the relevant stochastic variable is a function of space as well as time. It is clear that most Non-equilibrium processes studied in Physics comes under this class. We will explicitly discuss some of the important systems studied in this context, later in this chapter. For a general discussion of the features associated with Persistence in such systems, let us consider a space and time dependent field $\phi(\mathbf{x}, t)$ whose time

evolution at any point in space is also dependent on the field at neighboring points. In such systems, Persistence probability $P(t)$ is typically defined as the probability that the field $\phi(\mathbf{x}, t)$ at any point $\mathbf{x}$ remains above a certain reference level $\phi_0$ till time $t$. This definition, of course, requires an ensemble of similar systems. In practice, $P(t)$ is computed as the fraction of sites $\mathbf{x}$ in the system where the $\phi > \phi_0$ throughout the interval $[0 : t]$. This also gives rise to the notion of persistent and non-persistent sites in such a system, whose definition is obvious from the preceding discussion.

We now briefly describe some of the 'many-body' stochastic processes studied in Persistence. The simplest system is the Ising ferromagnet, whose Hamiltonian is

$$\mathcal{H} = -J \sum_{\langle ij \rangle} \sigma_i \sigma_j \tag{1.5}$$

where $\sigma = \pm 1$ are the Ising spin variables and $J > 0$. In general, the Ising model has two phases: the paramagnetic phase at high temperatures where the spins randomly take the values $\pm 1$ and the low temperature ferromagnetic phase where the configuration is predominantly 'up' or 'down'. The Ising model does not have any 'intrinsic' Hamiltonian dynamics, but the spin configuration can evolve by trading energy with an external heat bath. This purely dissipative dynamics is implemented in simulations usually through single spin-flip algorithms, where one spin is randomly picked at a time, and its state is changed with a certain probability (For a discussion of some of the common schemes, we refer the reader to Appendix A). The randomness imitates the action of the fast degrees of freedom, the heat bath variables like electrons or phonons which couple to the spins. The time evolution of the state of any single spin is a stochastic process. Moreover, the time evolutions of different spins are coupled, in general, because of the interaction between neighboring spins.

When an Ising ferromagnet is quenched from high to low temperatures, spins will start to realign themselves in the process of evolution of the system from paramagnetic to ferromagnetic (equilibrium) state. This arrangement of spins into *domains* of up and down phases is called *coarsening* of the system. In this problem, one may

consider the effective process at any single site, and ask for the probability that the spin at that site remains in the same phase for the time interval $[0 : t]$. This is the Persistence probability in the problem. A large amount of analytical and numerical effort has been devoted to the computation of the persistent fraction in kinetic Ising model and several other well-known Non-equilibrium stochastic processes. It has been fairly well established that for a large number of systems, Persistence follows a power-law decay and the exponent is, in general, non-trivial, and not related to the other exponents usually used in the characterization of a Non-equilibrium process.

In spatially extended systems with interactions, the time evolution naturally has an effect on the spatial correlations in the system. This is very obvious in the process of domain growth in coarsening systems, which occurs through the collective behaviour of spins. It is natural to enquire if Persistence decay is also mirrored in the spatial organization of the system in some way. The most direct way to see whether this happens, would be through very simple and direct questions, like, what is the probability of finding a persistent site at a distance $r$ from another persistent site at time $t$ ? This is the approach we shall take in this thesis, and as we shall see in detail in later chapters, spatial correlations associated with Persistence contain very rich and non-trivial features. In particular, we discovered dynamical scaling and scale-invariance in the distribution of persistent sites, which indicates that the Persistence decay at different points in space are very strongly correlated.

Before we get into more details on spatial correlations, it is worthwhile to understand in some more detail Persistence in a simple many-body system. The best choice to start is the one-dimensional kinetic Ising model. This model coarsen only at zero temperature. We start from a random initial distribution of $+$ and $-$ spins on a 1-dimensional lattice. The system is now quenched to $T = 0$, ie., assumed to be brought into contact with a heat bath at zero temperature. The spins are now updated one by one according to the Glauber dynamics. In this rule, a spin always flip if the resulting energy change $\Delta E < 0$, never flips if $\Delta E > 0$, and flips with probability $\frac{1}{2}$ is $\Delta E = 0$(Appendix A) . This dynamics is exactly soluble in one dimension. It is known that the mean size of domains $L(t) \sim t^{\frac{1}{2}}$, and the equal time pair correlation of spins has the scaling form $\langle \sigma_0 \sigma_k \rangle = g(\frac{k}{\sqrt{t}})$ where the scaling

function $g(z)$ is exactly known[10].

Let us now consider the Persistence properties of this model. The Persistence probability has been exactly solved for by Derrida *et. al*, and it is known that $P(t) \sim t^{-\theta}$ where the exponent $\theta$ has the non-trivial value 3/8[11]. The derivation of this result is a real *tour de force* in Mathematical Physics, and is not particularly illuminating. We try to motivate this result through a toy model[12, 13], which, although is a poor approximation to the original problem, captures the right physics.

It is well-known that the Glauber dynamics in 1D Ising model can be mapped to a reaction-diffusion problem. This is because the *interfaces* between + and − spins in the Ising problem, act like a set of independent random walkers under the Glauber dynamics, which annihilate each other when two of them meet. The number of these random walkers $n(t)$ at any time $t$ is simply the inverse of the mean domain length, and so $n(t) = L(t)^{-1} \sim t^{-\frac{1}{2}}$. Consider now the spin at the origin. The probability that this is persistent at time $t$ is $P(t)$, then the probability that it flips for the first time at $t$ is $P'(t)dt$. A spin will flip only when an interface moves across it. The probability that an interface which was at a distance $x$ at $t = 0$, will reach the origin for the first time between $t$ and $t + dt$ is $q(x,t) \sim \frac{x}{t^{3/2}} e^{-x^2/4t} dt$[4]. We now make the assumption that the interfaces, instead of annihilating upon contact, randomly disappear with a certain rate so that their average density still decays like $n(t)$. Thus each of the random walkers survive up to time $t$ with probability $n(t)$. This is clearly an approximation, as it neglects the correlations in the positions of the walkers arising from the annihilation. Under this approximation, we find that

$$P'(t)dt = -n(t)P(t)dt \int_{-\infty}^{\infty} dx q(x,t) \tag{1.6}$$

After substituting the expression for $q(x,t)$, we find $P(t) \sim t^{-\theta}$, where $\theta = \frac{\sqrt{2}}{\pi}$ for this toy model. We note that the crucial ingredients that produce the power-law decay in $P(t)$ are the diffusive motion of interfaces, and the overall decay in their density. While the former originates from the stochastic nature of the time evolution, the latter reflects the domain coarsening process. We conclude that Persistence decay is intimately related to domain coarsening process.

Before we start a detailed discussion on the models studied in this context, it is worthwhile to have a look at an interesting experimental study of Persistence[14]. This study, which was the first experimental study in Persistence, involved the study of growth and coalescence of droplets of a liquid that condense on a substrate (the so-called *breath figures*). It was observed that, in this case, the fraction of area in the substrate that has always remained dry up to time $t$ decays as a power of time, with exponent $\theta \approx 1$. It was further noted that the boundary of this *persistent* region with the rest of the substrate has a fractal distribution over small enough length scales and has a homogeneous distribution over larger length scales. The fractal dimension measured was nearly $d_f \approx 1.22$. The fractal nature in the distribution is a signature of non-trivial correlations in the spatial structure of the persistent region. The study of similar correlations in some simple models is one of the main themes of this thesis.

The interplay between Persistence and coarsening observed in the Ising model also led us to explore this connection in a system which is not *a priori* related to coarsening systems. The system we have is a fluctuating interface, like, for example, the interface between a liquid and its vapour, or a thin film grown by deposition of particles on a substrate. The dynamics of such an interface is usually represented by coarse-grained mesoscopic equations of the form

$$\frac{\partial h}{\partial t} = \mathcal{F}[h] + \eta(\mathbf{r}, t) \tag{1.7}$$

where the function $\mathcal{F}[h]$ is determined by symmetry requirements and the mechanisms of growth and relaxation[15]. The noise term $\eta$ represents the stochastic element in the growth, which could be thermal fluctuations or a random deposition event. The statistical mechanics of fluctuating interfaces has undergone extensive study in recent times and is one of the most advanced topics in Non-equilibrium Statistical Mechanics[16].

The Persistence properties of fluctuating interface has also been studied in fair detail[7]. The probability $P(t, t_0)$ that the height at any given point on the interface remains above or below its 'initial' height $h(\mathbf{x}, t = t_0)$ throughout the time interval

$[t_0, t]$ is defined as the Persistence probability. Analytical and numerical results have shown that for several classes of interfaces, this probability decays with time as a power-law, and the associated exponent, in general, is not simply related to the other exponents that are usually used to characterize surface growth. The question that we asked here was whether such an interface could be viewed as a coarsening system, evolving towards a phase separated *steady state*. In Chapter 4, we present the results of our investigation into this problem.

Finally, why is Persistence important ? As we had explained in the beginning of this chapter, Persistence has provided us with more information on even the most well-known processes, like, for example, simple diffusion. The Persistence exponent has already found its place among the family of similar exponents that characterize a Non-equilibrium dynamical process. The study of spatial correlations in Persistence has shown that there is much in Persistence that still remains to be understood.

In the coming sections of this chapter, we briefly discuss the basic scaling phenomenology of coarsening processes and the connections to Persistence. We present a brief review of some of the important and widely applied techniques used to compute the Persistence exponent. The problem of spatial correlations is a vary natural offshoot of these studies, and we use both analytical and numerical techniques to study this problem in some detail. Brief accounts of our work presented in thesis also appears alongside the general discussion. In the last section, we show that the problem of spatial correlations is one aspect of a more general problem, the interplay between Persistence decay and the underlying coarsening process. This aspect is explored further, and we show that a fluctuating interface may actually be viewed as a coarsening system, but with features which are, in general, different from most of the conventional coarsening systems.

## 1.2 General Review of Coarsening and Persistence

### 1.2.1 Domain growth in coarsening systems

The time evolution of an Ising ferromagnet following a quench from high to low temperatures is one of a class of similar processes called *coarsening*[17]. Coarsening systems are ubiquitous in nature. The time evolution of such systems from disordered to ordered phase has been one of the most well-studied processes in Non-equilibrium Physics. Examples of systems undergoing coarsening range from soap froth to binary alloys to galactic density distributions. Generically, coarsening is characterized by the growth of homogeneous *domains* of a single phase (in the Ising model, + and − spins) from a disordered initial condition (Fig. 1.1). In many cases, the typical domain size grows as a power-law with time, ie., $\mathcal{L}(t) \sim t^{1/z}$[17]. The exponent $z$ is the dynamical exponent of the coarsening process.

In this section, we briefly discuss the basic phenomenology of coarsening dynamics. A typical problem studied in Phase Ordering Kinetics is the phase segregation of a binary fluid. Consider a binary fluid AB which contains two species of fluids, A and B. At sufficiently high temperatures, the entropy dominates the energetics and the most probable state of the system is a completely mixed state. A standard method employed to segregate the species is to quench the system to low temperatures. If the final temperature is less than the critical temperature $T_c$ of the mixture, the fluids will phase segregate in course of time. This process is often called *spinodal decomposition*, which is actually a term used in metallurgy in connection with phase segregation of a binary alloy. In the late stages, one may identify three kinds of regions in a typical configuration of the system:

- Homogeneous *domains*, rich in one of the species, $A$ or $B$, whose characteristic length scale $\mathcal{L}(t) \sim t^{\frac{1}{3}}$[18] and
- The interface region which is the boundary between an $A$ and $B$ type of domain, with a *finite* width $\xi \ll \mathcal{L}(t)$.

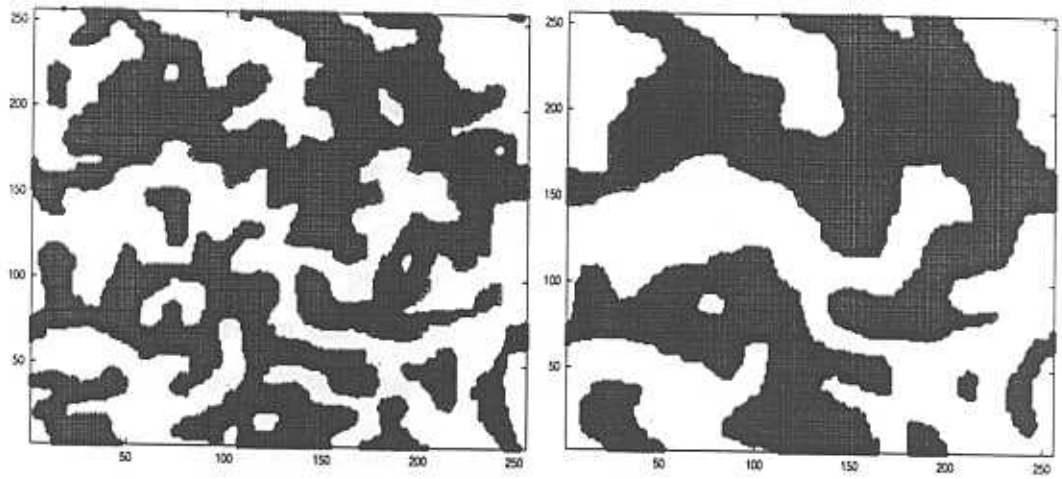


Figure 1.1: Snapshots of coarsening in 2D Ising model on a $256 \times 256$ lattice at times $t = 50$ and $t = 150$. The domain structure looks statistically self-similar, except for an overall scaling. This idea is quantified as the dynamical scaling hypothesis, which we discuss in the text.

In the binary fluid system, the amount of A and B material is separately conserved, unlike a ferromagnet where a single spin can flip sign locally. In the latter case, the absence of a conservation law makes the domains grow faster, resulting in a faster growth law of domains, $\mathcal{L}(t) \sim t^{\frac{1}{2}}$. The dynamics in the two cases are classified as *conserved* and *non-conserved* respectively. In the rest of this thesis, unless explicitly stated, we shall be dealing only with non-conserved dynamics.

The order parameter field in a phase ordering system may be discrete (eg. Ising spin) or continuous (eg. density difference in binary alloys), and in general, may be a vector (eg. Heisenberg spin) or even a tensor (Nematic order parameter in liquid crystals). We shall be dealing only with scalar order parameter, and it is often convenient to work with continuous variables. The Ising Hamiltonian defined in Eq.1.5 may be transformed into a continuum Free Energy functional through the Hubbard-Stratanovich transformation[6] followed by taking the continuum limit.

$$\mathrm{F}(\phi) = \int d^{\mathrm{d}}\mathrm{x}[\frac{\lambda}{2}|\nabla\phi|^2 + V(\phi)] \tag{1.8}$$

where $\phi(\mathrm{x}, t)$ is a coarse-grained magnetization, which is the average of $\sigma_i$ over a (mesoscopic) length scale $l$ ($a \ll l \ll \xi(T)$ where $\xi(T)$ is the equilibrium correlation

length and $a$ is the lattice spacing). The potential term has the form $V(\phi) = \frac{r}{2}\phi^2 + \frac{u}{4}\phi^4$, where $r \propto (T - T_c)$, $T_c$ being the ((mean-field) critical temperature. Clearly, if $T < T_c$, the potential has a double-well form, with minima at $\pm\sqrt{\frac{r}{u}}$. The gradient term in the Free Energy functional is very important, and takes into account the energy cost in having domain walls in the system.

Like the Ising model, the continuum model also has no inertial dynamics, since there is no time-dependent term in the Free Energy functional. However, one may write effective equations at a coarse-grained level to describe the dissipative dynamics of the system, when brought into contact with a heat bath. In the absence of any conservation laws, a suitable coarse-grained equation of motion is of the form (see Fig. 1.2)

$$\frac{\partial \phi}{\partial t} = -\Gamma \frac{\delta \mathbf{F}}{\delta \phi} + \eta(\mathbf{x}, t) \tag{1.9}$$

where $\Gamma$ is a friction constant and $\eta$ is the thermal noise, which is usually assumed to have zero mean, uncorrelated in space and time and variance fixed by Fluctuation-Dissipation Theorem[6].

$$\langle \eta(\mathbf{x}, t)\eta(\mathbf{x}', t)\rangle = 2\Gamma T \delta^d(\mathbf{x} - \mathbf{x}')\delta(t - t') \tag{1.10}$$

Eq.1.9 is often called the Time Dependent Ginzburg-Landau(TDGL) equation. The TDGL equation may be used to describe the ordering dynamics of the system following a quench from a random initial condition to a temperature $T < T_c$. In this case, it is supplemented by random, uncorrelated initial conditions in the ordering field, $\langle \phi(\mathbf{x}, 0)\phi(\mathbf{x}', 0)\rangle = \Delta\delta(\mathbf{x} - \mathbf{x}')$.

### 1.2.2 Dynamic scaling hypothesis

The most commonly used probe for the study of a coarsening process is the equal-time pair correlation function $C(r, t) = \langle \phi(\mathbf{x}, t)\phi(\mathbf{x} + \mathbf{r}, t)\rangle$ where the angular brackets indicate an average over initial conditions. The Fourier Transform of $C(r, t)$ is the equal time Structure Factor $S(\mathbf{k}, t) = \langle \phi_{\mathbf{k}}(t)\phi_{-\mathbf{k}}(t)\rangle$ where

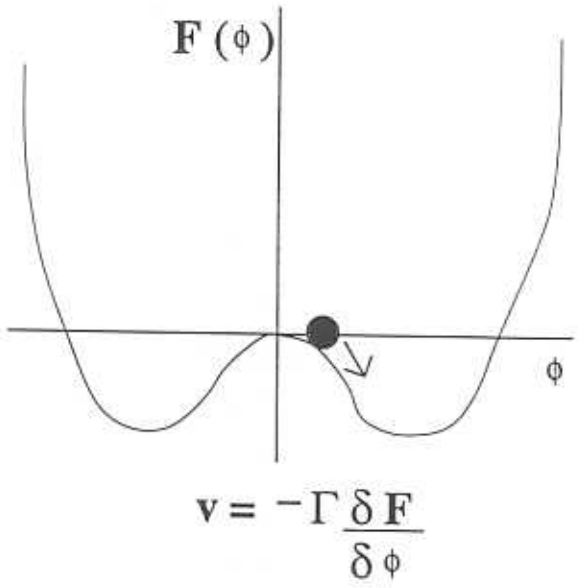


Figure 1.2: The picture shows the standard double well potential for a phase separating system. The system, starting from a disordered initial condition (corresponding to $\phi = 0$ is sliding down the potential valley, with a speed proportional to the local driving force.

$\phi_{\mathbf{k}}(t) = L^{-d/2} \int \phi(\mathbf{x}, t) e^{-i\mathbf{k}.\mathbf{r}} d^d\mathbf{r}$.

The dynamic scaling hypothesis states that at sufficiently late times $t$, the equal-time two-point spin correlation in a coarsening system satisfies the dynamic scaling form:

$$C(r,t) = f\left(\frac{r}{\mathcal{L}(t)}\right) \quad ; \quad r \gg \xi, t \gg t_0 \tag{1.11}$$

where the conditions on $r$ and $t$ define the *scaling regime* and $\xi$ and $t_0$ represent some microscopic length and time scales. $\mathcal{L}(t)$ is the characteristic length scale of the coarsening process which typically grows with time as a power-law; $\mathcal{L}(t) \sim t^{1/z}$. The exponent $z$ is the dynamical exponent of the coarsening process.

For a system of finite linear size $L$, in thermal equilibrium, the pair-correlation function satisfies Finite Size Scaling (FSS): $C(r, L) = f\left(\frac{r}{L}\right)$ for $r \gg \xi$, where $\xi$ is now the equilibrium correlation length. It is also important to look at the unequal time correlation function $C(r, t, t') = \langle \phi(\mathbf{x}, t)\phi(\mathbf{x} + \mathbf{r}, t') \rangle$ which, in the limit $\mathcal{L}(t) \gg \mathcal{L}(t')$, has the scaling form

$$C(r,t,t') \simeq \left(\frac{\mathcal{L}(t')}{\mathcal{L}(t)}\right)^{\lambda} f\left(\frac{r}{\mathcal{L}(t)}\right) \tag{1.12}$$

where $\lambda$ is a new non-trivial exponent[19]. From $C(r,t,t')$, we can also define the autocorrelation function $A(t) = C(0,t,t')$, which has the scaling form: $A(t) \sim \left(\frac{\mathcal{L}(t')}{\mathcal{L}(t)}\right)^{\lambda}$. The exponent $\lambda$ is called the autocorrelation exponent[19]. Conventionally, the dynamical exponent $z$ and the autocorrelation exponent $\lambda$ was considered to define the universality class of a coarsening process. The universality class is usually determined by the spatial dimension $d$, the symmetries of the order parameter, conservation laws and the nature of the correlations in noise (ie., whether long range or short range). In particular, the exponents are usually independent of the temperature of the heat bath, and the details of the dynamics (Monte Carlo methods and the TDGL equation should give identical results). The persistence exponent is a new addition to this set of Non-equilibrium exponents, and therefore it is important to investigate its universality properties.

It is possible to make some general statements about the short distance behaviour of the pair correlation (equivalently, the large k behaviour of the Structure Factor). For later reference, we briefly present these arguments here. We note that in the late stages of phase ordering, the system has a *few* large domains, with typical length scale $\sim \mathcal{L}(t)$. Consider the two-poin spin correlation function $C(\mathbf{r},t) = \langle \phi(\mathbf{x},t)\phi(\mathbf{x}+\mathbf{r},t)\rangle$, where the angular brackets denote average over all starting points $\mathbf{x}$ in a single spin configuration. Clearly, $C(\mathbf{r},t) = -1$ if $\mathbf{r}$ is intersected by a domain boundary (with typical width $\xi$, we are however considering only $r \gg \xi$) and 1 if it is not. If $r \ll \mathcal{L}(t)$, the probability that $\mathbf{r}$ will be intersected by a domain boundary is $p_1 \sim \frac{r}{\mathcal{L}(t)}$ and the probability that this doesn't happen is $p_2 = 1 - p_1$. Thus $C(\mathbf{r},t) = 1 - 2p_1 \approx 1 - 2\frac{r}{\mathcal{L}(t)}$ for $\frac{r}{\mathcal{L}(t)} \ll 1$. In Fourier space, this implies that

$$S(\mathbf{k},t) \sim \frac{1}{\mathcal{L}(t)} k^{-(d+1)} \tag{1.13}$$

This result is known as Porod law[20], and is valid quite generally for coarsening systems with scalar order parameter. Note that the result does not depend on whether the order parameter is conserved or non-conserved.

Substantial amount of analytical progress in the solution of the TDGL equation

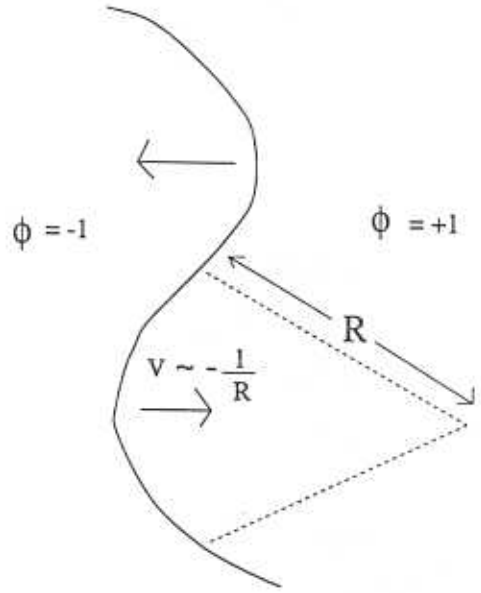


Figure 1.3: A schematic illustration of the Allen-Cahn law for motion of interfaces in a phase ordering system with non-conserved order parameter. The surface tension tends to flatten the domain wall by pulling in regions of positive curvature. The speed of motion is proportional to the mean local curvature.

turned out to be possible from understanding the structure and dynamics of domain walls. The most important result in this context is the Allen-Cahn equation[21], which we briefly discuss in the following section.

### 1.2.3 Motion of interfaces: The Allen-Cahn Equation

In this section, we present some phenomenological arguments regarding the motion of a domain wall. Consider the late stages of the coarsening regime, where the order parameter has attained value $\phi = \pm 1$ almost everywhere except at the domain boundaries. In this regime, the Free Energy of the system $F = \int (\nabla\phi)^2 d^d\mathbf{x} \sim \sigma\mathcal{R}$ where $\mathcal{R}$ is the total length of domain boundaries in the system and $\sigma$ is the surface tension.

Now let us consider a single (for simplicity, spherical) domain of radius $R$. The total surface energy is $\sim \sigma R^{d-1}$ in $d$ dimensions. Let $F$ be the force per unit area on the domain wall. The work done by the force in shrinking the domain by $\delta R$ is $\sim F R^{d-1}\delta R$ and the decrease in the surface energy is $\sim R^{d-2}\delta R$. Equating the two, we find $F \sim 1/R$, ie., the force on the domain wall is proportional to the local mean curvature. In purely dissipative dynamics, the velocity of motion of the domain wall will be proportional to the force : $\frac{dR}{dt} \sim -\frac{1}{R}$. This gives for the size of a domain at

time $t$, $R^2(t) = R^2(0) - at$, where $a$ is some constant. This means that the typical size of domains that disappears by time $t$ is about $\sqrt{t}$, and this gives the typical separation between domain walls at time $t$. Under the dynamical scaling hypothesis, the domain structure at late times is characterized by a single length scale $\mathcal{L}(t)$, and thus we conclude that for *non-conserved* dynamics, $\mathcal{L}(t) \sim t^{\frac{1}{2}}$ and the dynamical exponent $z = 2$. For general non-spherical domains, Allen and Cahn[21] derived the following equation, based on the assumption that the domain walls are *gently curving* in space.

$$v = -\nabla.\mathrm{g} \tag{1.14}$$

where g is a unit vector normal to the wall at any given point in space, and $K = -\nabla.\mathrm{g} = \frac{d-1}{R}$ where $R$ is the mean curvature of the domain wall at the given point. We note that the above results are based on very general arguments and is even independent of the spatial dimension $d$. The result is found to be satisfied by almost all models of coarsening with non-conserved order parameter in the asymptotic regime.

### 1.2.4 Approximate treatments in Phase Ordering Kinetics

After computation of the dynamical exponent $z$, the next task is the evaluation of the scaling function for the pair correlation, and the autocorrelation exponent. Except in the case of one dimensional Ising model with Glauber dynamics, there are no exact solutions in this front, and so one has to resort to approximate theories. In the remaining part of this section, we will discuss briefly two of the well-known approximate theories in Phase Ordering Kinetics with non-conserved dynamics.

*1. The Ohta-Jasnow-Kawasaki Theory*

The essential simplification in the OJK theory[22] is to replace the actual order parameter field $\phi$, which varies rather abruptly across domain boundaries, by the sign of a smoothly varying field $m(\mathbf{x}, t)$, ie., $\phi(\mathbf{x}, t) = sgn(m(\mathbf{x}, t))$. In terms of the new field, the TDGL equation may be written as

$$\frac{\partial m}{\partial t} = \nabla^2 m - n_a n_b \nabla_a \nabla_b m \tag{1.15}$$

where $\mathrm{n} = \frac{\nabla m}{|\nabla m|}$. The OJK approximation is to replace $n_a n_b$ by its spherical average $\langle n_a n_b \rangle = \delta_{ab}/d$, thus leading to the simple diffusion equation $\frac{\partial m}{\partial t} = D\nabla^2 m$, where $D = 1 - \frac{1}{d}$. The initial distribution of the field $m(\mathrm{x}, 0)$ is usually taken to be Gaussian, with delta-correlations. We shall come across the OJK approximation again in connection with Persistence of the diffusion problem. The OJK approximation is expected to work better as the spatial dimension $d$ is taken to higher and higher values. Hence, in the limit $d \to \infty$, the phase separation process is adequately described by the diffusion equation.

*2. Mazenko's Theory*

In Mazenko's theory[23], the order parameter field $\phi$ is expressed as a function of a variable $m$, which is physically interpreted as the perpendicular distance to the nearest domain wall. Then the TDGL equation can be cast in the form

$$\phi''(m) = V'(\phi) \tag{1.16}$$

The boundary conditions are $\phi(\pm\infty) = \pm 1$ and $\phi(m = 0) = 0$. Further treatment is simplified using the assumption that the field $m$ has a Gaussian distribution. Correct scaling behaviour is recovered for equal time and unequal time correlation functions and the numerical values of the autocorrelation exponent $\lambda$ was in very good agreement with simulations. Mazenko's theory is one of the most successful ones in Phase Ordering Dynamics, at least for non-conserved models.

### 1.2.5 Persistence in coarsening systems

The coarsening dynamics of the Ising model (and its continuum version), remains one of the most difficult problems in Persistence. The most important result in this field is the exact solution for 1-dimensional Ising model, which we had briefly mentioned in the introduction. This solution is in fact part of the solution to a more general problem, the coarsening dynamics of the one dimensional Potts model.

The kinetics of this model can be mapped to a reaction-diffusion problem. In this problem, a set of random walkers diffuse on the lattice, and when two of them meet, annihilate or coagulate with probability $\frac{1}{q-1}$ and $\frac{q-2}{q-1}$ respectively. A persistent spin at time $t$ is a site that is unvisited by any walker till $t$. By mapping the problem to an exactly soluble one-species coagulation model, Derrida, Hakim and Pasquier [11] showed that the fraction of unflipped spins $P(q,t)$ at time $t$ decays as $t^{-\theta(q)}$ where

$$\theta(q) = -\frac{1}{8} + \frac{2}{\pi^2}\left[cos^{-1}\left(\frac{2-q}{\sqrt{2}q}\right)\right]^2 \tag{1.17}$$

For $q = 2$ which is simply the Ising model, this equation gives $\theta = 3/8$, a highly non-trivial result. We studied the spatial distribution of persistent sites in this model both numerically and analytically[24]. The normalized pair-correlation for persistent spins was shown to have the scaling form

$$C(r,t) = P(t) f\left(\frac{r}{\xi(t)}\right) \tag{1.18}$$

where $\xi(t) \sim t^{\frac{1}{2}}$ and $f(x) \sim x^{-2\theta}$ for $x \ll 1$ and constant for $x \gg 1$. The scaling form in Eq.1.18 is one of the main results in this thesis. It follows that for $r \ll \xi(t)$, $C(r,t) \sim r^{-2\theta}$, which means that over length scales $\ll \xi(t)$, the set of persistent spins forms a fractal with fractal dimension $d_f = 1 - 2\theta = \frac{1}{4}$.

We outline the main steps in the derivation of Eq.1.18 here. We considered the length distribution $n(k,t)$ of intervals between consecutive persistent spins. The process of coalescence of these intervals was studied under the Independent Interval Approximation, where the lengths of adjacent intervals are treated as uncorrelated random variables. We constructed a rate equation for the time evolution of $n(k,t)$ based on this approximation, which was solved within a dynamic scaling ansatz. A scaling form was derived for $n(k,t)$, and was related to $C(r,t)$ under the IIA.

We extended this analysis to the coarsening of $q$-state Potts model in one dimension. We found that there are two distinct regimes appearing here. The IIA calculation shows that if $\theta(q) < \frac{1}{2}$, the persistent structure is a fractal over small length scales and homogeneous over large length scales. If $\theta(q) \geq \frac{1}{2}$, the distribution

is homogeneous over all length scales. These predictions agree with recent studies done by other authors[25].

The Persistence probability in one dimensional TDGL model has also been solved analytically. Unlike the Ising model, the characteristic length scale $\mathcal{L}(t)$ diverges only logarithmically with time[26]. It was shown that $P(t) \sim \mathcal{L}(t)^{-\theta'}$ where $\theta' \approx 0.17$ [27]. This work has the distinction of being one of the first analytical studies in Persistence.

The computation of the Persistence probability in the Ising model in higher dimensions is a very difficult task, and to date, analytic progress in this direction has been limited. In this section, we shall outline the difficulties in this problem, and attempts to get around them. However, substantial analytical progress has been possible in a simpler model, the diffusion equation[28], which is actually a coarsening system. Also, in the OJK approximation, the TDGL equation reduces to the simple diffusion equation when the ordering field is expressed in terms of the auxiliary field variable. As this approximation is believed to be exact in the $d \to \infty$ limit, results for the diffusion problem are directly relevant for the Ising model in the large $d$ limit.

Before we start our discussion, it is worth noting that all the many-body problems studied in Persistence are non-Markovian. Consider an Ising spin system evolving via Glauber dynamics. Let us consider the spin at any single site and study its persistence. It is clear that the probability that this spin will flip at any time $t$ depends on the state of its neighbours at that instant, which depends on the state of our test spin (and the state of the other neighbours also) at the *previous* instant, ie., at $t - \delta t$. We note here that the history dependence of the process has already gone beyond $t$, which makes the process non-Markovian. In general, for many body systems like the Ising model, this history dependence goes back till the origin of the process, which makes the process strongly non-Markovian. However, a number of analytical tools have been developed to deal with non-Markovian processes, which are Gaussian and stationary. Luckily, these conditions are not too restrictive, and as we shall see, the diffusion equation perfectly fits this class, while the Ising model can be approximately mapped to a Gaussian Stationary Process (GSP)under Mazenko's theory.

In this section, we briefly review some of the important analytical tools used to study Persistence in Gaussian Stationary Processes (GSP). The first two methods are used for the so-called *smooth* GSPs. Examples of problems that fall under this class are the diffusion problem and the randomly accelerating particle. In the third subsection, we consider a perturbation theory for GSPs that are not *smooth* but are very close to being Markovian. This scheme has been applied to study the Ising model under the Mazenko approximation.

Consider a general GSP $X(T)$ that has a stationary correlator $\langle X(0)X(T)\rangle = f(T)$. Let us consider the small $T$ behaviour of the function $f(T)$. In general, $f(T) \simeq 1 - aT^{\alpha} + ...$, where $\alpha \leq 2$. When $\alpha = 2$, the density of zero-crossings of the process is finite and the process is called *smooth*. On the other hand, if $\alpha < 2$, the zero-crossings have a fractal distribution. For the random walk (or, for that matter, any Markovian process), $f(T) \sim 1 - \lambda T$, so that $\alpha = 1$ and we conclude that Markov processes are not smooth. On the other hand, for the random acceleration problem, $f(T) = \frac{3}{2}exp(-\frac{T}{2}) - \frac{1}{2}exp(-3\frac{T}{2})$ which has the small $T$ behaviour, $f(T) \sim 1 - \frac{3}{8}T^2 + ..$ so that this process is smooth. Similar results hold for the diffusion problem, where $f(T) = [sech(T/2)]^{d/2}$ in $d$ dimensions. This process is also smooth as $f(T) \simeq 1 - \frac{d}{16}T^2 + ..$ near $T = 0$.

*The Independent Interval Approximation:*

For *smooth* Gaussian processes, one may obtain estimates of $\theta$ under an approximation. This is called the Independent Interval Approximation (IIA) which assumes the separations between two consecutive zero crossings are independent random variables drawn from some well-defined probability distribution. For the diffusion problem, this approach gave $\theta = 0.1203$ in $d = 1$ and $\theta = 0.1862$ and $0.2358$ in $d = 2$ and 3 respectively[28, 29]. These results are in very good agreement with the results of numerical simulations. The value of $\theta$ in $d = 1$ diffusion problem has also been recently verified experimentally[30]. For the random acceleration problem, the estimate was $\theta_{IIA} = 0.2647..$, in reasonable agreement with the exact value $\frac{1}{4}$.

*The Series expansion method:*

The IIA approach suffers from the drawback that it is difficult to systematically improve. A series expansion approach has been proposed which took care of this problem to some extent[31]. The basic idea is to start from the generating function

$$P(p,t) = \sum_{n=0}^{\infty} p^n P_n(t) \tag{1.19}$$

where $P_n(t)$ is the probability of $n$ zero-crossings till time $t$. For $p = 0$, this is just the usual persistent fraction $P(t)$. For general $p$, it was shown that $P(p,t) \sim t^{-\theta(p)}$ where the exponent $\theta(p)$ varies continuously with $p$, in general. For $p = 1$, clearly $P(1,t) = 0$ implying that $\theta(1) = 0$. From this approach, a series expansion for $\theta(1-\epsilon)$ in powers of $\epsilon$ was proposed, which gave very good results for the diffusion problem.

*Perturbation around a Markov Process:*

For processes that are close to Markovian, ie., with correlator $f(T) = e^{-\lambda' T} + \epsilon f_1(T)$, it is possible to express the persistence exponent $\theta$ in a series expansion in powers of $\epsilon$, ie., $\theta = \lambda' + O(\epsilon)$. The starting point of this method is to write $P(T)$ as the ratio of two path-integrals:

$$P(T) = \frac{2\int_{\phi>0} D\phi(\tau) exp(-S)}{\int D\phi(\tau) exp(-S)} \tag{1.20}$$

where the numerator is the total weight of all paths which never crossed zero, and the denominator is the weight of *all* paths. The action $S = \frac{1}{2}\int_0^T \int_0^T d\tau_1 d\tau_2 \phi(\tau_1) G(\tau_1 - \tau_2)\phi(\tau_2$ and $G(\tau)$ is the inverse matrix of the Gaussian correlator $f(\tau)$. It is possible to show that $\theta = E_1 - E_0$ where $E_0$ is the ground state of a quantum mechanical problem (harmonic oscillator with frequency $\lambda'$ for a Markov process) and $E_1$ is the corresponding quantity when a hard wall at the origin is added to the problem. This method was used for the solution of $\theta$ in kinetic Ising model, under the Mazenko scheme. The problem could be converted to a GSP approximately using Mazenko's auxiliary field variable: $s(\mathbf{x},t) = sgn[m(\mathbf{x},t)]$ where $m(\mathbf{x},t)$ is *assumed* to be a Gaussian variable within Mazenko's theory. The correlator $f(T)$ still could not be obtained in closed form above $d = 1$, and is obtained numerically as the solution to a

differential equation. It was confirmed that in all dimensions, $\alpha = 1$, so the process is non-smooth. Analytic predictions for $\theta$ were possible using the equality $\theta = E_1 - E_0$ described above, and estimating $E_1$ and $E_0$ using a variational approximation[32].

In Table 1.1, we have presented a summary of numerical and analytical estimates of persistence exponent $\theta$ in various coarsening models. We note that in the Ising model, numerical results for $T = 0$ Glauber dynamics points to a decrease in the value of $\theta$ with dimension. This is somewhat surprising, since, in general, we expect $\theta$ to increase with dimension. The argument in support of this conjecture is very simple: The more neighbours to interact with, lesser the chance of remaining in the same phase for a long time, and hence larger the value of $\theta$. This argument is also supported by the results (IIA and numerical) for the diffusion problem, TDGL model (FSS analysis) and semi-analytical estimates of $\theta$ in Ising model under the Mazenko theory.

What could be then wrong with the Ising model at $T = 0$ ? There has not been conclusive answers so far, but it seems possible that in zero temperature dynamics, the system often develops flat interfaces in the lattice, which considerably slows down the dynamics. It has been observed that in $d = 3$ Glauber dynamics, the characteristic length scale of domains grows much slower than $t^{\frac{1}{2}}$, as predicted by Allen-Kahn arguments[39]. We have independently verified this fact, and have also observed that in $d = 4$ it grows even slower than in $d = 3$. It is likely that since the average motion of interfaces is slower, Persistence probability also decays slower than usual. This conjecture is supported by numerical results in $d = 3$ for coarsening at non-zero temperatures. It is observed that for sufficiently high temperatures, $\theta$ actually becomes much higher, close to the TDGL and diffusion values.

Since the power-law decay of Persistence is established in higher dimensions also, it is natural to enquire about the spatial correlations in the distribution of these sites. We investigated this problem both through direct computation of pair correlations as well as an indirect Finite Size Scaling (FSS) analysis. For a coarsening process in $d$ dimensions characterized by dynamical exponent $z$, we showed that, if $z\theta < d$, the set of persistent sites forms a fractal structure over length scales $\ll t^{1/z}$ and will be randomly distributed beyond this length scale. In this case, persistent fraction

| model | $d=1$ | $d=2$ | $d=3$ | $d=4$ | $d \to \infty$ |
|---|---|---|---|---|---|
| Diffusion $(IIA)_{28}$ | 0.1203 | 0.1862 | 0.2358 | 0.2769 | $\sim \sqrt{d}$ |
| TDGL | $P(t) \sim (lnt)_{27}^{-0.17}$ | $0.20_{33}$ | $0.24_{FSS}$ | $0.27_{FSS}$ | $\sim \sqrt{d}$? |
| Ising($T=0$) | $3/8_{11}$ (exact) | $0.22_{32,34}$ | $0.16_{34}$ | $0.12_{36}$ | freezing $?_{34}$ |
| Ising($T>0$) | - | $0.22_{37,38}$ | $0.26_{38}$ | - | - |
| Ising(variational)$_{32}$ | 0.35 | 0.22 | 0.26 | - | - |

Table 1.1: The table shows comparison of numerical values of $\theta$ in different coarsening models. The notation FSS refers to finite size scaling techniques, which is described in detail in Chapter 3.

for finite lattices has the scaling form

$$P(t,L) = L^{-z\theta} f\left(\frac{t}{L^z}\right) \tag{1.21}$$

where $f(x) \sim x^{-\theta}$ for $x \ll 1$ and $f(x) \simeq$ constant for $x \gg 1$. We then showed that this scaling form actually leads to the dynamical scaling form Eq.1.18 in higher dimensions also. The FSS analysis was also used to study persistence in another well-known and common system, a diffusing field with inhomogeneous distribution of initial density. This system exhibits phase ordering similar to the TDGL model with characteristic domain size growing as $\mathcal{L}(t) \sim t^{1/2}$ in all dimensions. The persistence probability follows a power-law decay and approximate analytical estimates for $\theta$ are available for general spatial dimension $d$. We showed using FSS analysis up to $d=3$ that the set of persistent sites has a scale-invariant structure. We also argued that for the diffusion problem, this phenomenon will be present in all spatial dimension $d$[36]. This result is also relevant for the Ising model, since we expect the Persistence properties of both the models to be identical in the large $d$ limit.

### 1.2.6 Coarsening and Persistence in Fluctuating Interfaces

Fluctuating interfaces and growing surfaces form a class of systems that has undergone elaborate study in the past decades[16] In recent years, the persistence properties of fluctuating interfaces have also come under investigation[40, 41]. Con-

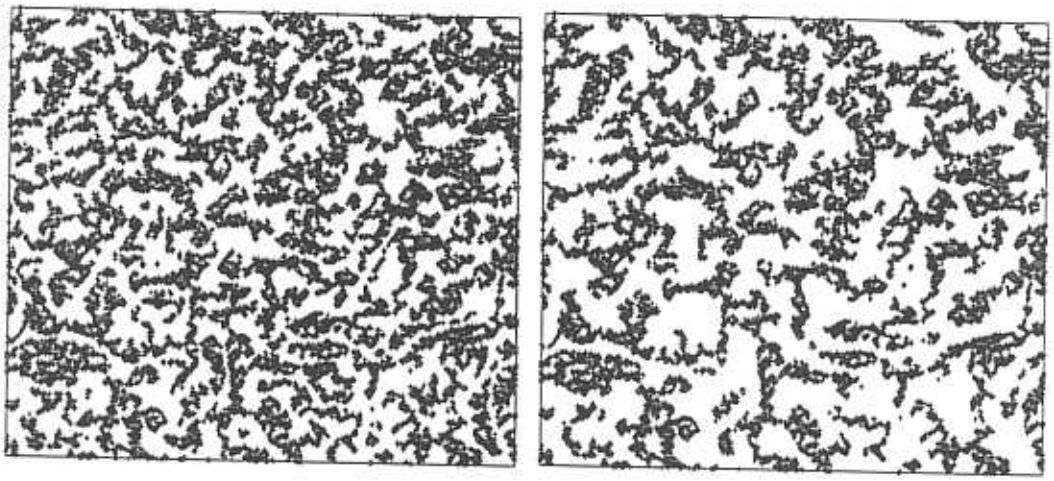

( A ) ( B )

Figure 1.4: Snapshots of the persistent region in 2D Ising model on a $256 \times 256$ lattice at times $t = 100$ and $t = 250$. The structure is evolving towards a fractal distribution, with fractal dimension $d_f \approx 1.56$.

sider a fluctuating interface characterized by a height field $h(\mathbf{x}, t)$, growing from a flat initial condition at $t = 0$. The probability $P(t, t_0)$ that the height at any given point on the interface remains above or below its 'initial' height $h(\mathbf{x}, t = t_0)$ throughout the time interval $[t_0, t]$ is defined as the Persistence probability. For interfaces whose average height $\langle h \rangle(t) = L^{-d} \sum h(\mathbf{x}, t)$ diverges with time (and in any case, for *any* interface defined on a *finite* lattice), it is natural to consider the relative height $h'(\mathbf{x}, t) = h(\mathbf{x}, t) - \langle h \rangle(t)$. In the rest of this section, we briefly summarize the known results on Interface Persistence.

*Gaussian Interfaces:*

For interfaces governed by a linear Langevin equation of the form

$$\frac{\partial h}{\partial t} = -(-\nabla^2)^{z/2} h + \eta(\mathbf{r}, t) \tag{1.22}$$

it was shown using analytic arguments and extensive numerical simulations that $P(t)$ shows a power-law decay at asymptotic times. The persistence exponent, however, depends on the choice of the 'starting' time $t_0$. Two temporal regimes were identified in this context.

- If $t_0 \ll L^z$ (the pre-steady state regime), $P(t, t_0) \sim t^{-\theta_0}$ where $\theta_0$ is a non-trivial exponent.

- If $t_0 \geq L^z$ (the steady state regime), $P(t, t_0) \sim (\frac{t}{t_0})^{-\theta_S}$ where $\theta_S = 1 - \beta$.

While the $\theta$ in steady state is directly related to the 'temporal roughness' exponent $\beta$, for $\theta_0$, it was possible to derive bounds which compared well with the results of numerical simulations.

*Persistence in KPZ surface:*

The up-down symmetry $h \to -h$ is broken in a KPZ surface, and in this case, we need to define two persistence probabilities, $P_{\pm}(t_0, t)$ corresponding to whether $h(\mathbf{x}, t) > h(\mathbf{x}, t_0)$ or $h(\mathbf{x}, t) < h(\mathbf{x}, t_0)$ respectively. In this case, analytical progress was limited on account of the non-linear nature of the evolution equation, and numerical results in $d = 1$ showed that

- If $t_0 \ll L^z$, $P_{\pm}(t_0, t) \sim t^{-\theta_0^{\pm}}$ where $\theta_0^+ < \theta_0^-$

- If $t_0 \geq L^z$, $P_{\pm}(t, t_0) \sim (\frac{t}{t_0})^{-\theta_S}$ where $\theta_S = 1 - \beta$.

Is it possible to view such an interface, evolving towards its self-affine steady state, as a coarsening system ? To answer this question, let us now characterize the height variations of the surface in terms of a discrete Ising-like variable $s(\mathbf{r})$ defined as follows: At a given instant in time, all points on the surface where the height is below a certain reference level $h_0$ is assigned a spin $s = 1$, and the others are assigned $s = -1$[42].

$$s(\mathbf{r}) = sgn\,[h(\mathbf{r}) - h_0] \tag{1.23}$$

We consider surfaces that are rough in the steady state ie., $\langle (h(\mathbf{x}, t) - h(\mathbf{x} + \mathbf{r}, t))^2 \rangle \sim r^{2\chi}$ for $t \gg L^z$. For Gaussian surfaces in steady state, (eg. the linear Edwards-Wilkinson surface), we showed analytically that the two-point spin correlator in steady state $C(r, L) = \langle s(\mathbf{x}) s(\mathbf{x} + \mathbf{r}) \rangle = f(\frac{r}{L})$. This scaling is characteristic of a phase separated system. In conventional phase separated systems, $f(x)$

decays linearly near origin ie., $1 - f(x) \sim x$[17]. In the present case, however,it is found that $1 - f(x) \sim x^{\chi}$ near $x = 0$[43]. The cuspy nature of the correlator near $r = 0$ shows that the ordered phase is not as homogeneous as in more conventional phase segregated systems (eg. binary fluid). While the largest domain is always of size $\sim L^2$, which signifies phase segregation, the smaller clusters have a broad distribution, which is reminiscent of critical systems.

For general non-Gaussian surfaces (eg. the Kardar-Parisi-Zhang surface in $d = 2$), we showed that these conclusions are still valid within the Independent Interval Approximation. We verified these predictions by numerical simulations of the EW and KPZ surfaces, and the results were in very good agreement with the analytical predictions. We also extended the simulations to explore the pre-steady state temporal regime ($t \ll L^z$) We found that the equal time correlator has the same scaling form with $L$ replaced by $\mathcal{L}(t)$, which is typical of a system undergoing domain coarsening. Scaling arguments suggest that $\mathcal{L}(t) \sim t^{1/z}$ where $z$ is the dynamical exponent for the surface fluctuations. For (2+1) dimensional KPZ and EW surfaces, we found that this argument is in excellent agreement with simulations. This result also agrees with a previous work on (1+1) dimensional surfaces[44].

## 1.3 A Note on Format

Each chapter in this thesis starts with an introduction, followed by a detailed analysis of the problem. We have tried to present all the details of calculations, as far as possible. For compactness and ease of reading, some calculations have been shifted to appendices at the end of each chapter. Each chapter ends with a summary of results and bibliography.

## 1.4 Appendix A

The dynamics of a thermodynamic system, ie., its transitions from one thermodynamic state to another, may be expressed through the following master equation:

$$\frac{\partial \mathcal{P}_\mu(t)}{\partial t} = \sum_\nu \mathcal{P}_\nu(t) W(\nu \to \mu, t) - \mathcal{P}_\mu(t) W(\mu \to \nu, t) \tag{1.24}$$

where $\mathcal{P}_\mu(t)$ is the probability of finding the system in a state with energy $E_\mu$ at time $t$ and $W(\nu \to \mu, t)$ is the transition probability between states $\mu$ and $\nu$ at time $t$. There is no general method to determine these transition probabilities and it is difficult to determine them unambiguously. The only guiding principle here is that, in thermodynamic equilibrium, all the quantities in the master equation becomes time-independent and $\mathcal{P}_\mu \propto e^{-\beta E_\mu}$, the Boltzmann-Gibbs distribution. This leads to the condition of detailed balance:

$$\frac{W(\mu \to \nu)}{W(\mu \to \nu)} = \frac{\mathcal{P}_\mu}{\mathcal{P}_\nu} = e^{-\beta(E_\nu - E_\mu)} \tag{1.25}$$

We now restrict ourselves to the case of the Ising ferromagnet with Hamiltonian involving only nearest neighbour exchange interaction between spins.

$$\mathcal{H} = -J \sum_{\langle ij \rangle} s_i s_j - h \sum_i s_i \tag{1.26}$$

To implement a dynamical scheme for this system, consistent with detailed balance, the simplest way is to consider only those transitions where the final state differs from the initial one by the flip of a single spin. Even with this simplification, is no unique choice for the transition rates, and the choice is often a matter of time-efficiency of the algorithm in a particular situation. The most common choice used is the Metropolis algorithm, where the transition rates are chosen as

$$\begin{aligned} P(\mu \to \nu) = e^{-\beta(E_\nu - E_\mu)} \;\; ; \;\; E_\nu > E_\mu \\ = 1 \;\; ; \;\; E_\nu < E_\mu \end{aligned} \tag{1.27}$$

Another popular choice is the Heat Bath algorithm:

$$P(\mu \to \nu) = \frac{e^{-\beta(E_\nu - E_\mu)}}{1 + e^{-\beta(E_\nu - E_\mu)}} \tag{1.28}$$

At $T = 0$, both Metropolis and Heat Bath algorithms behave identically.

$$\begin{aligned} P(\mu \to \nu) &= 0 \;\; ; \;\; E_\nu > E_\mu \\ &= \frac{1}{2} \;\; ; \;\; E_\nu = E_\mu \\ &= 1 \;\; ; \;\; E_\nu < E_\mu \end{aligned} \tag{1.29}$$

This is called Glauber dynamics. We note that both the algorithms are consistent with the condition of detailed balance, and both lead to the Gibbs-Boltzmann distribution in equilibrium.

In a system that is far from equilibrium, all quantities including the transition probabilities may be expected to depend on time. In such situations, however, it is conceivable that local equilibrium is established over small (but still macroscopic) regions in the system, where we may use the above results. In practice, both Metropolis and Heat Bath algorithms have been successfully used in Non-equilibrium simulations[45].

# Bibliography


[1] N. G. Van Kampen, *Stochastic Processes in Physics and Chemistry* (North Holland Publishing Company, Amsterdam, 1981).

[2] L. D. Landau and E. M. Lifshitz, *Statistical Physics* (Pergamon Press, 1980) Part 1.

[3] A. Einstein, *Investigations on the Theory of the Brownian movement* (Dover Publishing, New York, 1956).

[4] W. Feller, *Introduction to Probability Theory and Applications*, (Wiley, New York, 1966) Vol. I and II.

[5] S. Chandrasekhar, *Rev. Mod. Phys.* **15** 1 (1943).

[6] P. M. Chaikin and T. C. Lubensky, *Principles of Condensed Matter Physics* (Cambridge University Press, Cambridge, 1995)

[7] For a recent review, S. N. Majumdar, *Current Science* **77**, 370 (1999).

[8] D. Slepian, Bell Syst. Tech. J. **41**, 463 (1962).

[9] Y. G. Sinai, Theor. Math. Phys. **90**, 219 (1992); T. W. Burkhardt, J. Phys. A **26**, L1157 (1993).

[10] A. J. Bray, J. Phys. A **22**, L67 (1990); J. G. Amar and F. Family, Phys. Rev. A **41**, 3258 (1990); B. Derrida, C. Godreche and I. Yekutieli, **44**, 6241 (1991).

[11] B. Derrida, V. Hakim and V. Pasquier, Phys. Rev. Lett. **75**, 751 (1995); J. Stat. Phys. **85**, 763 (1996).

[12] G. Manoj, IMSc preprint/98/07/44. (unpublished).

[13] S. J. O'Donoghue and A. J. Bray, e-print cond-mat/0105074.

[14] M. Marcos-Martin, D. Beysens, J-P. Bouchad, C. Godrèche and I. Yekutieli, Physica D **214**, 396 (1995).

[15] A. L. Barabasi and H. E. Stanley, *Fractal Concepts in Surface Growth* (Cambridge University Press).

[16] For a recent review, J. Krug, Adv. Phys. **46**, 139 (1997).

[17] A. J. Bray, Adv. Phys. **43**, 357 (1994).

[18] I. M. Lifshitz, Sov. Phys. JETP **15**, 939 (1962); I. M. Lifshitz and V. V. Slyozov, J. Phys. Chem. Solids **19** 35, (1961); C. Wagner, Z. Elektrochem. **65**, 581 (1961).

[19] D. S. Fisher and D. A. Huse, Phys. Rev. B **38**, 373 (1988).

[20] G. Porod, Z. Kolloid **124**, 83 (1952).

[21] S. M. Allan and J. W. Cahn, Acta metall. **27**, 1085 (1979).

[22] T. Ohta, D. Jasnow and K. Kawasaki, Phys. Rev. Lett. **49**, 1223 (1982).

[23] G. F. Mazenko, Phys. Rev. Lett. **63**, 1605 (1989); Phys. Rev. B **42** 4487 (1990); Phys. Rev. B **43**, 5747 (1991).

[24] G. Manoj and P. Ray, J. Phys. A **33**, L109 (2000); *ibid.* 5489 (2000).

[25] A. J. Bray and S. J. O'Donoghue, Phys. Rev. E **62** 3366 (2000).

[26] T. Nagai and K. Kawasaki, Physica A **134** 483 (1986); A. D. Rutenberg and A. J. Bray, Phys. Rev. E **50**, 1900 (1994).

[27] A. J. Bray, B. Derrida and C. Godreche, Europhys. Lett. **27**, 175 (1994).

[28] S. N. Majumdar, C. Sire, A. J. Bray and S. J. Cornell, Phys. Rev. Lett. **77**, 2867 (1996); B. Derrida, V. Hakim and R. Zeitak, Phys. Rev. Lett. **77**, 2871 (1996).

[29] Very similar results were also obtained through a different method by T. J. Newman and Z. Toroczkai, Phys. Rev. E **58**, R2685 (1998).

[30] G. P. Wong, R. W. Mair and R. L. Walsworth, e-print physics/0008248 (2000).

[31] S. N. Majumdar and A. J. Bray, Phys. Rev. Lett. **81**, 2626 (1998).

[32] S. N. Majumdar and C. Sire, Phys. Rev. Lett. **77**, 1420 (1996).

[33] S. Cueille and C. Sire, Euro. Phys. J. B **7**, 111 (1999).

[34] D. Stauffer, J. Phys. A **27**, 5029 (1994).

[35] B. Derrida, A. J. Bray and C. Godrèche, J. Phys. A **27**, L357 (1994).

[36] G. Manoj and P. Ray, Phys. Rev. E **62**, 7455 (2000).

[37] B. Derrida, Phys. Rev. E **55**, 3705 (1997).

[38] D. Stauffer, Int. J. Mod. Phys. **8** No. 2, 361 (1997).

[39] J. D. Shore, M. Holzer and J. P. Sethna, Phys. Rev. B **46**, 11376 (1992).

[40] J. Krug, H. Kallabis, S. N. Majumdar, S. J. Cornell, A. J. Bray and C. Sire, Phys. Rev. E **56**, 2702 (1997).

[41] H. Kallabis and J. Krug, Europhys. Lett. **45**, 20 (1999).

[42] Such a characterization was first used in J. M. Kim, A. J. Bray and M. A. Moore, Phys. Rev. A **45**, 8546 (1992).

[43] G. Manoj and M. Barma, unpublished.

[44] D. Das and M. Barma, Phys. Rev. Lett. **85**, 1602 (2000).

[45] A more detailed account of Monte Carlo methods may be found in T. J. Newman and G. T. Barkema, *Monte Carlo methods in Statistical Physics* (Oxford University Press, 2000) and references therein.

# Chapter 2

# Spatial correlations in Persistence : $d = 1$

## 2.1 Introduction

In this chapter, we study the spatio-temporal evolution of the persistent region in a simple one-dimensional model. The model we choose is the one-dimensional $q$-state Potts-Glauber model. It is well-known that the dynamics of this model may be represented by the the reaction-diffusion model $A + A \rightarrow B$ where the product $B = \emptyset$ with probability $\frac{1}{q-1}$ and $B = A$ with probability $\frac{q-2}{q-1}$. The diffusing 'reactant' particles $A$ actually represent domain walls in the system, and persistent spins are the sites which are unvisited by any diffusing particle. We study the spatial correlations in the distribution of the persistent sites in these models. For concreteness, we present our formalism in the context of the $q = 2$ Potts model, which is simply the Ising model. We also briefly discuss about the extension of the techniques to general $q$-state Potts model.

Our approach here is two-fold:

- The study the distribution of the separations between nearest neighbour pairs of persistent sites. We call this the Empty Interval Distribution $n(k, t)$, defined as the number of occurrences where consecutive persistent sites are separated

by distance $k$ at time $t$.

- The pair correlation function $C(r,t)$, defined as the probability of finding a persistent site at a distance $r$ from another persistent site.

Both the quantities are good probes of the spatial correlations in the system. While the Empty Interval distribution proved to be more analytically tractable (in one dimension), the pair correlation function has the advantage of being easily generalisable to higher dimensions. In $d = 1$, we show that it is possible to relate the two quantities under an Independent Interval Approximation (IIA). We support our results with numerical simulations[1].

## 2.2 The Empty Interval Distribution

In this section, we study the time evolution of the size distribution $n(k,t)$ of these Empty Intervals. Persistence decay is identified with the irreversible coalescence of these intervals. The paper is organised as follows. In the next section we write a rate equation for the coalescence of these intervals under the approximation that the lengths of adjacent intervals are uncorrelated (IIA). We give phenomenological arguments about the asymptotically relevant dynamical length scale as well as the coalescence probability. These arguments, combined with the rate equation gives the dynamic scaling behaviour of $n(k,t)$ at late times $t$. We compare our predictions with numerical results. In section 3, we use the IIA to predict the two-point correlations in the distribution of persistent sites. The predictions are found to be in agreement with recent numerical results, showing that the IIA is valid.

In the $A+A \rightarrow \emptyset$ model, a set of particles are distributed at random on the lattice with average density $n_0$. Over one time step, all the particles make an attempted jump to either of the neighbouring sites with some probability $D$. If two particles meet each other, both disappear from the lattice. In one dimension, the density of particles decay with time as $n(t) \sim (8\pi Dt)^{-\frac{1}{2}}$ as $t \rightarrow \infty$[2]. Persistent sites in $A + A \rightarrow \emptyset$ model at any time $t$ are defined as the sites which remained unvisited by any diffusing particle throughout the time interval $[0 : t]$. Empty Intervals

(which we will call 'Interval' for simplicity henceforth) are defined as the separations between two consecutive persistent sites. By definition, an Interval cannot contain a persistent site, although it may contain one or more diffusing particles $A$. The total number (per site) of Intervals of length $k$ at time $t$ is denoted by $n(k,t)$ and is called the Empty Interval Distribution.

To start with, the the particles are put randomly on the lattice so that $n(k, t = 0) = n_0^2(1-n_0)^k \sim e^{-\lambda k}$ where $\lambda = -\log(1-n_0)$. With time, the particles diffuse on the lattice, making the sites non-persistent. $n(k,t)$ evolves satisfying the following normalisation conditions. If $I_m(t) = \sum_k k^m n(k,t) \approx \int_1^\infty n(s,t)s^m ds$ is the $m$-th moment of the distribution, then

$$I_0(t) = P(t) \sim t^{-\theta} \quad ; \quad I_1(t) = 1 \quad I_2(t) \equiv s(t) \tag{2.1}$$

The first condition follows from the definition of $n(k,t)$, the second one implies length conservation and the third condition gives the mean interval size $s(t)$. The probability distribution of interval lengths is $p(k,t) = \frac{n(k,t)}{\sum_k n(k,t)} = P(t)^{-1} n(k,t)$ so that $\sum_k p(k,t) = 1$.

Two neighbouring Intervals can coalesce when the persistent site between them is destroyed by a diffusing particle at the boundary of either of the Intervals. Note that this coalescence process is irreversible. For simplicity, we consider only binary coalescence in a single time step where two adjacent Intervals of lengths $k_1$ and $k_2$, separated by a persistent site, coalesce and form a new Interval of length $k_1 + k_2$ when the persistent site is 'killed' by a particle (Fig. 2.1). To study this process analytically, we invoke a mean-field approximation – the lengths of adjacent Intervals are treated as uncorrelated random variables with probability distribution $p(k,t)$. This is the Independent Interval Approximation (IIA), which has been used to study a variety of problems in one dimension[3, 4].

### 2.2.1 Rate Equation for Interval coalescence

Assuming that IIA is valid, the time evolution of $n(k,t)$ is given by the rate equation

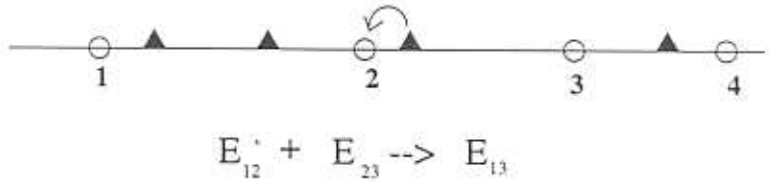


Figure 2.1: In the picture, white circles are persistent sites (numbered 1, 2, 3..) and dark triangles are diffusing particles. Two Empty Intervals $E_{12}$ and $E_{23}$ are shown to merge together to give a new Interval $E_{13}$ when the persistent site 2 at the boundary is killed by a diffusing particle.

$$\frac{\partial n(k,t)}{\partial t} = \frac{1}{2}\sum_{m=1}^{k-1} n(m,t)p(k-m,t)K(m,k-m,t) - n(k,t)\sum_{m=1}^{\infty} p(m,t)K(m,k,t) \tag{2.2}$$

where $K(m_1, m_2, t)$ is the probability that two adjacent Intervals of lengths $m_1$ and $m_2$ coalesce at time $t$. The first term in Eq.2.2 represents the increase in number of Intervals of size $k$ through coalescence of smaller intervals, while the second term is the loss term representing the decrease in number when Intervals of size $k$ merge with other Intervals.

To solve the above equation for $n(k,t)$, one need to know the form of the reaction kernel $K(m_1, m_2, t)$. The process of coalescence of Intervals involves the destruction of the persistent site in between them by a particle, which can come from either of the Intervals. So, quite generally,

$$K(m_1, m_2, t) = Q(m_1, t) + Q(m_2, t) \tag{2.3}$$

where $Q(m,t)$ is the fraction of intervals of size $m$ which is destroyed at time $t$.

$Q(m,t)$ satisfies the following condition by definition.

$$\sum_m n(m,t)Q(m,t) = -\frac{\partial P(t)}{\partial t} = \frac{\theta}{t}P(t) \tag{2.4}$$

where we have made use of the fact that $P(t) \sim t^{-\theta}$.

The form of $Q(m,t)$ can be argued for in the following way. An Interval of length $m$ at time $t$ can contain a particle anywhere inside it only if the interval length is at least of the order of the diffusive scale $\sqrt{Dt}$. That is, $Q(m,t) \simeq 0$ for $m \ll \sqrt{Dt}$. It is also known that the particle distribution is correlated over length scales $r \ll \sqrt{Dt}$, whereas it is completely random over $r \gg \sqrt{Dt}$[4]. So we expect that for $m \gg \sqrt{Dt}$, $Q(m,t) \to \alpha(t)$, independent of $m$. These physical considerations leads us to suggest the following dynamic scaling form for $Q(m,t)$.

$$Q(m,t) = \alpha(t)\beta(\frac{m}{\sqrt{Dt}}) \tag{2.5}$$

where the function $\beta(x)$ is expected to have a sigmoidal form, ie., $\beta(x) = 0$ for $x \ll 1$ and $\beta(x) \to 1$ for $x \gg 1$. The function $\alpha(t)$ will be determined later.

### 2.2.2 Dynamic scaling

We assume that at asymptotic times, the distribution $n(k,t)$ is characterised by a single dynamic length scale $s(t)$. We note that there are two relevant length scales in the problem. The first is the diffusive scale $\mathcal{L}_D(t) \sim \sqrt{Dt}$ entering the scaling form Eq.2.5 for the coalescence probability. On the other hand, the inverse of the persistent fraction $P(t)$ is also a length scale, which we shall call the persistence scale, denoted by $\mathcal{L}_p(t) \sim t^{\theta}$. The asymptotic behaviour is expected to be dominated by the larger of the two, ie., the diffusive scale $\mathcal{L}_D(t)$ in the present case (since $\theta < 1/2$).

We now invoke the dynamic scaling ansatz, ie., $n(k,t) \propto f(\frac{k}{s})$ with

$$s \sim t^{1/z},\ z = 2 \tag{2.6}$$

From the length conservation condition given by the second part of Eq. 2.1 it

follows that the prefactor is $\sim s^{-2}$. Thus, the scaling solution for $n(k,t)$ is written in the form

$$n(k,t) = s(t)^{-2} f\left(\frac{k}{s(t)}\right) \tag{2.7}$$

Substituting Eq. 2.7 and Eq. 2.5 in Eq. 2.4, we find $\alpha(t)$.

$$\alpha(t) = \frac{\theta}{t}\frac{s(t)P(t)}{B} \tag{2.8}$$

where $B = \int_0^\infty \beta(x)f(x)dx$. Substituting Eq.2.7 in the normalisation conditions Eq.2.1, we find the following conditions on the scaling function.

$$\int_{s^{-1}}^{\infty} f(x)dx = sP(t) \quad ; \quad \int_0^\infty f(x)xdx = 1 \tag{2.9}$$

In the first integral, the lower limit is set as $s(t)^{-1}$ to take care of any possible small argument divergence.

Substituting Eq.2.5, 2.6, 2.7,and 2.8 in Eq. 2.2, we find the following equation for the scaling function $f(x)$.

$$\frac{\eta}{z}\frac{\partial f}{\partial \eta} = -\frac{\theta}{B}\int_{s(t)^{-1}}^{\frac{\eta}{2}} f(x)f(\eta - x)[\beta(x) + \beta(\eta - x)]dx - \left[\frac{2}{z} - \theta - \frac{\theta}{B}s(t)P(t)\beta(\eta)\right] f(\eta) \tag{2.10}$$

where the scaling variable $\eta = \frac{k}{s(t)}$.

*Case* I: $\eta \ll 1$.

For $\eta \ll 1$, all $\beta(x) \simeq 0$ for $x \leq \eta$. This case corresponds to small Intervals, ie., those which are not large enough to contain a diffusing particle till time $t$. In this case, the equation reduces to $\eta\frac{\partial f}{\partial \eta} = -(2 - z\theta)f(\eta)$ which has the solution $f(\eta) \sim \eta^{-\tau}$ where the new exponent $\tau$ is related to $\theta$ through the scaling relation

$$\tau = 2 - z\theta \tag{2.11}$$

From Eq. 2.7 this implies that for $k \ll s$, $n(k,t) \sim t^{-\theta}k^{-\tau}$. For the model under consideration here, $\theta$ is known exactly to be 3/8 [5] which gives $\tau = 5/4$.

*Case* II: $\eta \gg 1$.

For general values of $\eta$, $\beta(\eta)$ is non-zero, and because $\tau > 1$, the first integral diverges near $x = 0$ as $x^{-(\tau-1)}$. There is another divergence in the last term, of the form $t^{1/z-\theta}$. It can be shown that this term can be exactly cancelled by the divergent part of the first integral. After carrying out this 'regularisation' (details to be found in Appendix A) and putting $z = 2$ in Eq.2.10 the equation for the scaling function $f(\eta)$ stands as

$$\frac{\eta}{2}\frac{\partial f}{\partial \eta} = -\frac{\theta}{B}\int_0^{\frac{\eta}{2}} f(x)f(\eta - x)[\beta(x) + \beta(\eta - x) - \beta(\eta)]dx - \frac{\theta}{B}\beta(\eta)\int_0^{\frac{\eta}{2}} f(x)[f(\eta - x) - f(\eta)]dx - \left[1 - \theta - \frac{\theta}{B}\beta(\eta)\int_{\frac{\eta}{2}}^{\infty} f(x)dx\right] f(\eta) \qquad (2.12)$$

A general solution of this equation requires the knowledge of the detailed form of the scaling function $\beta(\eta)$. However, for large values of $\eta$ where $\beta(\eta) \simeq 1$, one can simplify this equation. We define the point $\eta^*$ sufficiently large such that for $\eta \geq \eta^*$, $\beta(x) = 1$ within the limits of accuracy required. Without any loss of generality, one can put $\eta^* = 1$ by rescaling the length scale $s(t)$ accordingly. For $\eta \geq 1$, we define $f(\eta) \equiv h(\eta)$, whose equation is

$$\frac{\eta}{2}\frac{\partial h}{\partial \eta} = -\frac{\theta}{B}\left[2\int_1^{\frac{\eta}{2}} h(x)h(\eta - x)dx + \int_0^1 f(x)[h(\eta - x) - h(\eta)]dx\right] - (1 - 2\theta)h(\eta) \qquad (2.13)$$

This equation has a solution of the form $h(\eta) = Ge^{-\lambda\eta}$ as can be shown by direct substitution. The constants $G$ and $\lambda$ are related through the relations

$$\lambda B = 2\theta G \qquad (2.14)$$

and

$$\lambda + 2\theta = 1 + \frac{\theta}{B} F(\lambda) \tag{2.15}$$

where $F(\lambda) = \int_0^1 f(x) \left[ e^{\lambda x}(1 + \beta(x)) - 1 \right] dx$ and

$$B = \int_0^1 f(x)\beta(x)dx + \frac{G}{\lambda} e^{-\lambda} \tag{2.16}$$

by definition. Eq.2.14-2.16 formally gives the constants $\lambda$ and $G$. However, the actual evaluation of these constants requires the knowledge of the function $f(x)$ in the entire range [0:1] (and not just near $x = 0$, where $f(x) \sim x^{-\tau}$), which, in turn, is possible only if the detailed form of $\beta(x)$ is known. Hence we will restrict ourselves to showing that the parameter $\lambda > 0$, which is required for the solution to be physically reasonable.

In Eq. 2.16, we note that $B \geq \frac{G}{\lambda} e^{-\lambda}$, depending on how sharply $\beta(x)$ rises near $x = 1$. The equality holds for the step function $\beta(x) = \Theta(x - 1)$ where $\Theta(x) = 0$ for $x < 0$ and $\Theta(x) = 1$ for $x \geq 0$. After using this inequality in Eq.2.14, we find that $\lambda \geq -\log(2\theta)$. Since $\theta < 1/2$, it follows that $\lambda > 0$.

The formalism may be easily extended to the general $q$-state Potts model. From the general arguments about the competition between the Persistence scale $\mathcal{L}_p(t) \sim t^{\theta(q)}$ and the diffusive scale $\mathcal{L}_D(t) \sim t^{\frac{1}{2}}$, we may conclude that the above results will hold true for all $\theta(q) < \frac{1}{2}$. When $\theta(q) > \frac{1}{2}$, the mean separation between persistent sites grows faster than the correlation length for the random walkers. As a result, the disappearance of persistent sites may be expected to become uncorrelated at asymptotic times. This result is formally recovered from the rate equation, as we shall see below.

Since $\mathcal{L}_p(t)$ dominates over the diffusive scale, we may formally put $s(t) = 1/P(t) \sim t^{\theta(q)}$ so that the dynamical exponent $z = 1/\theta(q)$. Thus, the scaling solution for $n(k,t)$ has the form $n(k,t) \sim t^{-2\theta(q)} f(k/t^{\theta(q)})$, and the scaling variable is $\eta = k/t^{\theta(q)}$. The reaction probability $Q(k,t)$ may be expressed in terms of this new scaling variable as $Q(k,t) = \alpha(t)\beta(\eta t^{\theta(q)-\frac{1}{2}})$. As $t \to \infty$, the argument of the scaling

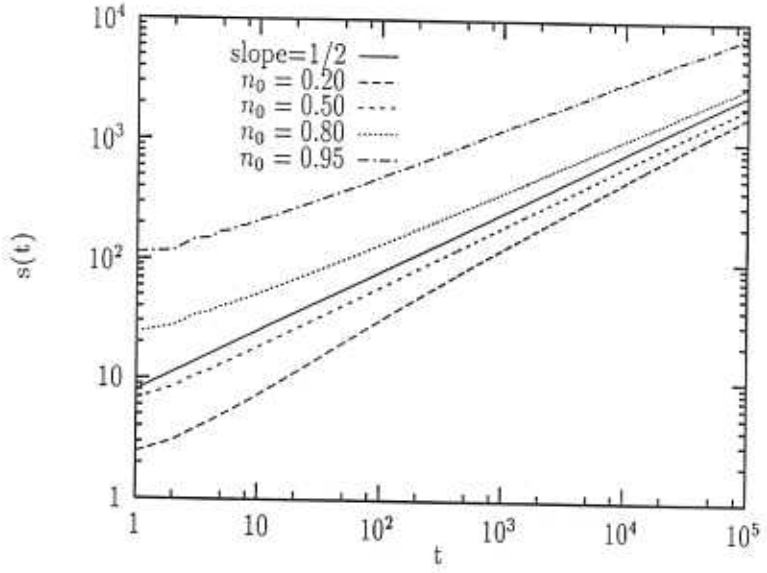


Figure 2.2: The length scale $s(t)$ is plotted as a function of time $t$. The straight line is a fit, with slope 1/2.

function is driven to $\infty$, so that for any value of $\eta$, $Q(m,t) \to \alpha(t)$ at asymptotic times. The equation for the scaling function $f(\eta)$ now becomes

$$\eta \frac{\partial f}{\partial \eta} = -\frac{1}{B}\int_0^{\frac{\eta}{2}} f(x)f(\eta - x)dx - \frac{1}{B}\int_0^{\frac{\eta}{2}} f(x)[f(\eta - x) - f(\eta)]dx - \left[\frac{1}{\theta} - 1 - \frac{1}{B}\int_{\frac{\eta}{2}}^{\infty} f(x)dx\right] f(\eta) \qquad (2.17)$$

We note that this equation is similar to Eq.2.13, and so the solution is exponential, $f(\eta) \sim e^{-\lambda'\eta}$, where $\lambda'$ is a constant. This scaling form is supported by simulations done by other authors[6].

### 2.2.3 Numerical Results

We determine the distribution $n(k,t)$ numerically by simulating $A+A \to \emptyset$ model on one dimensional lattice of size $N = 10^5$ with periodic boundary condition. Particles are initially distributed at random on the lattice with some average density $n_0$, and their positions are sequentially updated— each particle is made to move one step in either direction with probability $D = 1/2$. When two particles meet each other, both are removed from the lattice. The time evolution is observed up to $10^5$ Monte-Carlo steps (1 MC step is counted after all the particles in the lattice were touched

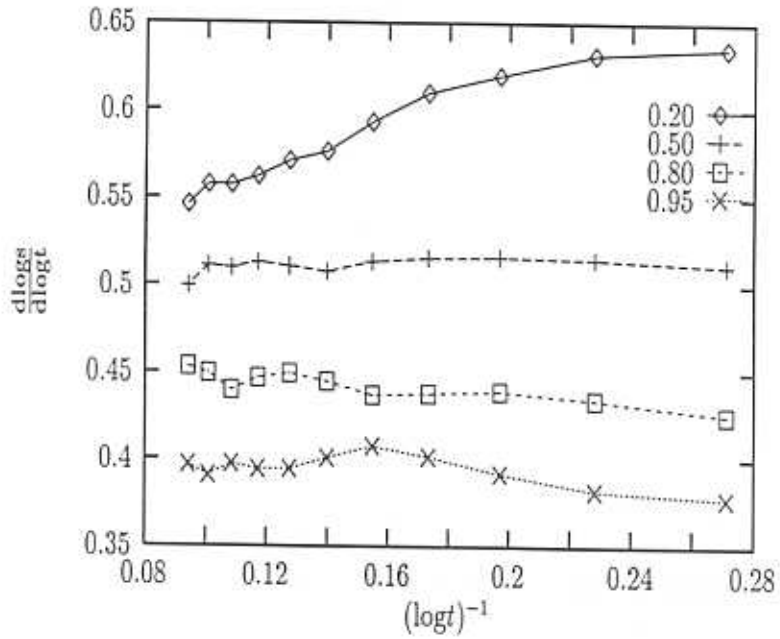


Figure 2.3: The effective exponent $\frac{d\log s}{d\log t}$ is plotted against $1/\log t$ for four values of starting density. For $n_0 = 0.5$, the exponent value is close to 0.5, expected from the scaling arguments. For other values of $n_0$, systematic deviations away from 0.5 is observed.

once). The simulation is repeated for several random starting configurations of the particles for any particular initial density and we repeat the entire simulation for four different initial density $n_0$. For any $n_0$, we determine the number of intervals of length $k$ (per site) at time $t$.

To compute the mean interval size $s(t)$, we ran the simulation up to $t = 10^5$ time steps, and averaged the results over 100 starting distributions of particles, with the same initial density. In Fig. 2.2, we plot $s(t)$ vs $t$ for four different values of $n_0$– 0.2, 0.5, 0.8 and 0.95. For $n_0 = 1/2$, we find that $s(t) \sim at^{1/z}$ with $z \simeq 1.97(1)$ and $a \simeq 5.96$. But for other values of $n_0$, we find that the observed value of $z$ is different from 2. In Fig. 2.3, the running exponent $d(\log s)/d(\log t)$ is plotted with $1/(\log t)$ and the results show the systematic deviation away from the value 1/2 expected from the scaling picture presented in the previous section. We will discuss about the possible origin of this deviation later.

In Fig. 2.4 we plot the scaling function $f(x) = s(t)^2 n(k,t)$ against the scaling variable $x = k/s(t)$ for $t = 10^4$ and $3.10^4$. To get the nature of the scaling function

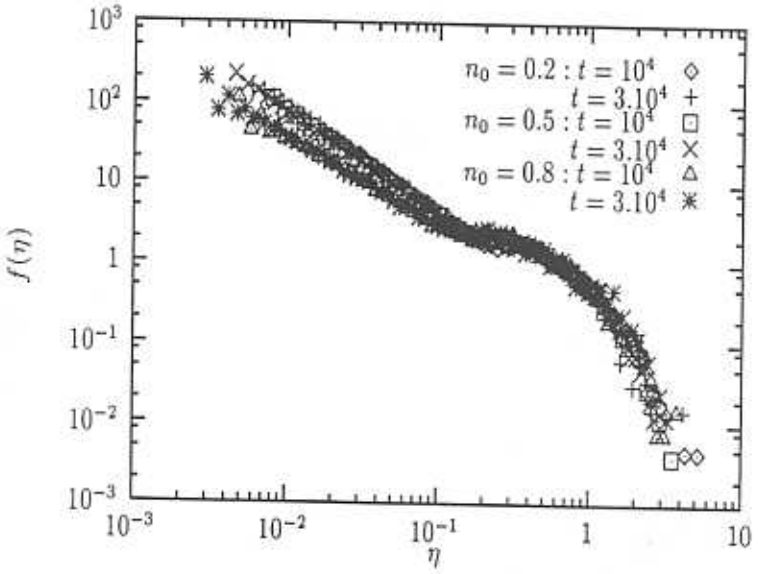


Figure 2.4: The scaling function $f(\eta) = s(t)^2 n(k,t)$ is plotted against the scaling variable $\eta = k/s(t)$ on a logarithmic scale. There is a power-law divergence at small $\eta$ and exponential decay at large $\eta$, as predicted by the IIA calculation. The observed value of $\tau$ for $n_0 = 0.8$ is seen to be appreciably different from that for other $n_0$.

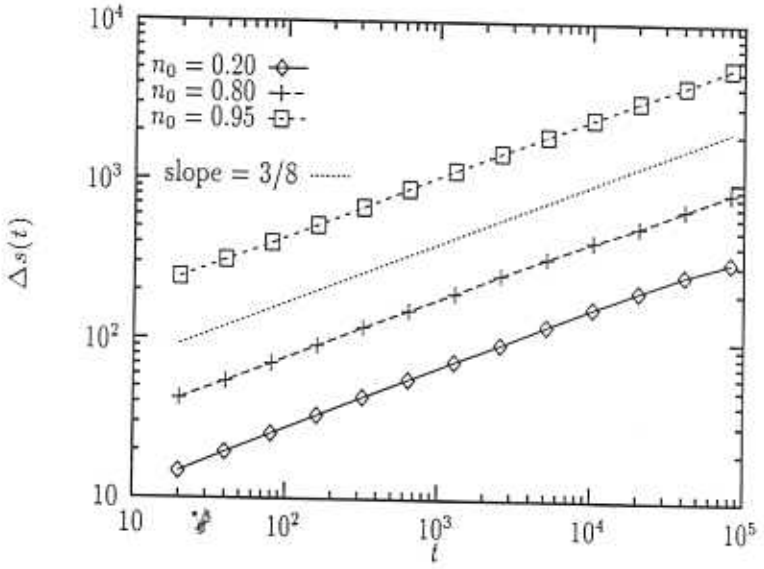


Figure 2.5: The difference $\Delta s(t) = |s(t) - s_{1/2}(t)|$ is plotted against $t$ for $n_0 = 0.2, 0.8$ and 0.95. The straight line is a fit with slope 3/8.

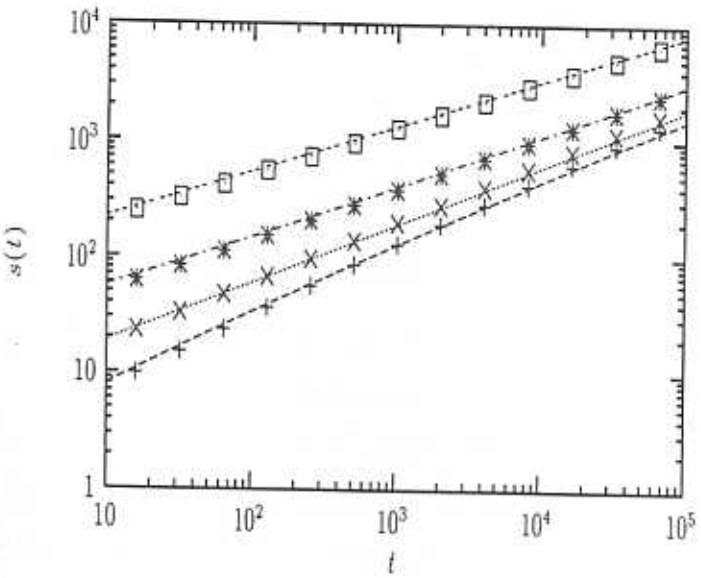


Figure 2.6: In the figure, we plot the observed $s(t)$ (points) with the proposed fitting form $at^{1/2} + bt^{\theta}$ (lines) for $n_0 = 0.2, 0.5, 0.8$ and 0.95 (bottom to top). We have used $a = 5.96$ and the $b$ values taken from Table I.

one needs to average over lots of configurations. This has restricted us to smaller time steps and data for three values of initial density, $n_0 = 0.2, 0.5$ and $0.8$ averaged over 500, 1000 and 1500 different initial distribution of particles respectively. For all $n_0$, we find that the scaling function $f(x) \sim x^{-\tau}$ for $x << 1$ and decays exponentially for higher values of $x$. For $n_0 = 0.5$, we find $\tau = 1.25(1)$ in accordance with the scaling relation Eq 2.11. For $n_0 = 0.2$, we find $\tau \simeq 1.32(2)$ while for $n_0 = 0.8$, the observed value of $\tau$ is 1.13(2). For all $n_0$, $\tau$ satisfies the scaling relation Eq. 2.11 if $z$ is replaced by its effective value.

For general values of $n_0$, we find that the numerical values of $s(t)$ supports the following form (within the time range studied)

$$s_{n_0}(t) \sim at^{1/z} + b(n_0)t^{\phi}. \tag{2.18}$$

The non-universal constant $b$ is $<, =$ or $> 0$ for $n_0 <, =$ or $> 0.5$. To compute the prefactor $b$ and the exponent $\phi$, we plot the difference $\Delta s_{n_0}(t) = |s_{n_0}(t) - s_{1/2}(t)|$ vs $t$, for $n_0 = 0.2, 0.8$ and $0.95$ (Fig. 2.5). The exponent $\phi$ is numerically found to be close to the persistence exponent $\theta = 0.375$ (Table 2.1). In Fig. 2.6, we show the simulation data together with the fitting form Eq.2.18 using the estimated numerical values of $a$ and $b$. We find that as $n_0 \to 1$, the constant $b$ undergoes a sharp rise so that the effective dynamical exponent of $s(t)$ is numerically close to $\theta$ for an appreciable range in time (Fig. 2.3). At the same time, we note that only the first term in Eq.2.18 is asymptotically relevant since $\phi < \frac{1}{2}$.

The two terms in Eq.2.18 can have their origin from the two dynamical length scales in the problem, the diffusive scale $\mathcal{L}_D(t) \sim t^{1/2}$ and the persistence scale $\mathcal{L}_p(t) \sim t^{\theta}$. For large $n_0$, the typical interval length between two consecutive persistent sites is determined by the decay of persistence only, rather than the diffusion of the particles. So, it is understandable that the dynamical behaviour of $s(t)$ coincides with that of $\mathcal{L}_p(t)$ at least at the initial times. However at late times, when the particle density falls down as a result of annihilation, the situation becomes same as that of starting with low $n_0$ and the decisive scale is $\mathcal{L}_D(t)$. However, the precise form and behaviour of the prefactor $b(n_0)$ with $n_0$ remains to be understood.

## 2.3 Two-point correlations

A good picture of the spatial distribution of the persistent sites and the presence of any possible correlation in their distribution is obtained from the two-point correlation $C(r,t)$, which is defined as the probability that site $\mathbf{x}+\mathbf{r}$ is persistent, given that site $\mathbf{x}$ is persistent (averaged over $\mathbf{x}$).

$$C(r,t) = \langle \rho(\mathbf{x},t) \rangle^{-1} \langle \rho(\mathbf{x},t)\rho(\mathbf{x}+\mathbf{r},t) \rangle \tag{2.19}$$

where the brackets denote average over the entire lattice and $\rho(\mathbf{x},t)$ is the density of persistent sites: ie., $\rho(\mathbf{x},t) = 1$ if site $\mathbf{x}$ is persistent at time $t$, and 0 otherwise. Clearly, $\langle \rho(\mathbf{x},t) \rangle = P(t)$ by definition.

Within the IIA, the relation between $C(r,t)$ and $n(r,t)$ (We consider $r \gg 1$, so that the discreteness of the underlying lattice can be ignored) can be written as the following infinite series:

$$\begin{aligned} C(r,t) = P(t)^{-1} n(r,t) + P(t)^{-2} \int_1^r dx\, n(x,t) n(r-x,t) + \\ P(t)^{-3} \int_1^r dx\, n(x,t) \int_1^{r-x} dy\, n(y,t) n(r-x-y,t) + .... \end{aligned} \tag{2.20}$$

The first term corresponds to the case where there is no other persistent site in the range $[0 : r]$, ie., a single Interval of length $r$. The second term gives the probability that the range is split into two Intervals of length $x$ and $r-x$ by the presence of a persistent site at $x$, the third term gives the probability for three Intervals and so on.

The above series can be rewritten as the following self-consistent equation for $C(r,t)$.

$$P(t) C(r,t) = n(r,t) + \int_1^r n(x,t) C(r-x,t) dx \tag{2.21}$$

In terms of the Laplace transforms $\tilde{C}(p,t) = \int_1^\infty C(r,t) e^{-pr} dr$ and $\tilde{n}(p,t) = \int_1^\infty n(s,t) e^{-ps} ds$ Eq. 2.21 becomes

$$\tilde{C}(p,t) = \frac{\tilde{n}(p,t)}{P(t) - \tilde{n}(p,t)} \tag{2.22}$$

From Eq.2.7, we find

$$\tilde{n}(p,t) = s^{-1}\tilde{f}(ps) \tag{2.23}$$

where $\tilde{f}(q) = \int_{s^{-1}}^{\infty} f(\eta)e^{-q\eta}d\eta$. which can be written in the following regularised form, using Eq.2.9.

$$\tilde{f}(q) = s(t)P(t) - f_1(q) \tag{2.24}$$

where

$$f_1(q) = \int_0^{\infty} f(\eta)[1 - e^{-q\eta}]d\eta. \tag{2.25}$$

Substituting Eq.2.23, 2.24 and Eq.2.25 into Eq.2.22 we find that

$$\tilde{C}(p,t) = \frac{s(t)P(t)}{f_1(ps)} - 1 \tag{2.26}$$

The second term in RHS can be neglected at late times, since $s(t)P(t)$ diverges as $t^{1/z-\theta}$. It follows that in this limit, $C(r,t)$ has the dynamic scaling form

$$C(r,t) = P(t)g\left(\frac{r}{s(t)}\right) \tag{2.27}$$

where

$$\tilde{g}(q) = \frac{1}{f_1(q)} \tag{2.28}$$

is the Laplace transform of $g(x)$: $\tilde{g}(q) = \int_0^{\infty} g(x)e^{-qx}dx$.

The preceding expressions can be used to deduce the limiting behaviour of the scaling function $g(\eta)$ for the cases $\eta \ll 1$ and $\eta \gg 1$, without needing to solve Eq.2.20 or 2.21 explicitly.

*Case* I: $\eta \gg 1$.

To find the asymptotic behaviour of $g(\eta)$, we note that $f_1(q)$ vanishes near $q = 0$ as $f_1(q) \sim q$. Thus $\tilde{g}(q) \sim \frac{1}{q}$ as $q \to 0$ from Eq.2.28. By standard results in the theory of Laplace transforms [7], this implies that $g(\eta) \sim 1$ as $\eta \to \infty$.

*Case* II: $\eta \ll 1$.

To analyse this case, consider the real-space relation Eq.2.20. For $\eta \ll 1$, or equivalently, $r \ll s$, we have shown that $n(r,t) \sim P(t)r^{-\tau}$. It is clear that in this range, the RHS of Eq.2.20 is time independent, so $C(r,t)$ in the LHS should also be time independent. From the dynamic scaling form Eq.2.27, we find that this is possible only if the scaling function is a power-law near the origin: $g(\eta) \sim \eta^{-\alpha}$ as $\eta \to 0$. After substituting in Eq.2.27 and requiring the resulting expression to be time independent, we find

$$\alpha = z\theta \tag{2.29}$$

We find $C(r,t) \sim r^{-\alpha}$ for $r \ll s$ and $C(r,t) \simeq P(t)$ for $r \gg s$. The power law decay at small distances is expected, because the RHS of Eq.2.20 contains only scale invariant terms in this limit, hence the LHS also should be likewise. In Appendix B, we show that this is also consistent with Eq.2.21.

We see that in the IIA calculation, the length scale $s(t)$ demarcates the correlated and uncorrelated regions for $C(r,t)$. In the correlated region ($r \ll s(t)$), the persistent sites form a fractal with fractal dimension $d_f = d - \alpha = \frac{1}{4}$, with the correlation length $s(t)$ increasing with time as $s \sim t^{1/2}$. The IIA results agree very well with that of numerical simulations [8], showing the validity of the approximation.

### 2.3.1 Numerical Results

In Fig. 2.7, the scaling function $f(x) = C(r,t)/P(t)$ is plotted against the scaled distance $x = r/t^{1/z}$ for two values of time separated by a decade. The initial density is $n_0 = 0.5$. Excellent data collapse is obtained for $z = 2$, and the measured value of the spatial exponent $\alpha \simeq 3/4$ is entirely in accordance with the scaling relation.

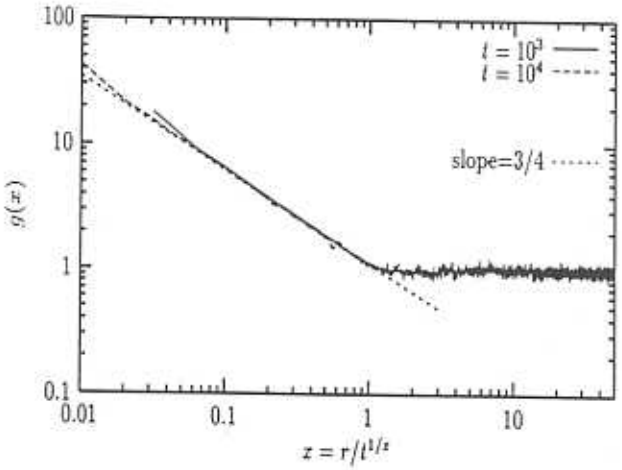


Figure 2.7: The scaling function for two-point correlation $f(x) = C(r,t)/P(t)$ plotted against the scaling variable $x = r/t^{1/z}$ on log-scale for two values of time $t = 10^3$ and $10^4$. The starting density of particles is $n_0 = 0.5$. The data for different times are seen to collapse into the same curve if scaling is done with $z = 2.0$. The observed $\alpha \simeq 0.75$ is in agreement with the proposed scaling relation (2).

The observed power-law decay of $C(r,t)$ with $r$ has a wider significance, apart from showing the strong spatial correlations in the distribution. It implies that, over length scales not too large, the underlying structure is a self-similar fractal. This is most easily seen with the 'box-counting' procedure [9]. We divide the entire lattice into boxes of size $l$, at time $t$. After discarding 'empty' boxes, ie., those which contain not even a single persistent site, let $M(l,t)$ be the average number of persistent sites in a box of length $l$. This quantity is related to $C(r,t)$ through $M(l,t) = \int_0^l C(r,t)dr$. Substituting the scaling form Eq. 2.27 for $C(r,t)$, one finds

$$M(l,t) \sim l^{1-\alpha} \quad l \ll s(t) \tag{2.30}$$

$$M(l,t) = lP(t) \quad l \gg s(t) \tag{2.31}$$

which can be summarised in the scaling form

$$M(l,t) = lP(t)h(l/s(t)) \tag{2.32}$$

with the scaling function $h(x) \sim x^{-\alpha}$ for $x \ll 1$ and $h(x) \simeq 1$ for $x \gg 1$. We see

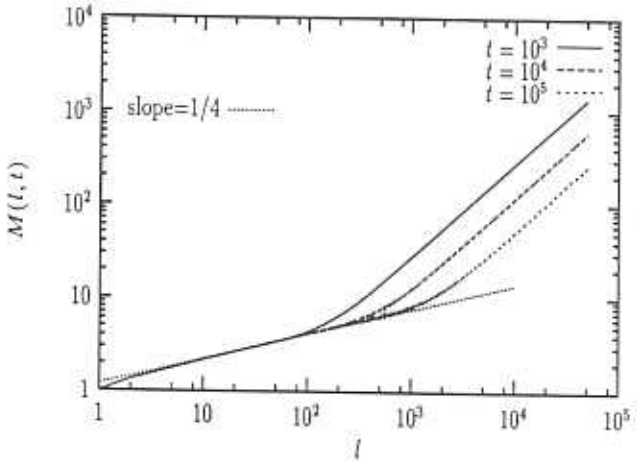


Figure 2.8: The average number of persistent sites $M(l,t)$ in a box of size $l$ at time $t$ is plotted against the box size $l$ for $t = 10^3, 10^4$ and $10^5$. The initial density of particles is $n_0 = 0.5$. The crossover from fractal (dimension $d_f \simeq 1/4$) to homogeneous ($d_f = d = 1$) distribution is clear from the figure.

that over small enough length-scales $l \ll s(t)$, the set of persistent sites form a self-similar fractal with fractal dimension $d_f = 1 - \alpha$, with a crossover to homogeneous behaviour at larger length scales. This crossover is illustrated in Fig.2.8, where we have $M(l,t)$ (measured from box-counting) plotted against the box size $l$ for three values of time. The initial density here is $n_0 = 0.5$, and we find $d_f \simeq 0.25$ in agreement with our result from study of the two-point correlation $C(r,t)$.

In Fig. 2.9, we compare the results from box-counting for different starting densities. For $n_0 = 0.2$, we see that the fractal region appears much later compared to higher values. This is presumably due to the large inter-particle separation at $t = 0$, and the consequent delay in reaching the scaling regime. For higher densities, the fractal dimension is seen to decrease continuously with $n_0$, approaching zero in the limit $n_0 \to 1$. We notice that although $s(t) \sim 10^3$ in terms of the lattice spacing, it is still much less than the lattice size $N$, so as to rule out finite-size effects.

In Fig. 2.10, we plot the scaling function $h(\eta) = M(l,t)/lP(t)$ against the scaling

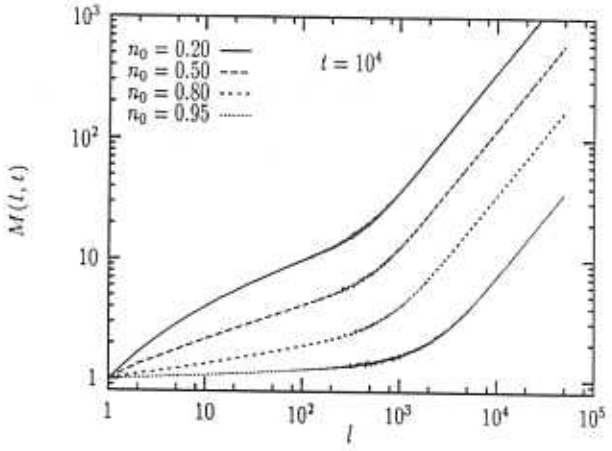


Figure 2.9: Same as Fig.2.8, for four starting densities $n_0 = 0.2, 0.5, 0.8$ and $0.95$. All plots correspond to $t = 10^4$. For $n_0 = 0.2$, the fractal region is reached late, but the asymptotic value is seen to be the same as that for $n_0 = 0.5$. For higher $n_0$, $d_f$ decreases continuously, approaching zero in the limit $n_0 \to 1$.

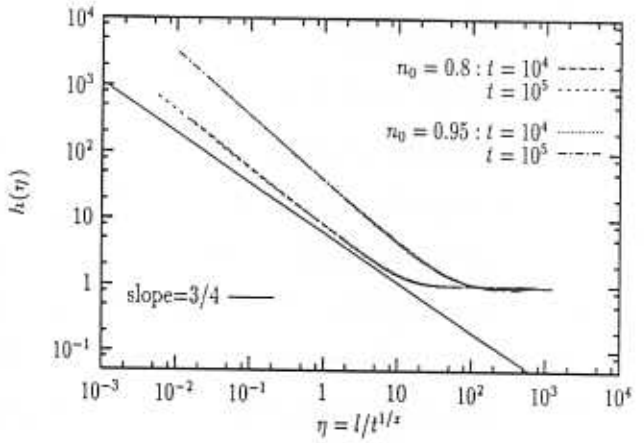


Figure 2.10: The scaling function for the mass-distribution $h(\eta) = M(l,t)/lP(t)$ plotted against the scaling variable $\eta = r/t^{1/z}$ for two values of time $t = 10^4, 10^5$ and two starting densities $n_0 = 0.8$ and $0.95$. The observed data collapse has been obtained with $1/z = 0.45 (n_0 = 0.8)$ and $1/z = 0.39 (n_0 = 0.95)$. The corresponding values for $\alpha$ are $\simeq 0.83$ and $0.95$. For comparison, a straight line with slope $0.75$ is also shown.

variable $\eta = l/t^z$ for two values of time separated by a decade. We have displayed results for $n_0 = 0.8$ and 0.95. For $n_0 = 0.8$ the best data collapse is obtained with $\frac{1}{z} \simeq 0.45$, whereas for $n_0 = 0.95$, the corresponding value is $\frac{1}{z} \simeq 0.39$. The exponent $\alpha$, measured from the small argument divergence of $h(\eta)$, also shows similar changes.

In Table 1.2, we have summarised our exponent values for four initial densities. All measurements were made using the data for the mass-distribution $M(l,t)$ rather than the correlator $C(r,t)$ on account of lesser statistical fluctuations. For the dynamical exponent $z$, we chose the value which gave the best collapse of data under dynamic scaling. Although it is difficult to measure the exponent very accurately using this method, we have verified by visual inspection that the error involved is less than the reported changes in the exponent values at least by a factor of two. We have omitted the case $n_0 = 0.2$ because no single value of $z$ was found to give good scaling behaviour in the time range studied.

Our numerical results are strongly suggestive of non-universal behaviour of exponents $\alpha$ and $z$. The non-universal exponent values have been observed to be valid over at least three decades of MC time (up to $10^5$ time steps). We note that there are *two length scales* at work here. For low $n_0$, the dynamics is dominated by diffusive motion of isolated particles, 'eating into' clusters of persistent sites. Due to annihilation, their average density decays as $n(t) = (8\pi Dt)^{-1/2}$ [10] and hence the average separation is the diffusive scale $\mathcal{L}_D(t) \sim t^{1/2}$. On the other hand, for $n_0 \to 1$, the initial separation of persistent sites $\sim 1/(1-n_0) \gg 1$. The short time behaviour is now dominated by persistent $\to$ non-persistent conversion of isolated sites, with characteristic length scale $\mathcal{L}_p(t) \sim t^{3/8}$. It is possible that the observed non-universal behaviour results from competition between these two scales. According to this picture, one should see a crossover to diffusion dominated regime at later times, but we are yet to see any signature of that. Further numerical work, at least a few orders of magnitude greater than what is reported here, would be required to establish conclusively the possibility of a temporal crossover.

| $n_0$ | $b$ | $\phi$ |
|---|---|---|
| 0.20 | $-6.621$ | 0.34372(11) |
| 0.50 | $\simeq 0$ | – |
| 0.80 | 15.701 | 0.35495(5) |
| 0.95 | 84.672 | 0.36572(4) |

Table 2.1: Results for the prefactor $b$ and exponent $\phi$ as measured from simulations. The numerical value of $\phi$ is found to be close to the persistence exponent $\theta$ whose exact value is 0.375. The figures in brackets represent statistical error in the last decimal place. Note the sharp rise in $b$ as $n_0 \to 1$.

## 2.4 Conclusion

Persistent sites are shown to have strong correlations in their spatial distribution. In one dimensional $A + A \to \emptyset$ reaction-diffusion system, we show that there is a length scale $s(t)$, diverging with time as $s(t) \sim t^{1/z}$, which demarcates the correlated region from the uncorrelated one. We argue that $z = 2$ at large $t$ . Persistent sites separated by distance $k \ll s(t)$ are highly unlikely to have a particle $A$ between them and so retains their persistent character. Only persistent sites separated by distance $\gg s(t)$ take part in the decay of persistence at subsequent times.

We find that if $k$ is the distance of separation between any two consecutive persistent sites, then for $k \ll s(t)$, the distribution of $k$ is scale-free and decays algebraically as $k^{-\tau}$ with $\tau = 2 - z\theta$. We show this using the IIA (Independent Interval Approximation), which assumes no correlation in the lengths of any two adjacent intervals. We have verified our results by numerical simulations which suggests the validity of the IIA. Under the IIA, our calculation for the two-point correlation shows that over length scales $r \ll s(t)$, the persistent site distribution over the lattice is a fractal with dimension $d_f = \tau - 1$. This prediction is verified using extensive numerical simulations. The interesting aspect of the present model is that the fractal dimension was found to be sensitive to the starting density of particles.

| $n_0$ | $\alpha$ | $1/z$ | $d_f = 1 - \alpha$ |
|---|---|---|---|
| 0.50 | 0.7342(8) | 0.50 | 0.27 |
| 0.80 | 0.8294(5) | 0.45 | 0.18 |
| 0.95 | 0.9517(3) | 0.39 | 0.05 |

Table 2.2: Observed values of exponent $\alpha$ as measured from box-counting method (details in text), for four values of initial density $n_0$. The quoted value of dynamical exponent $z$ is the one which gave the best data collapse over three decades of time, $t = 10^3, 10^4$ and $10^5$.

## 2.5 Appendix II A

The divergence in the first integral in Eq. 2.10 can be separated out as follows. We write $f(\eta - x) = f(\eta) + \Delta_x f(\eta)$ and $\beta(\eta - x) = \beta(\eta) + \Delta_x \beta(\eta)$. so that $\lim_{x\to 0} \Delta_x f(\eta) = \lim_{x\to 0} \Delta_x \beta(\eta) = 0$.

After substituting for $f(\eta - x)$ and $\beta(\eta - x)$, the divergent part of the integral separates into the following terms.

$$\int_{s(t)^{-1}}^{\frac{\eta}{2}} f(x)f(\eta - x)\beta(\eta - x)dx = f(\eta)\beta(\eta)\int_{s(t)^{-1}}^{\frac{\eta}{2}} f(x)dx + f(\eta)\int_0^{\frac{\eta}{2}} f(x)\Delta_x\beta(\eta)dx + \beta(\eta)\int_0^{\frac{\eta}{2}} f(x)\Delta_x f(\eta)dx + \int_0^{\frac{\eta}{2}} f(x)\Delta_x f(\eta)\Delta_x\beta(\eta)dx$$

The first term is divergent near the origin, while all other terms are finite by construction. Now we rewrite the first term using the equality $\int_{s(t)^{-1}}^{\infty} f(x)dx = s(t)P(t)$. After some simplifications, the integral becomes

$$\int_{s(t)^{-1}}^{\frac{\eta}{2}} f(x)f(\eta - x)\beta(\eta - x)dx = f(\eta)\beta(\eta)s(t)P(t) + \int_0^{\frac{\eta}{2}} f(x)f(\eta - x)\left[\beta(\eta - x) - \beta(\eta)\right]dx + \int_0^{\frac{\eta}{2}} f(x)\left[f(\eta - x) - f(\eta)\right] - \beta(\eta)f(\eta)\int_{\frac{\eta}{2}}^{\infty} f(x)dx$$

The first term is the divergent part of the integral, which exactly cancels the last term in Eq. 2.10, to give the regularised Eq. 2.12.

## 2.6 Appendix II B

For $r \gg 1$, it is reasonable to assume that the higher order terms in the RHS of Eq.2.20 will contribute more than the first term, ie., the range $[0 : r]$ is more likely to be covered with more than one Interval than a single one of length $r$. After using this approximation, and substituting $n(r,t) \simeq (\tau-1)P(t)r^{-\tau}$ in the continuum limit, Eq. 2.21 is simplified to

$$C(r,t) \simeq (\tau-1)\int_1^{r-1}(r-x)^{-\tau}C(x,t)dx$$

Our purpose is to see if the equation

$$r^{-\alpha} \simeq (\tau-1)\int_1^{r-1}x^{-\alpha}(r-x)^{-\tau}dx \tag{2.33}$$

is consistent for $\alpha = z\theta = 2-\tau$ (Eq.2.11) at $r \gg 1$.

The integral $I = \int_1^{r-1}x^{-\tau}(r-x)^{-\alpha}dx$ can be transformed by change of variables into the more standard form[11]

$$\int_0^{r-2}(1+y)^{-\tau}[r-1-y]^{-\alpha}dy \simeq \frac{r^{1-\alpha}}{1-\alpha}F(1,\tau;2-\alpha;-r) \quad for\ \alpha<1\ and\ r\gg 1.$$

where $F(a,b;c;z)$ is the Gauss Hyper-geometric function. For $b = c$, $F(a,b;b;z) = (1-z)^{-a}$ exactly, independent of $b$[12]. Thus, for $\alpha = 2-\tau$ we find

$$(\tau-1)I = r^{-\alpha}[1+o(\frac{1}{r})]$$

which is consistent with Eq. 2.33, at $r \gg 1$.

# Bibliography


[1] G. Manoj and P. Ray, J. Phys. A **33**, 5489 (2000).

[2] D. Toussaint and F. Wilczek, J. Chem. Phys. **78**, 2642 (1983); D. C. Torney and H. M. McConnell, J. Phys. Chem. **87**, 1941 (1983); A. A. Lushnikov, Phys. Lett. A **120**, 135 (1987); J. L. Spouge, Phys. Rev. Lett. **60**, 871 (1988).

[3] B. Derrida, C. Godrèche and Y. Yekutieli, Phys. Rev. A **44** 6241 (1991).

[4] P. A. Alemany, D. ben-Avraham, Phys. Lett. A **206**, 18 (1995).

[5] B. Derrida, V. Hakim and V. Pasquier, Phys. Rev. Lett. **75**, 751 (1995), and J. Stat. Phys. **85**, 763 (1996).

[6] A. J. Bray and S. J. O'Donoghue, Phys. Rev. E **62**, 3366 (2000).

[7] M. G. Smith, *Laplace Transform Theory*, D. Van Nostrand Company, London (1966).

[8] G. Manoj and P. Ray, J. Phys. A **33**, L109 (2000).

[9] A.-L. Barabasi and H. E. Stanley, *Fractal Concepts in Surface Growth* (Cambridge University Press, 1995); P. Meakin, *Fractals, scaling and growth far from equilibrium* (Cambridge University Press, 1998).

[10] A. A. Lushnikov, Phys. Lett. A **120**, 135 (1987); J. L. Spouge, Phys. Rev. Lett. **60**, 871 (1988).

[11] *Tables of Integral Transforms*, ed. A. Erdèlyi (McGraw Hill, 1954).

[12] *Handbook of Mathematical Functions*, ed. M. Abramovitz and I. A. Stegun (Dover, New York, 1968).

# Chapter 3

# Spatial correlations in Persistence : $d > 1$

## 3.1 Introduction

In the present chapter, we study the problem of spatial correlations associated with Persistence in various coarsening systems in higher spatial dimensions. As we had noted in the introductory chapter, the characteristic features of coarsening in spatial dimension $d > 1$ are very different from that in $d = 1$. For example, in $d = 1$ kinetic Ising model, domain walls are zero dimensional objects which diffuse and annihilate upon contact, while in $d > 1$, domain walls are spatially extended objects and their motion is curvature-driven.

In the last chapter, we had shown that in $d = 1$ Ising model, there is strong spatial correlation in the distribution of persistent sites. For length scales $\ll t^{\frac{1}{2}}$, the set of persistent sites was found to form a stationary structure, with power-law spatial correlations. The stationarity of the distribution was attributed to the annihilation process of the random walkers, which make them drift farther and farther away from each other, so that their average separation grows like $\sim t^{\frac{1}{2}}$. This is simply the domain growth process in $d = 1$, and it is natural to enquire whether the essential part of this argument could be carried forward to higher dimensions also. In the next section, we use finite size scaling arguments to obtain insights into

this problem.

## 3.2 Finite Size Scaling

Let us consider the Ising model in a $d$-dimensional geometry of linear size $L$. We start from an initial random configuration and quench the system, say, to the temperature $T = 0$. As a result, the spins evolve in time following the Glauber dynamics, lowering the total energy of the configuration in the process. In course of time, domains of positive and negative spins form, with characteristic length scale $\mathcal{L}(t)$ growing as a power-law in time ie., $\mathcal{L}(t) \sim t^{1/z}$, where $z$ is the dynamical exponent for the coarsening process[1]. The fraction of persistent spins decays as power of time : $P(t, L) \sim t^{-\theta}$ as long as $t \ll t^* \sim L^z$. Over time scales $t \sim t^*$, the domain growth is interrupted by the finite system size, and the system is expected to reach the symmetry-broken equilibrium state. For zero temperature dynamics, this implies that the persistence probability stops decaying beyond this point, attaining a limiting value $P(\infty, L) \sim L^{-z\theta}$. This happens as long as

$$\frac{z\theta}{d} < 1 \tag{3.1}$$

For $z\theta > d$, persistence probability will decay to zero for sufficiently large lattice size $L$. The above behaviour of the persistent fraction $P(t, L)$ for finite lattice sizes can be summarised in the following dynamical scaling form[2].

$$P(t, L) = L^{-z\theta} f(t/L^z) \tag{3.2}$$

where the scaling function $f(x) \sim x^{-\theta}$ for $x \ll 1$ and $f(x) \to$ constant at large $x$. Similar finite size scaling ideas have been used in a previous work in the context of global persistence exponent for nonequilibrium critical dynamics[3].

Recent Monte Carlo studies in kinetic Ising model[4] indicate that in $d = 2$, there is a finite probability for the system to end up in a metastable 'stripe' state (as opposed to a symmetry broken state), which is infinitely long-lived at $T = 0$.

At $T > 0$, however, the stripe state is unstable and the system undergoes a slow relaxation to the true equilibrium state over much larger time scales. Thus the proposed FSS form holds for $T = 0$ Glauber dynamics, but at $T > 0$ coarsening, non-trivial corrections are required. We will discuss this point in Section 3.3 of this chapter.

The FSS form for persistence is a very useful technique for the following reasons.

- The FSS form provides better estimates of the persistence exponent, especially in higher dimensions, where the system sizes are severely limited.
- The validity of the scaling form also guarantees the existence of scale-invariant spatial correlations in the distribution of persistent sites. This is especially useful in higher dimensions where direct computation of the pair correlation is tedious.

### 3.2.1 Pair correlation function from FSS

The finite-size scaling form given by Eq.3.2 implies the presence of scale-invariant spatial correlations in the system, characteristic of fractals. To show this, we consider the two-point correlation function $C(r,t)$, which we define as the probability of finding a persistent spin at a distance $r$ from another persistent spin. For a $d$-dimensional system, $C(r,t)$ satisfies the normalisation condition $\int_0^L C(r,t)d^dr = L^dP(t,L)$. After substituting Eq.3.2, this becomes

$$\int_0^L C(r,t)r^{d-1}dr \sim L^{d-z\theta}f(t/L^z) \tag{3.3}$$

Let us rewrite this equation in terms of a new function $F(a,b) = a^{z\theta}C(a,b)$ and dimensionless variables $x = r/L$ and $\tau = t/L^z$.

$$\int_0^1 F(Lx, L^z\tau)x^{d-1-z\theta}dx \sim f(\tau) \tag{3.4}$$

Since the RHS of the equation has no explicit $L$-dependence, LHS should also

be likewise. This is possible only if $F(a,b) = g(ba^{-z})$, where $g(\eta)$ is given by the integral relation

$$\tau^{\frac{d}{z}-\theta} \int_{\tau}^{\infty} \eta^{\theta-(1+\frac{d}{z})} g(\eta) d\eta \sim z f(\tau) \tag{3.5}$$

Using the above equation, the limiting behaviour of the function $g(\eta)$ for small and large values of the argument could be deduced from the known behaviour of the function $f(\tau)$. Consider $\tau \gg 1$, where $f(\tau)$ is constant. From Eq. 3.5, this implies that $g(\eta)$ is constant for large $\eta$. In the other extreme of $\tau \ll 1$, $f(\tau) \sim \tau^{-\theta}$. We split the integral in Eq. 3.5 as $\int_{\tau}^{\infty} = \int_{\tau}^{\alpha} + \int_{\alpha}^{\infty}$ and note that $g(\eta)$ is constant in the second integral for sufficiently large $\alpha$. The second integral vanishes as $\tau^{\frac{d}{z}-\theta}$ as $\tau \to 0$, whereas the RHS diverges as $\tau^{-\theta}$. This can be consistent only if the first integral diverges as $\tau^{-\theta}$, which would imply that $g(\eta) \sim \eta^{-\theta}$ as $\eta \to 0$. This leads to the following dynamical scaling form for $C(r,t)$.

$$C(r,t) = r^{-z\theta} g(\frac{t}{r^z}) \tag{3.6}$$

For small separations $r \ll t^{1/z}$, this scaling form implies scale-free correlations, ie., $C(r,t) \sim r^{-z\theta}$, characteristic of a fractal with fractal dimension $d_f = d - z\theta$. On the other hand, over larger length scales, $C(r,t) \sim t^{-\theta}$, which is indicative of the absence of any spatial correlations. This scaling description was introduced by us[5] in the context of $A + A \to \emptyset$ model, and later verified numerically in 2-dimensional Ising model[6] also.

### 3.2.2 Glauber-Ising model at $T = 0$

To check the finite-size scaling form given by Eq. 3.2, we simulate Ising spin systems of various sizes in spatial dimension $d = 1$ to 4. Starting from a random initial configuration, the spins are quenched to zero temperature and are updated sequentially using the Glauber updating rule by which a spin is always flipped if the resulting energy change $\Delta E < 0$, never flipped if $\Delta E > 0$, and flipped with probability $\frac{1}{2}$ if $\Delta E = 0$. One MC time step was counted after every spin in the lattice was updated

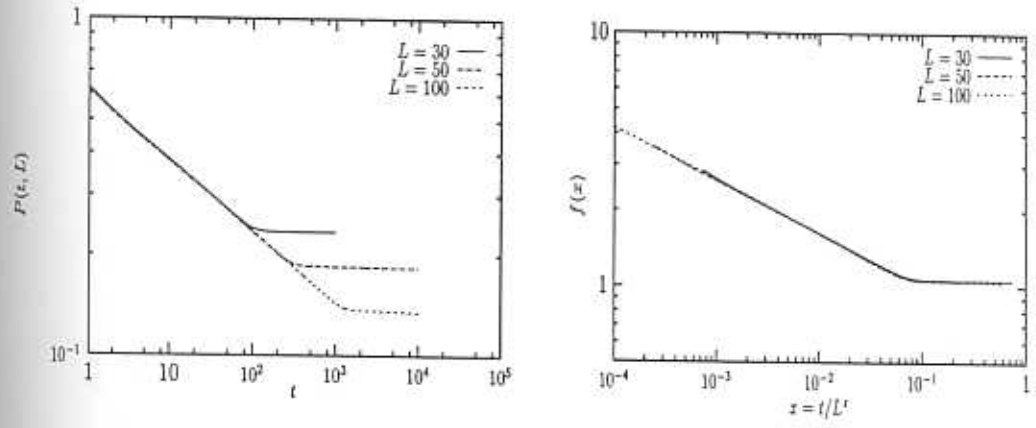


Figure 3.1: (A)The persistence probability $P(t, L)$ is plotted against time $t$ (measured in MC steps) for three different lattice sizes $L$ in $d = 2$ Glauber Ising model. (B) Same as Fig. 1, except that the scaling function $f(x) = L^{z\theta} P(t, L)$ is plotted against the dimensionless scaling variable $x = t/L^z$. The data for different $L$ values were found to collapse well to a single curve for $\theta = 0.21$ and $z = 2.12 \pm 0.05$.

once. The persistence probability at any time $t$ was determined as the fraction of spins that did not flip even once till time $t$ since the time evolution started. The data is averaged typically over 1000 starting random configurations for small $L$ and low $d$ and over 50 starting configurations for large $L$ and high $d$.

For $T = 0$ Glauber dynamics of Ising model, the persistence exponent $\theta$ is exactly known to be 3/8 in $d = 1$[7]. In higher dimensions, simulations predict $\theta \simeq 0.22(d = 2)$[8, 9, 10] and $\theta \simeq 0.16(d = 3)$ [8]. In our finite size scaling analysis of the simulation data, we adopt the following procedure. From the asymptotic fraction $P(t \to \infty, L) \sim L^{-z\theta}$, we estimate the exponent $\alpha = z\theta$. The scaling function is then computed as $f(x) = L^{\alpha} P(t, L)$, and is plotted against the scaling variable $x = t/L^z$ (Fig. 3.1 to 3.3). The value of the dynamical exponent $z$ is then adjusted for the best data collapse. The exponent $\theta$ could then be computed as $\theta = \frac{\alpha}{z}$. In Table 3.1, we have reported our results for the Glauber-Ising model in spatial dimension $d = 2$ to 4. In all cases, we find $z \simeq 2$, which is the accepted value of the coarsening exponent for non-conserved scalar models[1]. (In $d = 3$ Glauber dynamics, a slower $t^{1/3}$ coarsening has been observed before[11]. This is presumably due to lattice effects, but we have not seen any signature of this effect in our simulations). In $d = 4$, we find that $z \approx 2$, $\alpha \approx 0.24$ gives reasonably good data collapse over the time scales and system sizes studied. Fig. 3.3 shows the scaled data in $d = 4$. It may be mentioned that in $d = 4$, earlier simulations



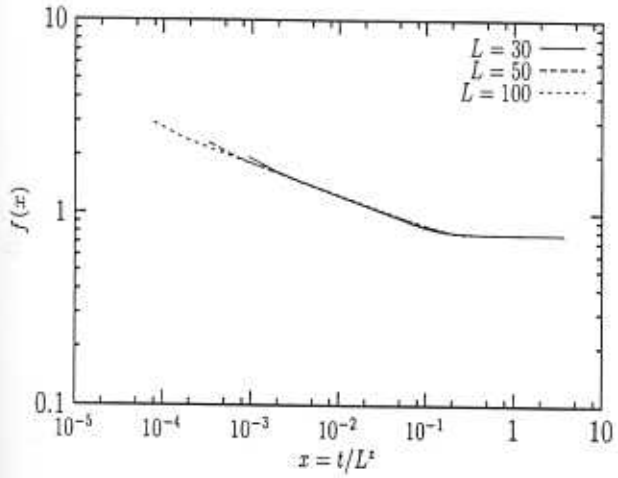


Figure 3.2: The scaling function $f(x) = L^{z\theta}P(t, L)$ is plotted against the dimensionless scaled time $x = t/L^z$ for three $L$-values in $d = 3$ Glauber Ising model. The observed data collapse has been obtained for $z = 2.05$ and $\theta = 0.166$.

| dimension | $\alpha$ | $z$ | $\theta = \frac{\alpha}{z}$ | $d_f = d - \alpha$ |
|---|---|---|---|---|
| $d = 2$ | 0.45 | 2.12 | 0.21 | 1.55 |
| $d = 3$ | 0.32 | 2.05 | 0.1561 | 2.68 |
| $d = 4$ | 0.24 | 2.0 | 0.12 | 3.76 |

Table 3.1: A table of results for the FSS analysis in kinetic Ising model at $T = 0$.

had suggested that the persistence decay might be slower than a power-law, and perhaps logarithmic[8]. However, the agreement of our data with the scaling form Eq.3.2 suggests that persistence follows a power-law decay in $d = 4$ also. For $d > 4$, blocking of spins has been shown to lead to a limiting value of $P(t, L)$ as $t \to \infty$, which is independent of $L$[8]. We could simulate only small lattice sizes for $d = 5$ from which we cannot make any conclusive remark at this stage.

### 3.2.3 The TDGL model

We now turn to a discussion on the continuum kinetic Ising model, which is described by the TDGL equation.

$$\frac{\partial\phi(\mathrm{x}, t)}{\partial t} = \nabla^2\phi - \phi + \phi^3 \;\; ; \;\; \langle\phi(\mathrm{x}, 0)\phi(\mathrm{x}', 0)\rangle = \delta^d(\mathrm{x} - \mathrm{x}') \qquad (3.7)$$

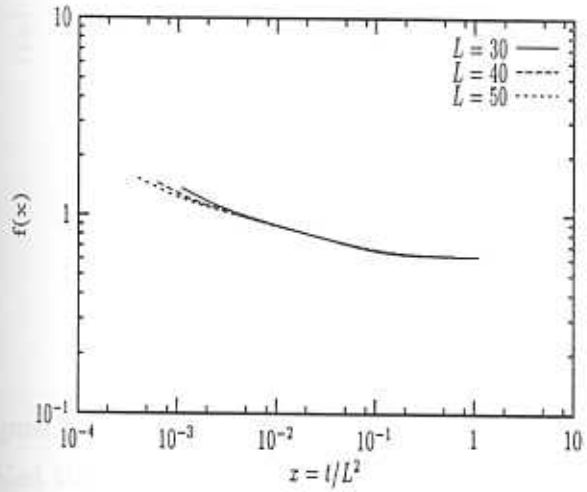


Figure 3.3: The figure shows the scaled probability plotted against the dimensionless scaled time in $d = 4$ Glauber Ising model. We have found that $z\theta \simeq 0.24$, and $z = 2$ gives the best collapse pf data, so that $\theta = 0.12 \pm 0.02$

To simulate Eq. 3.7 numerically, we use the finite difference Euler discretization scheme on cubic lattices of $L^d$ sites [13, 14].

$$\phi(\mathbf{x}, t + \Delta t) = \phi(\mathbf{x}, t) + a\left[\sum_{\mathbf{x}'} \phi(\mathbf{x}', t) - 2d\phi(\mathbf{x}, t)\right] + \Delta t[\phi(\mathbf{x}, t) - \phi^3(\mathbf{x}, t)] \quad (3.8)$$

where $a = \frac{\Delta t}{(\Delta x)^2}$. The TDGL model in $d = 1$ coarsens only logarithmically, and hence the FSS form does not hold in this case. We checked the FSS form numerically in spatial dimension $d = 2$ to 4. In $d = 2$, we find that the best scaling collapse is obtained for $z\theta = 0.375$ and $z = 1.94$ (Fig. 3.4), which gives $\theta = 0.19$, in agreement with previously known results[12]. In $d = 3$, we find $z\theta \approx 0.49$ and $z \approx 2.02$, which gives $\theta \approx 0.25$. This value is higher than the corresponding Ising model value at $T = 0$, perhaps because the lattice effects which impede domain growth in Glauber dynamics are absent here. This value also agrees with the high temperature value of $\theta$ in Ising model, as we shall see later in this chapter. Similarly, in $d = 4$, we observe $\theta \simeq 0.27$ (Fig. 3.5), again much higher than the corresponding Ising value at $T = 0$. A more detailed discussion of this point will be made in Section 3.3.

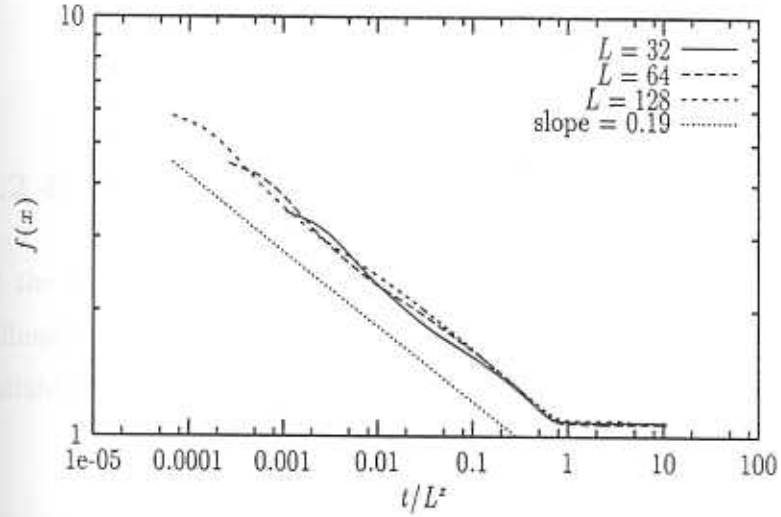


Figure 3.4: The figure shows the scaled probability plotted against the dimensionless scaled time in $d = 2$ TDGL model. The data collapse is obtained for $z\theta = 0.375$, $z = 1.94$ which gives $\theta \approx 0.19$.

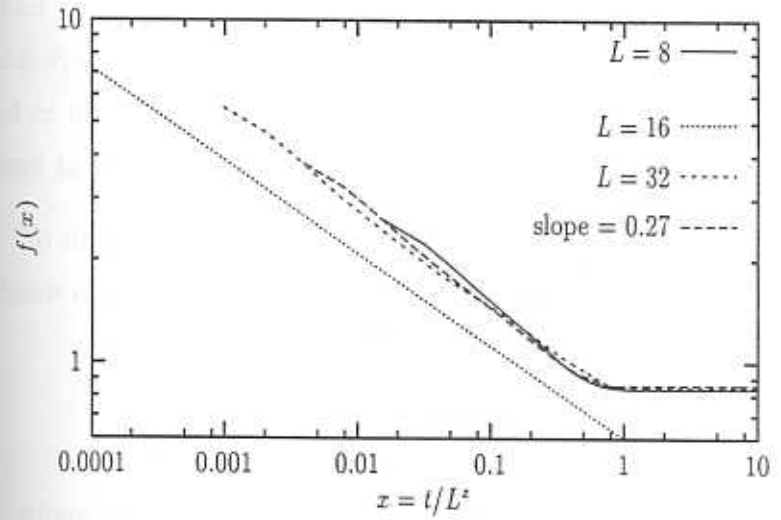


Figure 3.5: The figure shows the scaled probability plotted against the dimensionless scaled time in $d = 4$ TDGL model. The data collapse is obtained for $z\theta = 0.54$, $z = 2.0$ which gives $\theta \approx 0.27$.

| dimension | $\alpha$ | $z$ | $\theta = \frac{\alpha}{z}$ | $d_f = d - \alpha$ |
|---|---|---|---|---|
| $d = 2$ | 0.37 | 1.94 | 0.19 | 1.63 |
| $d = 3$ | 0.49 | 2.05 | 0.25 | 2.48 |
| $d = 4$ | 0.54 | 2.0 | 0.27 | 3.46 |

Table 3.2: A table of results for the FSS analysis in TDGL model.

### 3.2.4 The Diffusion Equation

In the diffusion problem, we have a scalar field $\phi(\mathbf{x},t)$ evolving according to the diffusion equation. The initial values $\phi(\mathbf{x},0)$ are taken to be independent random variables with zero mean.

$$\frac{\partial\phi(\mathbf{x},t)}{\partial t} = \nabla^2\phi(\mathbf{x},t) \;\; ; \;\; \langle\phi(\mathbf{x},0)\phi(\mathbf{x}',0)\rangle = \delta^d(\mathbf{x}-\mathbf{x}') \tag{3.9}$$

For this problem, it has been shown using approximate analytic theories[13, 14, 15]that $P(t) \sim t^{-\theta}$ in all dimensions. The predicted exponent values in low dimensions were in good agreement with simulation results. The exponent was found to increase with dimension, and has been suggested to have the asymptotic value $\theta(d) \simeq \alpha\sqrt{d}$ as $d \to \infty$. The constant $\alpha$ has been estimated to be $\simeq 0.14$[13, 14] and $\simeq 0.18$[15] by different authors. For $d = 1, 2$ and 3, the exponent values are found to be $\theta \simeq 0.12, 0.18$ and 0.23 respectively.

To simulate Eq. 3.9 numerically, we use the finite difference Euler discretization scheme on cubic lattices of $L^d$ sites [13, 14].

$$\phi(\mathbf{x},t+\Delta t) = \phi(\mathbf{x},t) + a\left[\sum_{\mathbf{x}'}\phi(\mathbf{x}',t) - 2d\phi(\mathbf{x},t)\right] \tag{3.10}$$

where $\mathbf{x}'$ runs over all the $2d$ nearest neighbour lattice sites of $\mathbf{x}$ in the cubic lattice and $a = \frac{\Delta t}{(\Delta x)^2} < \frac{1}{2d}$ for stability of the discretization scheme. We have taken $a = \frac{1}{4d}$ in our simulations as this value has been observed to provide the fastest approach to the asymptotic regime[13].

For the diffusion problem, simple scaling arguments suggest that the dynamical exponent $z = 2$ in all dimensions. In all dimensions studied, we found excellent scaling collapse with $z \simeq 2$ and the $\theta$ values quoted above. Upon substitution of the exponent values into Eq. 3.1, it can be easily seen that the condition for fractal formation is satisfied for $d = 1, 2$ and 3. For $d = 1$, this has already been confirmed by an earlier numerical study[16]. Our results for the persistence probability and the scaling function for three different lattice sizes in $d = 2$ is displayed in Fig.3.6.

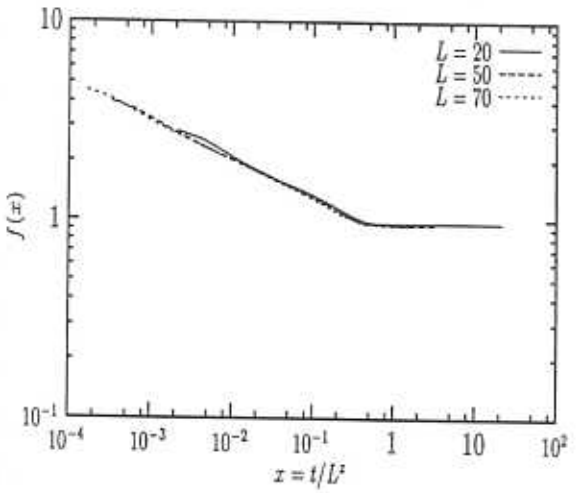


Figure 3.6: The scaling function $f(x) = L^{z\theta}P(t, L)$ for the 2D diffusion problem is plotted against the dimensionless scaling variable $x = t/L^z$. The data for different $L$ values were found to collapse well to a single curve for $\theta = 0.186$ and $z = 2.05 \pm 0.04$.

It is also possible to extrapolate these results to the $d \to \infty$ limit using the asymptotic form suggested for $\theta$. We see that in this limit, the LHS of Eq. 3.1 vanishes as $\frac{1}{\sqrt{d}}$, leading us to conjecture that fractal formation persists in all dimensions for the diffusion problem.

This result is also significant for the TDGL (and Ising) model. Consider the OJK approximation[17] to phase ordering where we define an auxiliary field $m(\mathbf{x}, t)$ through the nonlinear transformation $\phi = sgn(m)$. It was shown that in the limit $d \to \infty$, $m(\mathbf{x}, t)$ obeys the simple diffusion equation and thus, in this limit, Persistence properties of both the models are identical. We thus conclude that fractal formation in the Ising model is present in all spatial dimension $d$ ( at least at sufficiently high temperatures where lattice effects are overcome and the dynamics is adequately described by the continuum equation).

## 3.3 Spatial correlations at $T > 0$

For coarsening at non-zero temperatures, it is necessary to clearly distinguish between spin flips that contribute to the ordering process and spin flips that are purely

due to thermal fluctuations inside a domain. If one computes the fraction of persistent spins naively, the random thermal spin flips make $P(t)$ to decay faster than a power-law, almost exponentially.

Derrida suggested a scheme[18] that gets around this problem in a simple manner. His idea is to consider two identical systems, one at a disordered initial configuration (system A)and another at a completely ordered initial configuration (system B), both subject to the same realization of thermal noise. If a spin flips in A, and not in B, one concludes that the thermal noise is not strong enough to disturb spins inside a domain, and this flip is associated with the domain growth process. Such spin flips are counted when computing the persistent fraction. On the other hand, if a spin flips in both A and B simultaneously, one may safely conclude that it is due to thermal noise and need not be counted.

Derrida and later Stauffer[19], showed that with this modification, $P(t)$ decays as power-law in the entire subcritical range of temperatures in $d = 2$ Ising model. The exponent $\theta$ was also found to be independent of temperature, as long as $T < T_c$. This was also confirmed by block scaling studies done by Sire et.al. The situation is, however, different in three dimensions. In this case, the implementation of Derrida's scheme again leads to a power-law decay of $P(t)$ for $0 \leq T < T_c$. However, while $\theta$ at $T = 0$ is nearly 0.16, $\theta$ crosses over to a larger value, $\approx 0.26$ at higher temperatures. The latter value also agrees with the corresponding value in $d = 3$ TDGL model. Naively, these observations seem to suggest that the exponent $\theta$ varies with temperature and is non-universal. Similar discrepancy is also present in $d = 4$, where $\theta_{T=0} \simeq 0.12$ in the Ising model, while $\theta_{TDGL} \simeq 0.28$ in $d = 4$.

Majumdar and Sire[10] argued that the problem could be resolved and universality restored, if $P(t)$ is expressed in terms of the characteristic length scale of domains, $L(t)$. In general, $L(t) \sim t^{\frac{1}{z_D}}$ where we denote by $z_D$ the dynamical exponent associated with domain growth, and we expect $z_D = 2$ from Allen-Kahn arguments. However, it is known that for $T = 0$ dynamics of Ising model in $d = 3$, the dynamical exponent of domain growth is closer to 0.35 than 1/2[11], presumably due to lattice effects, which trap the system in certain configurations. We confirmed independently through simulations that this is indeed so, and also found that in

$d = 4$, the domain growth is even slower, with $L(t) \sim t^{0.21}$ (Fig. 3.7). Thus it is perhaps not surprising that the numerical value of $\theta$ in Ising model at $T = 0$ is lower than that for the corresponding continuum models, where such effects are absent. Also, the lattice effects might be overcome at sufficiently high temperature, so for large enough $T$, $\theta$ for Ising model approaches its continuum counterpart.

The argument of MS is that if we express $P(t) \sim L(t)^{-\overline{\theta}}$, then $\overline{\theta} \simeq 0.48$ in $d = 3$ and $\overline{\theta} \simeq 0.57$ in $d = 4$. Now, let us conjecture that $\overline{\theta}$ is universal, and is the same for discrete and continuum models. Since $L(t) \sim t^{\frac{1}{2}}$ for continuum TDGL model in $d \geq 2$, we find

$$\theta_{TDGL} = \theta_{T>0} = \frac{\theta_{T=0} z_D}{2} \tag{3.11}$$

Substitution of numerical values in the RHS give $\theta_{TDGL} \simeq 0.24$ in $d = 3$ and $\approx 0.28$ in $d = 4$ in reasonable agreement with independent numerical estimates.

Before concluding this section, we would like to remark that several questions remain unanswered in this problem. The argument about the universality of $\overline{\theta}$, as opposed to $\theta$ is supported by numerical data, but needs to be justified with physical arguments. Also, for Glauber dynamics in $d = 3$ and $d = 4$, the correlation length for distribution of persistent sites appears to have a different time dependence from the mean domain size. We have seen that while $\xi(t) \sim t^{\frac{1}{2}}$ in all dimensions studied, the exponent of $L(t)$ seems to be affected by the lattice severely in $d \geq 3$. Thus the persistence correlation length $\xi(t)$ seems to be a more robust length scale than the mean domain size.

We now present our numerical studies on pair correlation for persistent spins in Ising model at $T > 0$. As we had explained in a previous section, one cannot use the FSS analysis here on account of the occurence of slowly relaxing metastable states in $d \geq 2$. Hence, we did a direct computation of the two-point correlation, which restricted our system sizes to $L = 100$ in $d = 2$ and $L = 50$ in $d = 3$. This also restricted our studies to low temperatures ($T/T_c < 0.25$). At higher temperatures, $P(t)$ takes a long time to reach the power-law regime, and the interval between the onset of this regime and the saturation time ($\sim L^2$) was too small to make

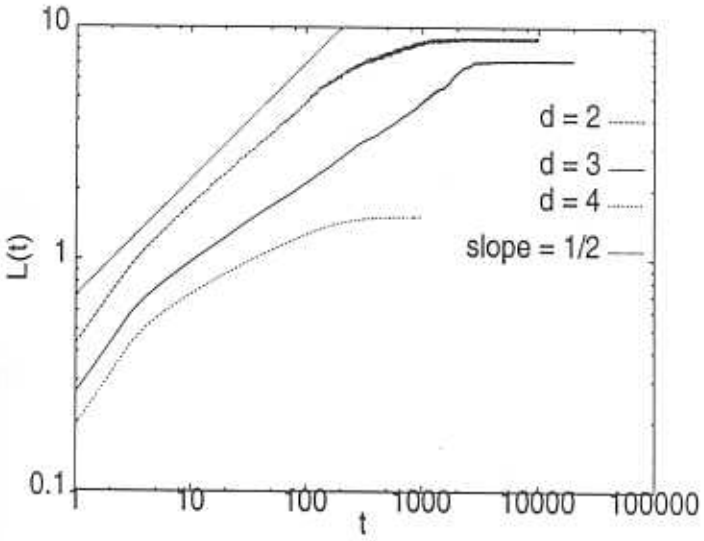


Figure 3.7: The figure shows the characteristic length scale $L(t)$ as a function of time $t$ for $T = 0$ Glauber dynamics in the Ising model in spatial dimension $d = 2$ to 4. We observe that except for $d = 2$, the slope is appreciably different from $1/2$. For $d = 3$, the slope is closer to 0.35 wheras for $d = 4$ it is only about 0.21. The system size is $L = 100$ for $d = 2$ and $d = 3$ and $L = 40$ for $d = 4$.

measurements of time dependent correlations.

Our principal results are outlined here. In the temperature and time ranges studied, we found that $C(r,t)$ satisfies the dynamical scaling form given by Eq. 3.6 For $r \ll t^{1/z}$, we observed power-law decay of correlations, which signifies the formation of stationary fractal structure over these length scales.

We started from a random initial configuration of spins with roughly equal number of + and − spins. The spins were evolved according to heat bath dynamics at fixed values of $T/T_c$. In order to measure Persistence probability under Derda's scheme, two replicas were also prepared, with all-up (replica A) and all-down (replica B)starting configurations. The original system and the replicas were then subject to the same realisation of thermal noise at all times. In simulation, we implemented this by using the same initial seed for updates in all systems. Further, all the systems were updated sequentially.

We measured the Persistence probability as follows. Let us denote the spins in the original system by $\sigma(\mathbf{x},t)$ and the replica spins as $\sigma_A(\mathbf{x},t)$ and $\sigma_B(\mathbf{x},t)$ respectively. All the + spins were initially synchronised with corresponding spins in replica A, and all − spins with corresponding spins in replica B. This means that a + spin

$\sigma(\mathrm{x},t)$ will be regarded as persistent upto time $t$, if the product

$$\Pi_{t'\leq t}\sigma(\mathrm{x},t')\sigma_A(\mathrm{x},t') > 0$$

For $-$ spins, the analogous condition is

$$\Pi_{t'\leq t}\sigma(\mathrm{x},t')\sigma_B(\mathrm{x},t') > 0$$

The Persistence probability is thus given by the expression

$$P(t) = L^{-d}\sum_{\mathrm{x}} \frac{1+\sigma(\mathrm{x},t)}{2}\Pi_{t'\leq t}\sigma(\mathrm{x},t')\sigma_A(\mathrm{x},t') + \frac{1-\sigma(\mathrm{x},t)}{2}\Pi_{t'\leq t}\sigma(\mathrm{x},t')\sigma_B(\mathrm{x},t') \tag{3.12}$$

To compute the pair correlation $C(r,t)$, we defined the persistence density index $n(\mathrm{x},t)$, such that $n(\mathrm{x},t) = 1$ if the spin at x is persistent at time $t$, and 0 otherwise. Then,

$$C(r,t) = [L^d P(t)]^{-1}\sum_{\mathrm{x},\Omega} n(\mathrm{x},t)n(\mathrm{x}+\mathrm{r},t) \tag{3.13}$$

where, $\Omega$ in the RHS represents angular averaging.

$d = 2$

In Fig. 3.8, we show the numerical results for $C(r,t)$ in $d = 2$ Ising model evolved using heat bath dynamics at a temperature $T = 0.25T_c$. We found that $C(r,t)$ is very well described by the dynamical scaling form

$$C(r,t) = t^{-\theta}h(r/t^{1/2}) \tag{3.14}$$

where $\theta \simeq 0.21$, which agrees with previous numerical estimates. For $r \ll t^{1/2}$, we find that $C(r,t) \sim r^{-2\theta}$, which is characteristic of fractal structure.

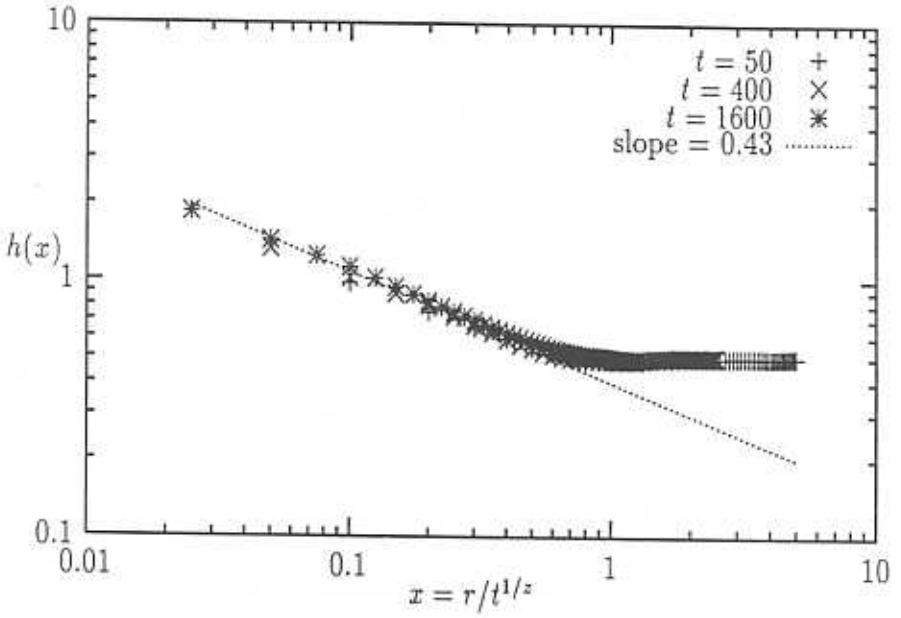


Figure 3.8: The figure shows the scaled two-point correlation function for persistent spins in $d = 2$ Ising model at $T/T_c = 0.25$. The scaling collapse was obtained for $z \simeq 2.0$.

$d = 3$

In Fig. 3.9, we show the numerical results for $C(r,t)$ in $d = 3$ Ising model evolved using heat bath dynamics at a temperature $T = 0.22T_c$. We found that $C(r,t)$ is very well described by the dynamical scaling form

$$C(r,t) = t^{-\theta} h(r/t^{1/z}) \tag{3.15}$$

where $\theta \simeq 0.18$ and $z \simeq 2.13$. The value of $\theta$ is slightly higher than previous estimates for zero temperature, but much lower than the continuum value $\approx 0.26$. It is possible that for small non-zero temperatures, $\theta$ exhibits a a slow crossover from 0.16 to 0.26.

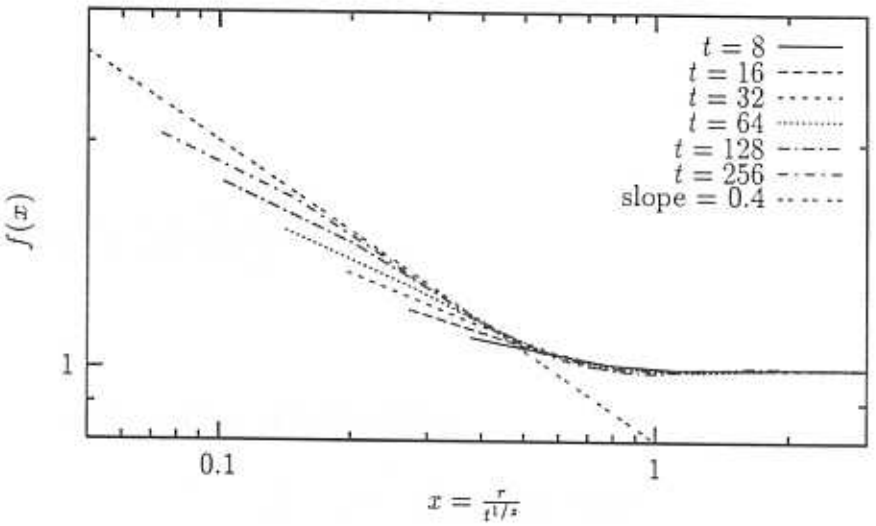


Figure 3.9: The figure shows the scaled two-point correlation function for persistent spins in $d = 3$ Ising model at $T/T_c = 0.22$. The scaling collapse was obtained for $z \simeq 2.13$.

## 3.4 Conclusion

In this chapter, we proposed a finite size scaling ansatz for the persistence probability in a coarsening system. The scaling form corresponds to the fractal structure and dynamic scaling characterising the spatio-temporal evolution of the persistent set. We checked the scaling form numerically for Glauber-Ising model, TDGL model and for the diffusion problem. Finite size scaling enabled us to study persistence reliably in higher dimensions. Our results agree with the known values of $\theta$ in the case of Ising model(from $d = 1$ to 3) and in the diffusion problem (we have checked upto $d = 3$). For $d = 4$ Ising model, we find the signature of algebraic decay of persistence with $\theta \simeq 0.12$, in contrast with what had been reported earlier[8]. We also verified by direct computation of pair correlation that the fractal formation is also present at non-zero temperatures, below the critical temperature.

# Bibliography


[1] A. J. Bray, Adv. Phys. **43**, 357 (1994).

[2] G. Manoj and P. Ray, Phys. Rev. E **62**, 7455 (2000).

[3] S. N. Majumdar, A. J. Bray, S. J. Cornell and C. Sire, Phys. Rev. Lett. **77**, 3704 (1996).

[4] V. Spirin, P. L. Krapivsky and S. Redner, Phys. Rev. E **63**, 036118 (2001).

[5] G. Manoj and P. Ray, J. Phys. A **33** L109; **33**, 5489 (2000).

[6] S. Jain and H. Flynn, preprint cond-mat/0004148.

[7] B. Derrida, V. Hakim and V. Pasquier, Phys. Rev. Lett. **75**, 751 (1995).

[8] D. Stauffer, J. Phys. A **27**, 5029 (1994).

[9] B. Derrida, A. J. Bray and C. Godrèche, J. Phys. A **27**, L357 (1994).

[10] S. N. Majumdar and C. Sire, Phys. Rev. Lett. **77**, 1420 (1996).

[11] J. D. Shore, M. Holzer and J. P. Sethna, Phys. Rev. B **46**, 11376 (1992).

[12] S. Cuielle and C. Sire, J. Phys. A **30**, L791 (1997); Eur. Phys. J. B **7**, 111 (1999).

[13] S. N. Majumdar, C. Sire, A. J. Bray and S. J. Cornell, Phys. Rev. Lett. **77**, 2867 (1996).

[14] B. Derrida, V. Hakim and R. Zeitak, Phys. Rev. Lett. **77**, 2871 (1996).

[15] T. J. Newman and Z. Toroczkai, Phys. Rev. E **58**, 2685 (1998).

[16] D. H. Zanette, Phys. Rev. E **55**, 2462 (1997).

[17] T. Ohta, D. Jasnow and K. Kawasaki, Phys. Rev. Lett. **49**, 1223 (1982).

[18] B. Derrida, Phys. Rev. E **55**, 3705 (1997).

[19] D. Stauffer, Int. J. Mod. Phys. C **8**, 361 (1997).

# Chapter 4

# Phase separation in fluctuating Interfaces

## 4.1 Introduction

The problem that we address in this chapter is somewhat different from that in the previous chapters, where we had investigated the spatial structure of the persistent region in various coarsening systems. In this chapter, on the other hand, we study fluctuating interfaces, which are not coarsening systems in a conventional sense. However, fluctuating interfaces do exhibit power-law decay of Persistence probability, as we had briefly discussed in the introductory chapter. In coarsening systems, we have seen that Persistence decay is intimately connected to the underlying domain growth, and the interplay of these effects causes strong correlations to develop in the spatial distribution of persistent regions. Our idea is to explore this connection further and see whether an interface with power-law persistence may be viewed as a coarsening system, evolving towards a phase separated steady state.

It is useful to recall some basic phenomenology associated with surface growth to obtain an insight to the problem. Let us consider a surface described by a single valued height function $h(\mathbf{r}, t)$, whose time evolution over large length and time scales is described an equation of the form Eq. 1.7. In general, the unequal time height correlation of the surface assumes the scaling form[1] $\langle [h(\mathbf{0}, t) - h(\mathbf{r}, t + T)]^2 \rangle =$

$r^{2\chi} f\left(\frac{T}{r^z}\right)$ where $f(x) \sim x^{2\beta}$ for $x \ll 1$ and $f(x) \to$ constant for $x \gg 1$. The exponent $\beta$ is related to $\chi$ and $z$ as $z\beta = \chi$. The dynamical exponent $z$ and roughness exponent $\chi$ depends on the mechanism of growth and relaxation of the surface and the correlations in the noise term. In a finite system of linear dimension $L$, the steady state is reached over a time scale $\tau \sim L^z$. In this state, the correlation becomes time-independent and the surface is self-affine over all length scales.

Is it possible to view such an interface, evolving towards its self-affine steady state, as a coarsening system ? To answer this question, let us now characterise the height fluctuations of the surface in terms of a coarse-grained Ising-like variable $s(\mathbf{r})$ defined as follows: At a given instant in time, all points on the surface where the height is below a certain reference level $h_0$ is assigned a spin $s = -1$, and the others are assigned $s = +1$.

$$s(\mathbf{r}) = sgn\left[h(\mathbf{r}) - h_0\right] \tag{4.1}$$

These spins will be referred to as *Coarse-grained Depth* (CD) spins henceforth, and the description of an interface in terms of these spins shall be called a CD model. Since the RMS width of the surface is $w \sim L^{\chi}$, it makes sense to consider only reference levels $h_0 \sim \langle h \rangle(t, L) + aL^{\chi}$ where $\langle h \rangle(t)$ is the instantaneous mean height and $a \simeq O(1)$. In the present work, we shall only deal with the case $a = 0$. The effects of changing the reference level are currently under investigation, and will be reported elsewhere.

Before we start our detailed study, we try to give a very simple picture of the coarsening properties of an interface. When an interface starts growing from a 'flat'(uncorrelated) initial condition, in course of time, self-affine height correlations appear over length scales $\mathcal{L}_h(t) \sim t^{1/z}$. The self-affine scaling of height fluctuations leads to the occurrence of *valleys* on the surface, which are simply connected clusters of positive spins. In course of time, a valley will be overturned to become a *hill*, which is a connected cluster of $-$ spins. The survival time scale of a valley $\tau \sim \xi^z$ where $\xi$ is the average linear extension of the valley. Thus, the longest valley that is overturned at time $t$ has typical size $\sim t^{1/z}$, and this defines the characteristic

length scale for coarsening in the problem. Therefore the interface 'coarsens', and in the steady state, the correlation length of height fluctuations $\mathcal{L}_h(t)$ approaches the system size $L$. In this state, the interface 'phase separates', and the size of the largest valley is of the order of the system size.

In this chapter, we focus mostly on steady state properties (of interfaces), unlike earlier chapters where we were almost exclusively concerned with time-dependent phenomena. This choice is motivated by the possibility of making analytical predictions, which could be done most directly in the steady state on account to the self-affine scaling of height fluctuations over all length scales. However, most of the results that we derive here could be easily extended to the coarsening regime also by the standard method of replacing the finite-size cut-off with the dynamical correlation length.

In this chapter, we will be mostly concerned with (2+1) dimensional interfaces. The problem of 'domain growth' in (1+1)-dimensional surfaces was studied earlier by Kim, Bray and Moore[2] and more recently by Das, Barma and Majumdar[4]. In general, it was shown that the equal time pair correlation for spins satisfies dynamical scaling, $\langle s(\mathbf{x},t)s(\mathbf{x}+\mathbf{r},t)\rangle = f(r/t^{1/z})$ where $z$ is the dynamical exponent for interface fluctuations. The dynamical scaling form is characteristic of a coarsening system, evolving towards a phase separated state, and is consistent with the general arguments in the preceding paragraph. However, unlike the conventional coarsening systems discussed in Chapter 1, the mean domain length scales differently from the correlation length, which resulted in a cusp in the correlation function (as opposed to linear decay in conventional systems) and the consequent breakdown of Porod Law (see Sec. 1.2.2). This feature is a direct consequence of the power-law distribution of domain sizes, which was shown to be closely related to the self-affine scaling of height fluctuations. Further, the order parameter in the phase separated steady state was found to experience strong fluctuations, with a finite variance in the thermodynamic limit. This is again unlike typical Equilibrium systems, where the variance in the order parameter vanishes in the thermodynamic limit.

It is natural to ask whether similar 'fluctuation dominated' phase separated state exists in higher dimensions also. In the present paper we show that 2+1 dimensional

rough surfaces indeed show features very similar to what was found in 1+1 dimensions. In particular, the power-law decay of the cluster size distribution, the cusp in the pair-correlation and the finite width of the order parameter distribution in the thermodynamic limit are, in general, present in two dimensions also. However, there are also additional features, for example, the cluster size distribution, in addition to the power-law part, may also have a distinct infinite cluster (Sec. 4.3), which might even be 'dominant' compared to the power-law sector.

The rest of this chapter is arranged as follows. In the next section, we present an overview of the basic phenomenology of the steady state of rough interfaces. This section forms the theoretical background of most of the material discussed in this paper. We consider the steady state of a rough interface, characterised by a certain roughness exponent $\chi$. For Gaussian surfaces, we show exactly that the pair correlation of CD spins shows finite size scaling, which is indicative of phase segregation of $+$ and $-$ spins. For non-Gaussian surfaces like the KPZ surface, this result is again shown to be true within an approximation. We further argue that the largest spin cluster in the system has typically $\sim L^2$ spins. These results are supported by extensive numerical simulations, which we present in Section 4.3, where we introduce the specific models we study here and the numerical procedure followed. We show that the study of two-point correlations and size distribution of particle clusters provide unambiguous evidence for phase separation of CD spins in rough surfaces. In order to characterize the ordered state, we define an appropriate order parameter and study its probability distribution. We find that similar to (1+1)-dimensional surfaces, the probability distribution appears to remain broad in the thermodynamic limit (Section 4.4). We argue that this feature arises from large fluctuations in the size of the extremal spin clusters. In Section 4.5, we conclude the chapter with a summary of our results.

## 4.2 Phase separation in (2+1) dimensional interfaces in steady state

### 4.2.1 Long Valleys in a Rough Surface

We start our analysis by considering a 2 dimensional surface in steady state, intersected by an imaginary horizontal plane at height $h_0$ as discussed in the introduction of this chapter. In order to assign a domain structure to the surface, we define Ising-like spin variables on the surface, relative to this reference height. Following the convention in DB, we shall call the new spin variables *Coarse-grained Depth* (CD) spins. The intersection of a rough surface with a horizontal plane forms a set of non-intersecting contour lines on the surface (Fig. 4.1). It can be shown from scaling arguments that for a self-affine rough surface, these contour lines have a fractal distribution on the surface, with fractal dimension $D = 2 - \chi$[7, 8] (Also see Appendix 4A for a detailed analysis). In spin language, these contours are identified as the interfaces between clusters of $s = +1$ and $s = -1$. The area enclosed by a contour is called an 'island', which typically contains one spin domain and several smaller islands. The perimeter of any single island is itself a fractal, and scales with the enclosed area $\mathcal{A}$ as $\mathcal{P} \sim \mathcal{A}^{\frac{D_c}{2}}$[6] where the fractal dimension $D_c \leq D$. The size distribution of 'islands' formed by contours can be shown to follow a scale invariant distribution[8, 9]:

$$N(m) \sim \Gamma_L m^{-\tau^*} \tag{4.2}$$

where

$$\tau^* = 2 - \frac{\chi}{2} \tag{4.3}$$

and $m$ is the area of the island and $\Gamma_L$ is the total number of islands. To find $\Gamma_L$, we use the normalisation condition for the perimeter lengths of all islands :

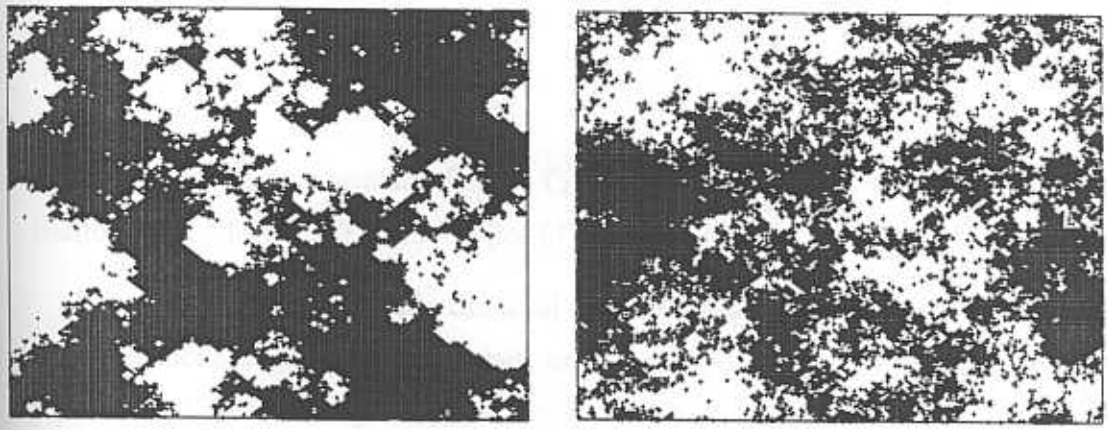

( A ) ( B )

Figure 4.1: Typical CD spin configurations for KPZ surface (A) and EW surface (B) in the steady state. The white part represent regions where $h \leq \langle h \rangle$ and the dark part regions are where $h > \langle h \rangle$.

$$\int_a^{bL^2} N(m) m^{D_c/2} dm \sim \mathcal{M}(L) \tag{4.4}$$

where $\mathcal{M}(L)$ is the total perimeter of all islands (the total contour length) discussed in Appendix A. The upper limit is taken to be proportional to the total area, since the island sizes are limited only by the finite system size. Clearly, if $D_c < D$, the integral converges to a constant, and we have $\Gamma_L \sim \mathcal{M}(L)$. On the other hand, if $D_c = D$, the integral diverges logarithmically and $\Gamma_L \sim \mathcal{M}(L)/\log L$.

Kondev *et.al* has recently suggested that $D_c = (3 - \chi)/2$[10]. If true, this result would mean that $D_c < D$ for all $0 \leq \chi < 1$ and $D_c = D$ for $\chi = 1$. Using these results, we find $\Gamma_L \sim L^{2-\chi}$ for $0 < \chi < 1$. In the marginal case of logarithmic roughness ($\chi = 0$), $\Gamma_L \sim L^2[\log L]^{-\frac{1}{2}}$ whereas for $\chi = 1$, the logarithmic factors cancel out and we find $\Gamma_L \sim L$.

We now proceed to find the typical area of the largest island in the system. For this purpose, we use an approximate argument concerning the statistics of extremal values in a given power-law distribution. It can be shown using extremal statistics arguments that in an ensemble of $N$ variables $X_1 ... X_N$ randomly drawn from a power-law probability distribution $p(X) \sim X^{-(1+\alpha)}$, the typical value of the maximum of $X$ scales as $X_{max} \sim N^{1/\alpha}$ (see Appendix B for details). If we make

the approximate replacement of $N$ by $\Gamma_L$, we find that the typical size of the largest island is $\sim L^2$ for $\chi > 0$ and $\sim L^2[\log L]^{-\frac{1}{2}}$ for $\chi = 0$.

It is also of interest to study the total area covered by *all* the islands in the system, which we denote by $\mathcal{A}'$. Since islands are typically found inside larger islands, it is clear that $\mathcal{A}'$ is bound by the following inequality.

$$\mathcal{A}' < \mathcal{A} = \int_a^{bL^2} N(m) m dm \tag{4.5}$$

For $\chi > 0$, it is straightforward to show that $\mathcal{A} \sim L^2$. Thus the total area covered by all islands is at most a finite fraction of the system size. Since the overall island distribution is self-similar, it is reasonable to assume that this property is true for each individual island also, ie., the total area covered by smaller islands is a finite fraction of the total island area (This assertion, however, needs to be proven rigorously). Since each island typically consists of one lake (which is a connected cluster of CD spins) and several small islands, it follows that the lake also occupies a finite fraction of the total area of the island. Since the area of the largest island is $\sim L^2$, this implies the presence of at least one domain with size $\sim L^2$, a characteristic of phase separation.

For $\chi = 0$, logarithmic corrections to the power-law in Eq.4.2 have to be taken into account, and the calculation gives $\mathcal{A} \sim L^2 \log L$. This result is identical to an exact result for the corresponding quantity in critical 2D Ising model[11] and the extra logarithmic factor is indicative of the dense distribution of contour loops in this case. From the general arguments presented above, we conclude that the size of the largest CD spin domain scales as $\sim L^2$, with possible logarithmic corrections.

Having established the existence of an infinite cluster, and thus the existence of phase separation in CD spin model using scaling arguments, we now proceed to the study of two-point functions. For Gaussian rough surfaces, we compute exactly the two-point spin correlations in the steady state. For general non-Gaussian surfaces, there is no analogous result, but we use an approximation that is expected to hold good at least in the vicinity of $\chi = \frac{1}{2}$. Both the approaches predict finite size scaling of the two-point correlation function, another characteristic of phase ordered state.

### 4.2.2 Steady State Correlations in CD models

The two-point spin correlator for CD spins is defined as follows:

$$\mathcal{C}(\mathbf{r}, L) \equiv \langle s(\mathbf{x})s(\mathbf{x}+\mathbf{r})\rangle \tag{4.6}$$

where the average is taken over an ensemble of steady state configurations. The remaining part of this section is devoted to the evaluation of $\mathcal{C}(r, L)$ analytically for different surfaces, characterised by the roughness exponent $\chi$. In the first subsection, we show that for a Gaussian rough surface with $0 < \chi < 1$ in 2+1 dimensions, $\mathcal{C}(\mathbf{r}, L) = \Phi(\frac{r}{L})$ and $1 - \Phi(x) \sim x^{\chi}+$ higher order terms. In Appendix 4C, we show that this result is valid also for 1+1 dimensional surfaces, in agreement with [4]. It is tempting to conjecture that this result might in fact be super-universal for Gaussian surfaces. However, we have not been able to compute $\mathcal{C}(r, L)$ for general $d$ dimensions, except for the special (marginal) values $\chi = 0$ and 1. In these cases, we find logarithmic corrections to the above results.

#### Gaussian rough surfaces

We consider a Gaussian rough surface in the steady state with probability distribution

$$\mathcal{P}[h] \sim exp\left(-\sum_{\mathbf{q}} q^{2(1+\chi)} h_{\mathbf{q}} h_{-\mathbf{q}}\right) \tag{4.7}$$

where $\chi$ is the roughness exponent for the surface and $h_{\mathbf{q}} = L^{-1}\int d^2\mathbf{x} h(\mathbf{x}) e^{-i\mathbf{q}.\mathbf{x}}$. For finite lattices, $h(\mathbf{r})$ is defined relative to the instantaneous mean value $\langle h\rangle = L^{-2}\int h(\mathbf{x}) d^2\mathbf{x}$.

Consider the two-point height correlator $\mathcal{G}(\mathbf{r}, L) \equiv \langle h(\mathbf{x})h(\mathbf{x}+\mathbf{r})\rangle$ and its Fourier Transform $\Xi(\mathbf{k}, L) = \langle h_{\mathbf{k}} h_{-\mathbf{k}}\rangle$. For the Gaussian probability distribution Eq. 4.7, it is clear that

$$\Xi(\mathbf{k}, L) \sim k^{-2(1+\chi)} \tag{4.8}$$

so that

$$\mathcal{G}(r,L) \sim \int_{\frac{2\pi}{L}}^{\frac{\pi r}{a}} dk k^{-(1+2\chi)} J_0(kr) \tag{4.9}$$

where $J_0(x)$ is the zeroth order Bessel function and $a$ is a microscopic sut-off length scale. For $\chi > 0$, there is a continuum limit and the constant $a$ can be effectively put to zero for large enough $L$. (See Appendix 4C for a discussion on this point). We consider this case first. After making this simplification, we express Eq.4.9 in terms of the scaled variable $\xi = 2\pi r/L$.

$$\mathcal{G}(r,L) \sim L^{2\chi}\left[\frac{1}{2\chi} - \xi^{2\chi} I(\xi)\right] \tag{4.10}$$

where

$$I(\xi) = \int_{\xi}^{\infty} dx[1 - J_0(x)]x^{-(1+2\chi)} \tag{4.11}$$

After expanding $I(\xi)$ in powers of $\xi$ near $\xi = 0$[18] and substituting, we find that

$$\mathcal{G}(r,L) = \frac{L^{2\chi}}{2\chi}\left(1 - \Delta\xi^{2\chi} + .....\right) \tag{4.12}$$

where

$$\Delta = \frac{2^{-2\chi}\Gamma(1-\chi)}{\chi\Gamma(\chi)}.$$

For Gaussian surfaces, $\mathcal{G}(r,L)$ and $\mathcal{C}(r,L)$ are related through the equation[19] (also, Appendix 4D)

$$\mathcal{C}(r,L) = \frac{2}{\pi} arcsin\left[\frac{\mathcal{G}(r,L)}{\mathcal{G}(0,L)}\right] \tag{4.13}$$

After substituting for $\mathcal{G}(r)$ and expanding $\arcsin(1-x) = \frac{\pi}{2} - \sqrt{2x}(1 + ....)$ near $x = 0$[20], we find

$$\mathcal{C}(r,L) = 1 - \Delta'\xi^{\chi} + ..... \tag{4.14}$$

where $\Delta' = \frac{2\sqrt{2}}{\pi}\Delta$ . After doing the Fourier transform, we find the Structure Factor:

$$S(k, L) \sim k^{-(2+\chi)} \tag{4.15}$$

If $\chi = 0$, there is no continuum limit and we need a non-zero length scale $a$. After proceeding with the calculation, the final result is

$$C(r, L) \simeq 1 - \frac{2\sqrt{2}}{\pi}\sqrt{\frac{ln(\chi r/a)}{ln(L/2a)}} + ... \tag{4.16}$$

for $\xi \ll 1$, where $\chi = \frac{\pi}{2}e^{\gamma}$ and $\gamma = 0.5772..$ is Eulers constant. Eq.4.16 is valid for all dimensions. The details of the calculation may be found in Appendix C.

### The Independent Interval Approximation

Due to the isotropy of the problem, the two-point correlator $C(r, L)$ is expected to depend only on the magnitude of **r** and not on its direction. So the computation of $C(r, L)$ is essentially a one-dimensional problem, one need to compute the two-point spin correlation only along an arbitrary linear cut on the surface. The vertical cross-section of the surface along such a linear cut is effectively a 1+1 dimensional surface, with the same roughness exponent as the original 2+1 dimensional surface.

It can be shown from scaling arguments that the separations between consecutive zero crossings (ie., its intersections with any reference level, like the mean height $\langle h \rangle$) of this 1+1 dimensional surface follow a power-law distribution. Let $Q_L(l)$ be the average number of consecutive zero crossings separated by a distance $l$, along an arbitrary linear cut along the surface. Since the average number of zero-crossings along a linear cut scales as $L^{1-\chi}$, we have the equation

$$\int_a^L dl Q_L(l) \sim L^{1-\chi} \tag{4.17}$$

together with the normalisation $\int_a^L dl Q_L(l) l = L$. To solve, we use the scaling ansatz $Q_L(l) = L^{-1} f(l/L)$ where $\int_0^1 dx f(x) x = 1$ from normalisation. Upon

substitution into Eq. 4.17, we find $\int_{a/L}^{1} dx f(x) \sim L^{1-\chi}$. This condition implies a small-argument divergence of the scaling function: $f(x) \sim x^{-(2-\chi)}$ near $x = 0$. Thus $Q_L(l) \sim L^{1-\chi} l^{-(2-\chi)}$ for $l \ll L$. Let $P(l)$ be the probability that two consecutive zero-crossings are separated by a distance $l$ along the linear cut, then

$$P(l) = \frac{Q_L(l)}{\int Q_L(l)} \sim l^{-\theta} \tag{4.18}$$

with $\theta = 2 - \chi$. In the spin language, this is the size distribution of domains of $+$ and $-$ CD spins along any linear cut on the surface.

A particularly interesting case is when the roughness exponent $\chi = \frac{1}{2}$, so that any vertical cross-section of the surface has the statistics of a one dimensional Brownian random walk, which is a Markovian process. For a random walk in one dimension, the intervals between successive zero crossings are independent random variables. In this case, it can be shown that $C(r, L) = 1 - a(\frac{r}{L})^{2-\theta}$ for $r \ll L$[4]. After substituting for $\theta$, we find

$$C(r, L) \simeq 1 - a(\frac{r}{L})^{\chi} + .... \tag{4.19}$$

where $a$ is a constant of order unity. In Fourier space, this implies that $S(k, L) \sim k^{-(2+\chi)}$ in 2 dimensions.

For general $\chi \neq \frac{1}{2}$, the analog of random walk is a fractional Brownian motion(fBm)[7, 12]. Unlike the Random walk, an fBm is non-Markovian, ie., past and future increments are correlated. In this case, it is not *a priori* clear whether successive zero crossings can be treated as independent random variables. However, near $\chi = \frac{1}{2}$ one may use Eq.4.19 as an approximation. (The Independent Interval Approximation, or IIA, which is exact for random walk). For example, the KPZ surface in 2+1 dimensions is rough with $\chi \simeq 0.4$, not very far from the Brownian value $\frac{1}{2}$. In this case, we find that the IIA prediction is in very good agreement with results form simulations.

## 4.3 Numerical Simulations

In this section, we present our numerical results on phase separation in SP and CD problems for two different models of surface fluctuations: the Edwards–Wilkinson model[13] and Kardar-Parisi-Zhang [14] model, whose evolution equations are respectively

$$\frac{\partial h}{\partial t} = \nu \nabla^2 h + \eta(\mathbf{r}, t) \tag{4.20}$$

$$\frac{\partial h}{\partial t} = \nu \nabla^2 h - \lambda (\nabla h)^2 + \eta(\mathbf{r}, t) \tag{4.21}$$

We briefly summarize some of the properties of the models. The EW surface describes symmetric surface fluctuations while the KPZ surface grows in one of the perpendicular directions, and hence breaks the $h \rightarrow -h$ symmetry. The height fluctuations in EW surface has a steady state probability distribution that remains Gaussian in all dimensions, whereas for KPZ surface this holds only in $d = 1$. It is fairly well-established that the KPZ surface is rough in (2+1) dimensions, and the mean square width of the surface $w^2(L) = \langle h^2 \rangle - \langle h \rangle^2 \sim L^{2\chi}$ where $\chi \approx 0.4$ from simulations. For the linear EW surface, $d = 2$ is the upper critical dimension, and $w^2(L) \sim \log(L/a)$[21].

### 4.3.1 The single-step algorithm

We simulated a single-step SOS model of the surface on a square lattice of $L^2$ sites[6]. The initial configuration was constructed as follows. Let the ordered pair $(k, m)$ represent the points on the lattice, with $k, m = 1, 2, ..L$. Then $h(k, m) = 1$ if $k + m$ is odd and zero if even. Thus it is ensured that all 'columns' of height 1 have four nearest neighbours with height 0 and vice-versa.

The dynamics of growth of the surface is as follows. In each move, one site of the lattice is selected at random. The height of the column is increased by 2 with probability $p_+$ if all four nearest neighbours are at greater height, and decreased by 2 with probability $p_-$ if all four nearest neighbours are at lower height. If either of

these conditions is not satisfied, the column is undisturbed. The former corresponds to deposition of particles on the surface followed by adsorption, whereas the latter corresponds to desorption and evaporation of particles from the surface.

The dynamics ensures that the height difference between any two nearest neighbour columns stays at $\pm 1$. One Monte Carlo time step is counted after $L^2$ such moves, so that every site in the lattice is counted once, on an average, in each step. If $p_+ = p_-$, the surface has no net growth in either direction (in the limit $L \to \infty$), and the large distance-long time properties of the model are identical to those of 2-dimensional Edwards-Wilkinson equation[13]. On the other hand if $p_+ > p_-$ (or vice-versa), the surface grows in $z$-direction, and the asymptotic properties fall in the KPZ universality class[14] with $\lambda \propto (p_+ - p_-)$[1]. The noise $\eta$ has zero mean and short range correlations in space and time. In our simulations we have chosen $p_- = 0$ and $p_+ = 1$ for KPZ dynamics, ie., we have simulated a KPZ surface growing *against* gravity. For EW dynamics, we fixed $p_+ = p_- = \frac{1}{2}$.

### 4.3.2 The steady state measurements

We studied both the time evolution of the system as well as the steady state. For the surface, the steady state regime is identified by studying the time evolution of its mean-square width $w(L,t) = \sqrt{\langle h^2(\mathbf{r},t)\rangle - \langle h(\mathbf{r},t)\rangle^2}$. For a self-affine rough surface, it is known that $w(L,t) \sim t^\beta$ for $t \ll L^z$ and $w(L,t) \sim L^\chi$ at large times. Here $z$ is the dynamic exponent, $\chi$ is the roughness exponent and $z\beta = \chi$. This behaviour is summarised in the following scaling form[1].

$$w(L,t) = L^\chi f(t/L^z) \tag{4.22}$$

where $f(x) \sim x^\beta$ for $x \ll 1$ and $f(x) \to$ constant for $x \gg 1$.

We measured the exponents $z$ and $\chi$ for KPZ surface independently by computing $w(L,t)$ numerically for three system sizes, $L = 32, 64$ and $128$. The data was fitted into the scaling form Eq.4.22, and the exponents giving the best data collapse were selected. We found that the best values were $\chi \simeq 0.37$ and $z \simeq 1.65$, which are

reasonably close to the accepted values, $\approx 0.4$ and 1.6[15, 10]. From the data the width of the surface was found to saturate by a time of about $\tau \simeq 10L^z$. Accordingly, in our simulations, we fixed the equilibration time $\tau_{eq}$ for the surface configurations to be $\sim 10\tau$. These time scales were found to be sufficient for reaching steady state. For a given starting configuration the steady state measurements were made at equally spaced points in time, with an interval of about $0.1\tau_{eq}$.

For the EW surface, the dynamical exponent $z = 2$ in all dimensions from simple scaling. Since 2 is the upper critical dimension, the width $w(L,t) \sim \sqrt{logL}$ in the long time limit $t \gg L^2$ and $w(L,t) \sim \sqrt{logt}$ for $t \ll L^2$[1].

### 4.3.3 Two-point correlations

We start our study of coarsening in Sliding Particle model with two-point spin correlations in the coarsening regime ($t \ll L^z$).

$$C(\mathbf{r},t) \equiv \langle \sigma(\mathbf{x},t)\sigma(\mathbf{x}+\mathbf{r},t) \rangle \tag{4.23}$$

where the average is taken over all lattice points $\mathbf{x}$ and over all starting configurations. Also, on account of the isotropy in space, the set of all vectors $\mathbf{r}$ differing only in direction give identical results. The direction averaged two point correlation function $C(r,t)$ is well represented by the dynamical scaling form (Fig.4.2) in the scaling limit ($r \gg 1, t \gg 1$).

$$C(r,t) = f\left(\frac{r}{t^{1/z}}\right) \tag{4.24}$$

This scaling form is characteristic of systems undergoing domain coarsening, where $\mathcal{L}(t) \sim t^{1/z}$ is the dynamic correlation length[3]. The data collapses best with $z \approx 1.6$ for KPZ surface and $z \simeq 2.0$ for EW surface. This is in accordance with our arguments in the introductory section.

For $t \gg L^z$, we observe finite-size scaling in the correlations.

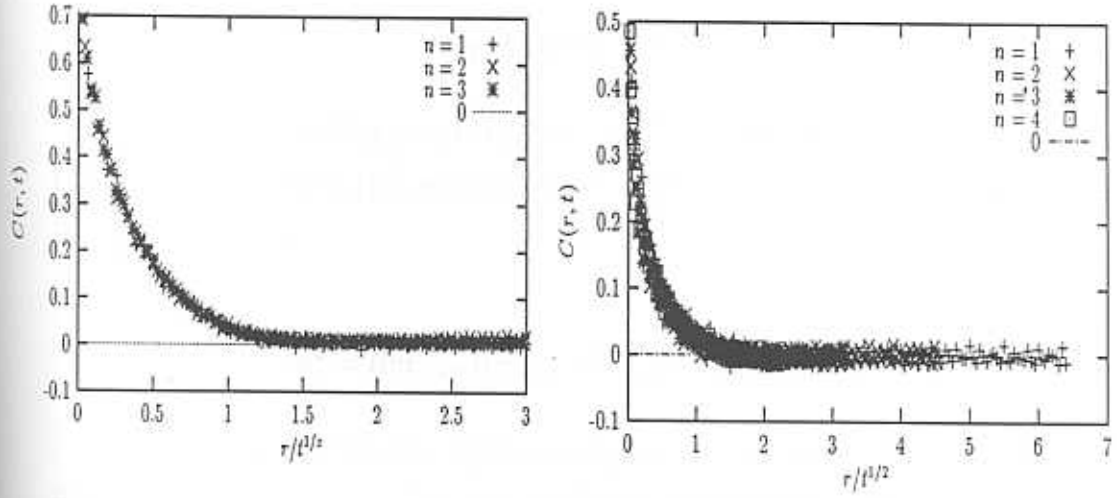


( A ) ( B )

Figure 4.2: The figures show the two-point spin correlation as a function of the scaled variable $r/t^{1/z}$ for a (A) KPZ surface and (B) EW surface in a lattice of linear size $L = 256$. The data represents an average over 100 different realisations of the noise distribution in time. The data collapse was obtained for $z = 1.6$ in KPZ surface and $z = 2$ in EW surface. The time scales of measurements are $t = 200 \times 2^n$, $n = 1, 2, 3.....$

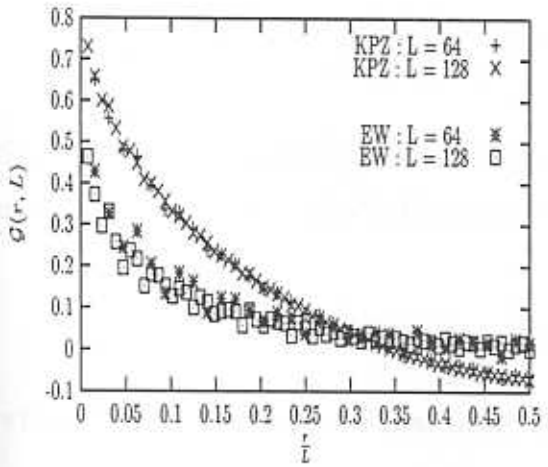


Figure 4.3: $C(r, L)$ for CD spins is plotted against the scaled variable $r/L$ for KPZ (top, steep) and EW (bottom, flat) surfaces. The cuspy behaviour of the correlations is evident from the plots.

$$C(\mathbf{r}, L) = f\left(\frac{r}{L}\right) \quad ; \quad r \gg 1 \tag{4.25}$$

The finite-size scaling points to the ordered nature of the steady state. Analogous to equilibrium systems[16], we define the steady state spontaneous magnetisation $m_c$ in the CD model.

$$m_c^2 = lim_{r\to\infty} lim_{L\to\infty} C(r, L) = lim_{x\to 0} f(x) = c_0 \tag{4.26}$$

In Fig.4.2 and Fig.4.3, upon extrapolation to the origin, it is seen that $\lim_{x\to 0} f(x) = c_0 < 1$. The measured values (see Sec. III B)give $c_0 \simeq 0.8$ for KPZ surface and $c_0 \simeq 0.5$ for EW surface. This feature shows that the ordered phase is not very homogeneous, but contains droplets of the other species also. This is similar to the equilibrium state of $d = 2$ Ising model, at temperatures $0 < T < T_c$.

The dynamic and finite-size scaling forms Eq.4.24 and Eq.4.25 describe the behaviour of the correlations in the regime $r \gg \xi, t \gg t_0$, where the microscopic length and time scales $\xi$ and $t_0$ define the scaling limit. In general, there is a short-range analytic part in $C(r, L)$.

$$C(\mathbf{r}, L) = g\left(\frac{r}{\xi}\right) + f\left(\frac{r}{L}\right) \tag{4.27}$$

Since $C(0, L) = 1$ trivially, the short range function may be approximated by a $\delta$-function: $g(r/\xi) \approx (1 - c_0)\delta^2(\mathbf{r})$ in the limit $\frac{\xi}{L} \to 0$, so that

$$C(r, L) \approx [1 - c_0]\delta^2(\mathbf{r}) + f\left(\frac{r}{L}\right) \tag{4.28}$$

where $\delta^2(\mathbf{r})$ is the 2-dimensional Dirac delta function on the lattice.

We observe that both $C(r, t)$ and $C(r, L)$ are nonlinear for the entire range of the relevant scaling variable. This is quite unlike conventional phase ordering systems where $C(\mathbf{r}, t) \simeq 1 - r/\mathcal{L}(t)$ for $r \ll \mathcal{L}(t)$, ie., the fall of the correlation with distance is linear over small $r$[3](see chapter 1). The latter result, more correctly, its Fourier transformed version is well-known as the Porod Law[17], which holds true if the

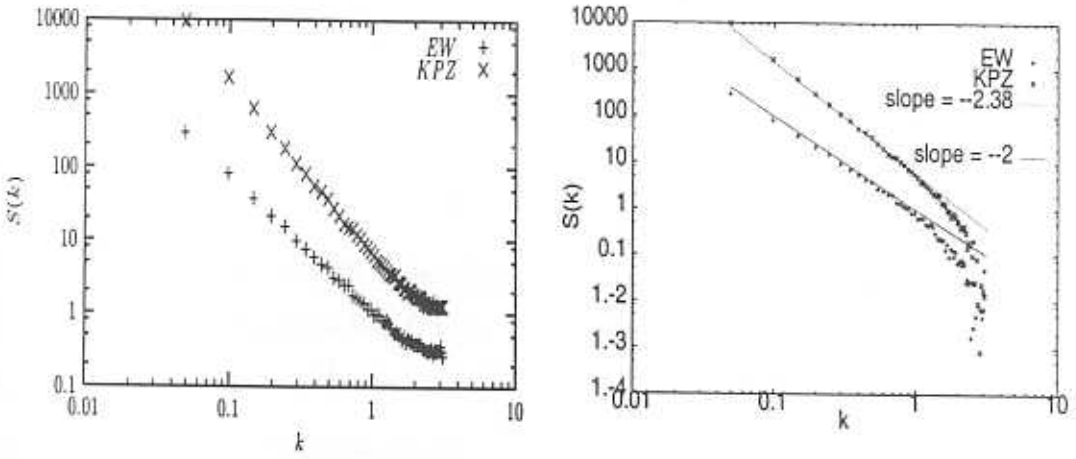


( A ) ( B )

Figure 4.4: (A) The structure factor $S(\mathbf{k}, L)$ for EW (top) and KPZ (bottom) is plotted against k in the (1,0) direction. The KPZ plot have been shifted upwards by a factor of 10 for clarity. (B) The direction averaged structure factor after subtraction of the flat part for KPZ (top) and EW (bottom) surfaces.

average domain size is of the same order as the correlation length. The observed deviation from this law mean that although the correlations extends over the entire system, the domains are not compact, but are ridden with holes. In order to quantify this deviation, it is helpful to study the structure factor at small wavelengths.

### 4.3.4 The Structure Factor

The structure factor is defined as

$$S(\mathbf{k}, L) \equiv \int_0^L d^2\mathbf{r} C(\mathbf{r}, L) e^{-i\mathbf{k}.\mathbf{r}} \tag{4.29}$$

We computed $S(\mathbf{k}, L)$ along (1,0), (0,1), (1,1) and (1,-1) directions. No significant direction dependence was observed, which also reflects the isotropy of $C(\mathbf{r}, L)$. From Eq.4.28 $S(k, L)$ has the following scaling form.

$$S(\mathbf{k}, L) \simeq 1 - c_0 + L^2 g(kL) \tag{4.30}$$

where

$$g(q) = \int_0^1 dy f(y) J_0(qy) y$$

and $J_0(y)$ is the zeroth order Bessel function. For a fully phase separated system with sharp domain walls, $f(x) \simeq 1 - ax$ for $x \ll 1$[3]. In Fourier space, this would mean that $g(q) \sim q^{-3}$ as $q \to \infty$[17] in two dimensions.

Due to the presence of the non-scaling factor $1 - c_0$ in Eq.4.30, the structure factor does not vanish at large $k$, but approaches a constant value $1 - c_0$ (Fig. 4.4A). The value of $c_0$ can be thus measured from the flat part of the structure factor. The observed values are $c_0 \simeq 0.8$ for KPZ surface and $\simeq 0.5$ for EW surface. To find the short wavelength behaviour of $g(q)$, we first subtract the flat part from $S(k, L)$ and then do the finite size scaling. In Fig. 4.4B, we have plotted $S(k, L)$ after subtraction of the flat part. The power-law decay at large $k$ is expressed in terms of the scaling function as

$$g(q) \sim q^{-(2+\alpha)} \tag{4.31}$$

with $\alpha \simeq 0.38$ for KPZ-CD spins. For EW surface, we find that $g(q) \sim q^{-2}$( Fig.4.4B).

For $\alpha > 0$, Eq.4.31 implies a cusp in real space for $C(r, L)$ at small arguments:

$$f(x) \simeq c_0 - c_1 x^{\alpha} + ... \tag{4.32}$$

at $x \ll 1$. We observe that for KPZ surface, $\alpha$ is numerically close to $\chi$, in agreement with the analytical prediction based on IIA (Sec. 4.3.2). For $\alpha \approx 0$ (EW surface), we expect logarithmic corrections to appear near the origin, which also agrees with our exact results for Gaussian surfaces.

### 4.3.5 Domain size distribution of CD spins

To find the size distribution of CD spin domains, one can extend the ideas in Section II A to make analytic predictions.

Let us recall the CD spin distribution inside a typical island. In general, it consists of a *lake* and smaller islands (which might have still smaller islands inside them). A *lake* is just a CD spin domain. In section 4.2.1, we argued that since the island structure is expected to be self-similar, the total area covered by the small islands inside an island (and hence the area of the large *lake*) is a finite fraction of the total area of the island.

We denote by $N_{\pm}(s)$ the number of domains of + and − CD spins respectively, which is bound by the following normalisation conditions:

$$\begin{aligned} \int_a^{p_{\pm}L^2} ds N_{\pm}(s) s &= p_{\pm} L^2 \\ \int_a^{p_{\pm}L^2} ds N_{\pm}(s) s^{D_c/2} &\sim L^{2-\chi} \end{aligned} \tag{4.33}$$

where $p_{\pm}$ is the area ratio of + and − CD spins (the ratio of the area covered by CD spins to the total system area, which, we assume to be well-defined numbers with zero variance in the thermodynamic limit). In addition, since the total number of islands follow a power-law distribution given by Eq. 4.2, we have

$$N_+(s) + N_-(s) \sim \Gamma_L s^{-\tau^*} \tag{4.34}$$

where $\tau^*$ is given by Eq. 4.3. This, of course, implies that at least one of the distributions $N_{\pm}(s)$ has to have the form in the RHS for large $s$. In general, let us assume the power-law forms $N_{\pm}(s) \sim L^{\beta_{\pm}} s^{-\tau_{\pm}}$. Then clearly

$$\begin{aligned} \beta_{\pm} \leq 2 - \chi \;\; ; \;\; max(\beta_+, \beta_-) &= 2 - \chi \\ \tau_{\pm} \geq \tau^* \;\; ; \;\; min(\tau_+, \tau_-) &= \tau^* \end{aligned} \tag{4.35}$$

It remains to predict the values of $\beta_{\pm}$ and $\tau_{\pm}$ from the above normalisation conditions. In general, $N_{\pm}(s)$ may have a well-separated infinite peak of the form $\epsilon_{\pm}\delta(s - \alpha_{\pm}L^2)$. If the infinite peak is not *dominant* (say, for − spins) ie., if $lim_{L\to\infty}\epsilon_-\alpha_- < p_-$, then the non-infinite part of $N_-(s)$ satisfies Eq. 4.33 separately. In this case, one can show from simple scaling arguments that $N_-(s) \sim L^{2-\chi}s^{-\tau^*}$[9].

On the other hand, it is possible that the distribution for one of the spins (say, + spins) has a *dominant* infinite cluster, ie., $lim_{L\to\infty}\epsilon_+\alpha_+ = p_+$. In this case, the

total area covered by the non-infinite part of the distribution is sub-dominant in comparison to $L^2$, in the thermodynamic limit. After combining this condition with Eq. 4.33, we arrive at the following set of equations.

$$\beta_+ = 2 - \chi \;\; ; \;\; \tau_+ > \tau^* \tag{4.36}$$

We observe that these conditions are consistent with Eq. 4.35.

We now proceed to numerical results. In Fig. 4.5A, we show the size distribution of domains of CD spins for KPZ surface. The size distributions follow power-law decay, as expected. The exponents for + and − spins, $\tau_+$ and $\tau_-$ have different values with $\tau_+ > \tau_-$, indicating the presence of a dominant infinite cluster in + spins (This property is more a manifestation of the reference level chosen for the definition of CD spins, than any fundamental characteristic of the surface. A detailed study of the effect of a change in reference level will be given elsewhere). Note that an infinite cluster also occurs for − spins, but it is not distinct from the power-law part and it is not *dominant*. These features are consistent with the theoretical predictions based on island-size distribution. The asymmetry in the distribution of hills and valleys is due to the breaking of $h \rightarrow -h$ symmetry in KPZ growth. For EW surface (Fig. 4.5B), both the exponents are nearly the same within numerical errors, and very close to $\tau^* \approx 2$. This is reasonable because EW surface has symmetric surface fluctuations.

*We recall the CD spin configurations for KPZ and EW surfaces shown in the* last section (Fig. 4.1). For KPZ surface, there is a distinct asymmetry between + and − spins. For − spins (denoted by white in the picture), clusters appear in all sizes, and the largest cluster is a compact object which seems to occupy a finite fraction of the system area. The features point to a broad distribution of cluster sizes which continues upto the system size. For + spins, on the other hand, we observe an *ocean* which percolates through the system and a few small *lakes* scattered here and there. The percolating ocean is the dominant infinite cluster discussed in the previous section. For EW surface, there is visible symmetry between + and − spins.

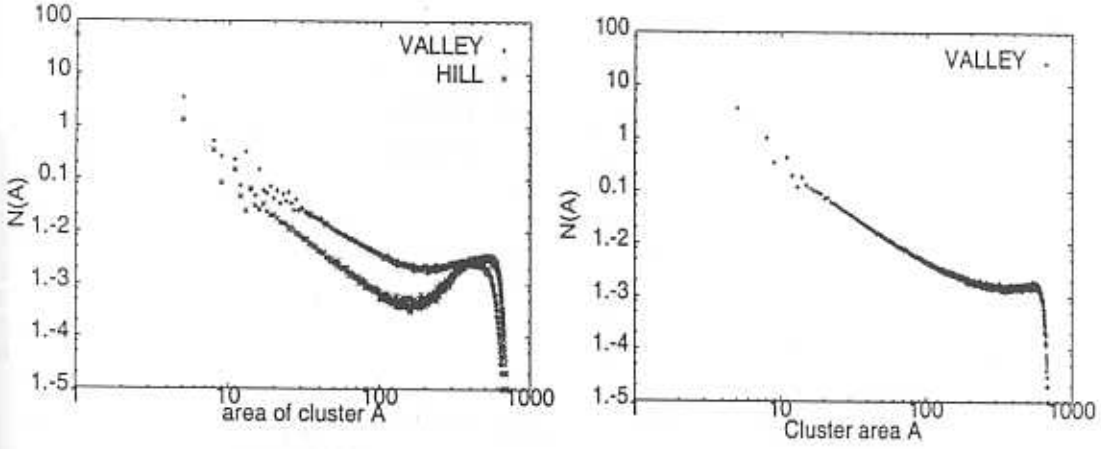


( A ) ( B )

Figure 4.5: The figure shows the normalized size distribution of domains for (A) − (valley) and +(hill) spins for KPZ-CD model and (B) for + spins in EW model. For KPZ, the exponents are different, with values $\simeq 1.83$ and 2.13 respectively. There is a distinct infinite cluster appearing in the distribution of + spins, which is absent for − spins. For EW spins, the distributions are identical for both kinds of spins and the exponent is $\approx 2$.

### 4.3.6 Extremal statistics of cluster sizes in CD models

We studied the statistics of the size of the extremal clusters numerically for models in KPZ and EW surfaces. For CD models, we studied hill ($s = +1$) and valley ($s = -1$) clusters separately. In general, the distributions were found to be different for KPZ surface, but identical for EW surface.

For KPZ and EW CD models, we find that the normalised distribution for both particles and holes fits well into the following scaling form:

$$P(s_m, L) = \langle s_m \rangle^{-1} g\left(\frac{s_m}{\langle s_m \rangle}\right) \tag{4.37}$$

In Fig. 4.6A, we plot the mean extremal cluster size $\langle s_m \rangle(L)$ for particles and holes in KPZ surface, for three system sizes. It is seen that $\langle s_m \rangle \sim L^2$ for KPZ surface, indicating that the extremal cluster appearing outside the power-law distribution actually has size $s^* \sim L^2$. For EW, the mean size $\langle s_m \rangle \sim L^x$ (Fig. 4.6B) with an effective exponent $x < 2$, which presumably is an indication of the presence of logarithmic corrections.

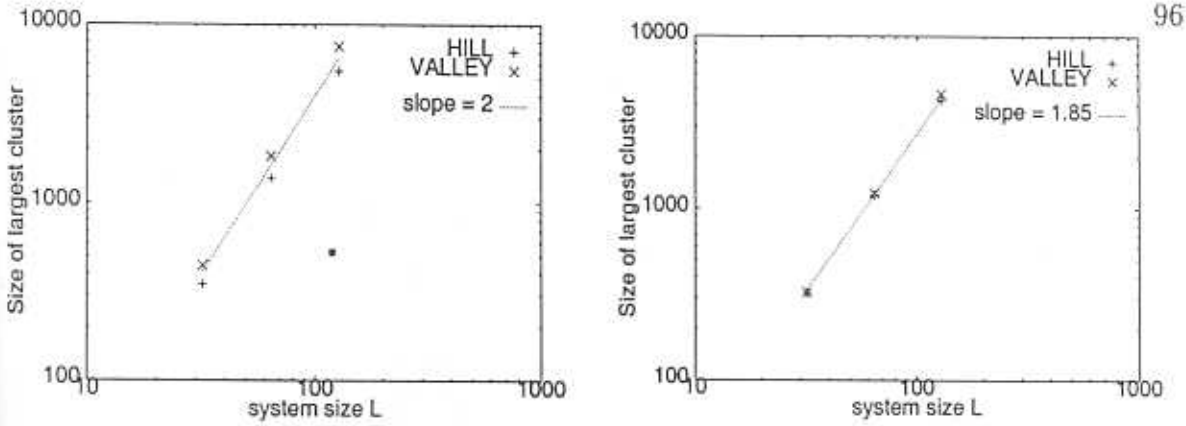


Figure 4.6: The figure shows mean size of the extremal cluster for $s = +1$ and $s = -1$ CD spins for (A) KPZ surface and (B) EW surface.

Unlike the EW-CD model, the corresponding CD model in the case of KPZ surface shows a great deal of difference between $s = +1$ and $s = -1$. This difference was discussed in the previous section, where it was shown that for $s = +1$ (the *valley* regions), in the thermodynamic limit, *all* the spins form part of an infinite cluster that percolates through the system. Consequently, the scaled probability distribution for the size of the maximal cluster narrows down with increase in system size (Fig. 4.7), and may be expected to approach a $\delta$-function form in the thermodynamic limit: $lim_{L\to\infty} g_{-}(x) = \delta(x - p_{-})$. For $s = -1$, on the other hand, there is no *dominant* infinite cluster, and the scaling function is well-defined in the thermodynamic limit (Fig. 4.8A).

For EW surface, the scaling function is similar for $s = +1$ and $s = -1$, and is much broader compared to KPZ surface. This is natural because the width of the EW surface scales only as $\sim \sqrt{logL}$, and hence the cluster sizes are very sensitive to (configuration-wise ) fluctuations in $\langle h \rangle$. The maximal cluster size for EW CD model scales as $\sim L^{y}$ where the effective exponent $y \simeq 1.85$, indicating logarithmic corrections to $L^2$ (Fig. 4.6B).

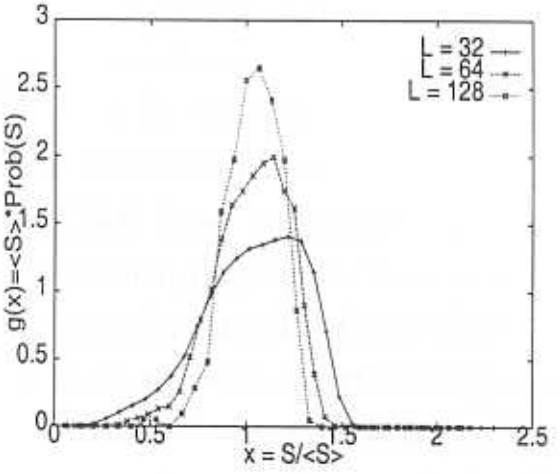


Figure 4.7: The scaled probability distribution for the extremal cluster size of $s = +1$ spins in KPZ-CD model.

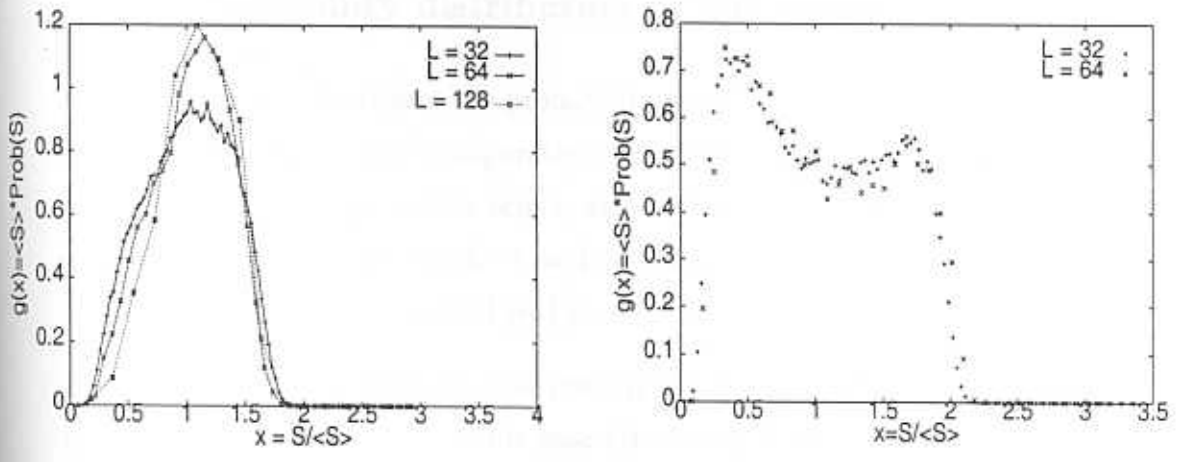


( A ) ( B )

Figure 4.8: The scaled probability distribution for the extremal cluster size of $s = -1$ spins in (A) KPZ-CD model and (B) EW-CD model.

## 4.4 The Order Parameter Distribution

In this section, we explore various definitions of a suitable order parameter to characterise the ordered state in CD models. We recall that in the CD models that we have used so far, the spins are defined with respect to a fixed reference height (in this case, the instantaneous mean height). In this definition, the magnetisation $m = L^{-2}\sum_{\mathbf{r}} s(\mathbf{r})$ is not conserved by default. In conventional ordered states in thermal equilibrium, $\langle m \rangle$ remains finite and the variance $\langle m^2 \rangle$ vanishes in the thermodynamic limit for the ordered state (For the disordered state, $\langle m \rangle = \langle m^2 \rangle = 0$). In general terms, we would expect that a good order parameter should satisfy both these requirements. However, we shall see that while the former requirement is, in general, satisfied in the problems that we studied, the latter is not. A comprehensive discussion of these issues may be found in [4], in the context of (1+1)-dimensional surfaces. In conserved models where the global magnetisation $m$ is strictly conserved, we have to choose a suitable quantity to monitor the degree of phase separation. One such quantity that is commonly used is the magnitude of the longest wavelength Fourier component of the density field.

### 4.4.1 Probability distribution of CD magnetisation

In Fig.4.9A, we have shown the probability distribution of CD spin magnetisation over several steady state configurations in a KPZ surface. We observe that the distribution peaks close to the origin, although one cannot rule out the possibility of having a finite $\langle m \rangle$ in the $L \to \infty$ limit, since the KPZ surface breaks $h \to -h$ symmetry. For $L = 128$, we find $\langle m \rangle \approx -0.06$ with a variance $\approx 0.101$.

For EW surface (Fig4.9B), the convergence of the distribution is slower compared to the KPZ surface. In this case also, we observe a small non-zero value for the mean magnetisation, $\langle m \rangle \approx 0.021$, with variance $\approx 0.18$ for $L = 128$. For EW surface, the symmetric nature of the height fluctuations rule out the possibility of a non-zero value of $\langle m \rangle$ in the $L \to \infty$ limit, so we may safely conclude that the observed non-zero values are only statistical fluctuations. However, the situation is less clear regarding the variance $\langle m^2 \rangle$, and in general, the behaviour of the probability

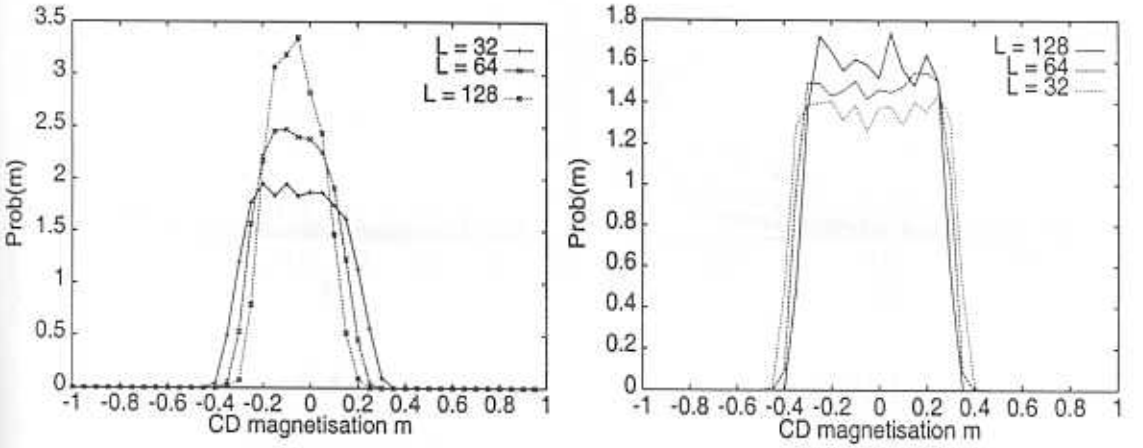


( A ) ( B )

Figure 4.9: The probability distribution of CD spin magnetisation for three lattice sizes for in (A) KPZ surface and (B) EW surface.

distribution $P(m)$ in the thermodynamic limit. From the numerical data, it is not convincingly clear that this distribution narrows down in the thermodynamic limit, and it has been shown that for Gaussian rough surfaces (like EW), the variance remains finite in this limit[9].

### 4.4.2 Order Parameter for the CD models

For a system with conserved magnetisation, an appropriate quantity to characterise the ordered state is the steady state average of the magnitude of the Fourier components of the density, defined as follows:

$$Q(\mathbf{k}) = \langle |L^{-2} \sum_{\mathbf{r}} n(\mathbf{r}) e^{-i\mathbf{k}.\mathbf{r}}| \rangle \tag{4.38}$$

Here, $n(\mathbf{r})$ is the discrete density variable defined as $n(\mathbf{r}) = \frac{1+s(\mathbf{r})}{2}$ and $\mathbf{r}$ runs over all the sites in the lattice. The wave vectors $\mathbf{k}$ are quantised in the lattice in the usual way: $\mathbf{k} = \frac{2\pi}{L}(n_x, n_y)$ and $|\mathbf{k}| < \pi$.

In Fig.4.10A and B, we plot $Q(\mathbf{k})$ along the (1,0) direction for three different lattice sizes. It is seen that for any fixed $k$, $Q(k = n2\pi/L)$ vanishes in the thermo-

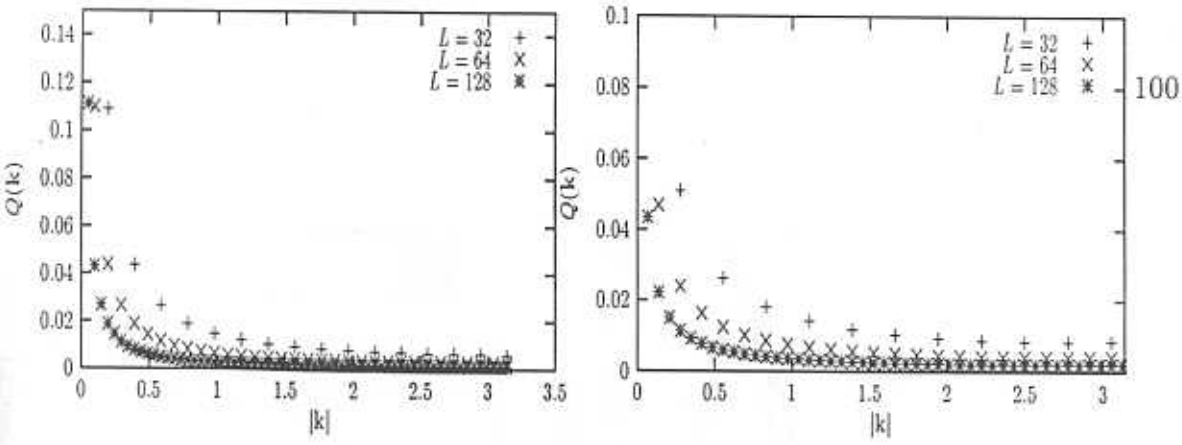


( A ) ( B )

Figure 4.10: $Q(k)$ is plotted against wave vector $k$ for three lattice sizes for (A) KPZ surface and (B) EW surface.

dynamic limit, (except at $k \to 0$), which is an indication that the system is in phase separated state. However, for fixed small values of $n$, $Q(k)$ approaches a non-zero constant value in this limit. Thus a suitable order parameter in this case would be $Q^* = Q(\frac{2\pi}{L}, 0)$ (Another equally good choice would be $Q(\frac{2\pi}{L}, \frac{2\pi}{L})$. In general, any $Q(\frac{n_x 2\pi}{L}, \frac{n_y 2\pi}{L})$ is a valid choice, as long as $n_x, n_y \ll L$).

In Fig.4.11A, we present the probability distribution for $Q^*$ for a KPZ surface. The distribution seems to remain broad in the limit $L \to \infty$, with $\langle Q^* \rangle \approx 0.11$ and variance $\approx 0.02$. The non-vanishing of the RMS fluctuation in the order parameter in the thermodynamic limit is in contrast with most conventional phase separating systems, and this phenomenon was named Fluctuation-Dominated Phase Ordering(FDPO) by DBM[4].

Although we do not yet have a sound theoretical understanding of FDPO, the following arguments appear plausible. Consider the SP or CD model in a rough surface. We found that in steady state, spin domains appear in all sizes, following a power-law distribution, with one (maybe a few) very large clusters of size $\sim L^2$. These clusters predominantly give a non-zero contribution to the Fourier sum in $Q^*$, with the other smaller clusters contributing nearly zero. However, the actual size of the largest cluster(s) also fluctuates (with RMS fluctuation $\sim L^2$), and these fluctuations get reflected in the broadness of the probability distribution.

It is interesting to see whether FDPO exists also in EW surface, which is only

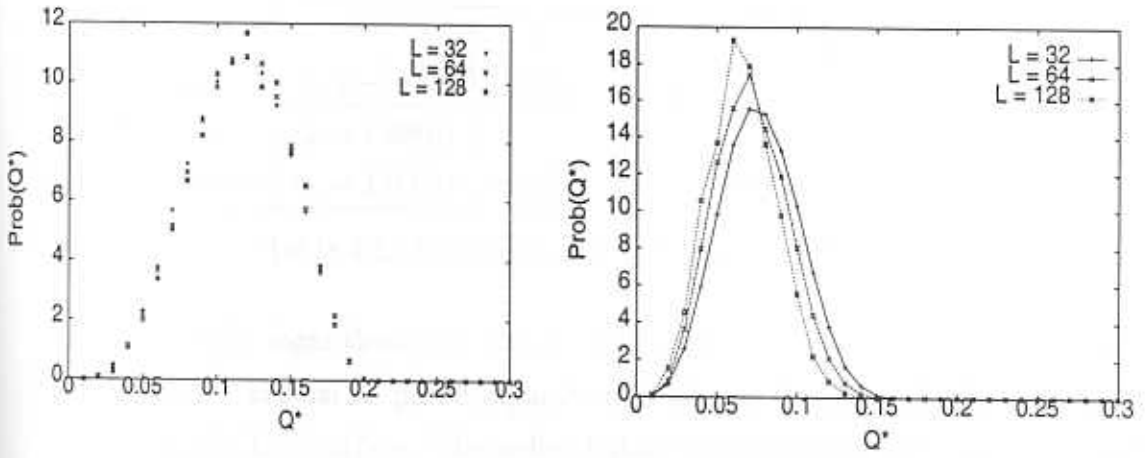


Figure 4.11: The probability distribution of the order parameter $Q^*$ for three lattice sizes for the CD problem on a (A) KPZ surface and (B) EW surface.

| model | $\tau$ | $\alpha$ | $\langle s_m \rangle$ |
|---|---|---|---|
| KPZ-CD (Theory) | $\geq 2 - \chi/2$ | $\chi$(IIA) $\approx 0.37$ | $\sim L^2$ |
| KPZ-CD (Simulation) | $\tau_+ = 1.83(4)$ $\tau_- = 2.13(8)$ | 0.38(1) | $\sim L^2$ |

Table 4.1: A summary of properties of KPZ-CD model.

logarithmically rough. In this case, the logarithmic corrections to the size of the extremal cluster seems to produce a slow shift of $\langle Q^* \rangle$ (and its variance) towards zero in the large $L$ limit (Fig.4.11B).

## 4.5 Conclusion

In this chapter, we showed that a two-dimensional fluctuating rough interface growing from a flat initial condition may be mapped to a coarsening system, characterised by the same dynamical exponent. For concreteness, we have considered two types of surface fluctuations, KPZ surface which is rough in steady state and EW surface

| model | $\tau$ | $\alpha$ | $\langle s_m \rangle$ |
|---|---|---|---|
| EW-CD (Theory) | $\geq 2 - \chi/2$ | $\chi$ 0(log) | $\sim L^2/(logL)^x$ |
| EW-CD (Simulation) | $\tau_+ = 1.98(6)$ $\tau_- = 1.90(4)$ | -0.03(2) | $\sim L^{1.85}$ |

Table 4.2: A summary of properties of EW-CD model.

which is only logarithmically rough. The roughness properties of the surface are found to be crucial in phase separation, which is complete for KPZ surface and marginal for EW surface. The ordered state is characterised by some very distinct features. The bulk magnetisation is less than its maximum value and the two-point correlation has a cusp at small arguments. The size distribution of domains follows a power-law decay. All these features indicate that the ordered phase is not very homogeneous, but has a non-compact structure.

In Tables 4.1 and 4.2, we have listed the properties of EW and KPZ CD spin models in the steady state. From the typical size of the extremal cluster, we see that there is complete phase separation in KPZ surface, wheras phase separation is marginal for EW surface. The size distribution of spin domains follows power-law decay in both models, with different exponents for + and − spins in KPZ surface. We also observed that in case of KPZ surface, most of the − spins actually form part of an infinite (ie., a cluster with $\sim L^2$ spins) percolating cluster, and the rest of the spins are present in much smaller clusters which follow a power-law distribution. In the case of + spins, however, the infinite cluster appears as part of the power-law distribution, and it is not distinct. This is also true for EW surface, irrespective of the sign of spin. In this case, the size of the largest cluster appears to scale with $L$ with an effective exponent $y < 2$. We argued that this is indicative of logarithmic corrections.

The pair correlation for CD spins in both models showed finite size scaling. However, the scaling function did not decay linearly near the origin, as in conventional coarsening models like the kinetic Ising model. Instead, the scaling function had a cusp near the origin, $f(x) \approx c_0 - c_1 x^a + ....$ We showed that for surfaces whose

steady state probability distribution for height fluctuations is Gaussian, the cusp exponent $\alpha$ is exactly equal to the roughness exponent $\chi$. For more general surfaces, we arrived at the same conclusion under the Independent Interval Approximation, which is expected to hold good in the vicinity of $\chi = \frac{1}{2}$. These predictions were in good agreement with observations for both EW and KPZ surfaces.

To characterise the ordered state of the system, we used an appropriate order parameter. For KPZ surface, the order parameter has a non-zero mean value in the ordered state, but its variance appears to remain finite in the thermodynamic limit. We argued that this feature could be attributed to large fluctuations in the size of extremal spin clusters. For EW surface, the mean value was observed to slowly shift towards zero in the $L \to \infty$ limit, perhaps because of logarithmic corrections. A more thorough study of these features is currently in progress.

## 4.6 Appendix IV A

We essentially follow the arguments of Matsushita *et. al*[8] in this section. Consider a (2+1) Gaussian surface with probability distribution

$$\mathcal{P}[h] \sim exp\left(-\sum_{\mathbf{q}} q^{2(1+\chi)} h_{\mathbf{q}} h_{-\mathbf{q}}\right) \tag{4.39}$$

where $\chi$ is the roughness exponent for the surface. We measure the height of the surface relative to a reference level $h_0$. Along an arbitrary linear cut on the surface, let $Q_X(z)$ be the probability that $h(X) = z$, where the origin is any one of the points where $h = 0$. Then $Q_X(z) = \frac{Z_1}{Z_0}$ where

$$Z_1 = \int \mathcal{D}h\delta[h(X) - h(0) - z]\mathcal{P}[h]$$

and

$$Z_0 = \int \mathcal{D}h\mathcal{P}[h]$$

The integrals are straightforward to do, and the result is

$$Q_X(z) \sim \frac{1}{\xi} exp[-\frac{z^2}{\xi^2}]$$

where

$$\xi^2 \sim \sum_{\mathbf{q}} \frac{1 - cos(\mathbf{q}.\mathbf{X})}{q^{2(1+\chi)}}$$

For $\chi > 0$, $\xi^2 \sim X^{2\chi}$ and for $\chi = 0$, $\xi^2 \sim \ln(X/a)$, where $a$ is a microscopic length scale.

For general non-Gaussian surfaces, it is difficult to derive an exact form for $Q_X(z)$. However, it is reasonable to think that in general, $Q_X(z)$ has a scaling form

$$Q_X(z) \sim \frac{1}{\xi} f\left(\frac{z}{\xi}\right)$$

By analogy with the case of Gaussian surfaces, we argue that $f(x)$ remains finite in the limit $x \to 0$. The probability of return to origin at $X$ is $P_0(X) = Q_X(0) \sim \frac{1}{\xi}$. Thus $P_0(X) \sim X^{-\chi}$ for $\chi > 0$ and $P_0(X) \sim [\log(X/a)]^{-\frac{1}{2}}$ for $\chi = 0$.

The average number of returns to origin up-to $X$ is

$$N_0(X) = \int_a^X dY P_0(Y)$$

and $N_0(X) \sim X^{1-\chi}$ for $0 < \chi < 1$. For $\chi = 0$, $N_0(X) \sim X[\log(X/a)]^{-\frac{1}{2}}$ while for $\chi = 1$, $N_0(X) \sim \log(X/a)$. For $\chi > 1$, $N_0(X)$ is a constant, independent of $X$.

It follows that along any arbitrary linear cut on the surface, the surface will touch a chosen reference level $\simeq L^{1-\chi}$ times on an average, if $\chi < 1$ and a constant number of times if $\chi > 1$, with logarithmic corrections at $\chi = 0$ and $\chi = 1$. Since this is true for each linear cut, and since one may have $\sim L$ independent linear cuts on the surface, the total length of the contour lines, which forms the boundary between regions where $h < h_0$ and $h > h_0$, scales as $\mathcal{M}(L) \sim L^{2-\chi}$ for $0 < \chi < 1$ and $\mathcal{M}(L) \sim L$ for $\chi > 1$. For $\chi = 0$, $\mathcal{M}(L) \sim L^2[\log L]^{-\frac{1}{2}}$ and for $\chi = 1$, $\mathcal{M}(L) \sim L \log L$.

## 4.7 Appendix IV B

Consider a continuous variable $X$ which can take values in the range $[a : b]$, with probability distribution $p(X)$. We would like to compute the probability $L_N(Y)dY$ that the maximum value of $X$ in an ensemble of $N$ randomly selected samples from $[a : b]$ lies between $Y$ and $Y + dY$.

The probability $p_>(Y)$ that $X_{max} \leq Y$ is the probability of randomly picking $N$ variables, all less than $Y$. Thus

$$p_>(Y) = \left[\int_a^Y p(X)dX\right]^N \tag{4.40}$$

It follows that the required probability

$$L_N(Y) = \frac{dp_>(Y)}{dY} \tag{4.41}$$

As a special case, let us consider the power-law distribution $p(X) \sim X^{-(1+\alpha)}$ where $\alpha > 0$. It is easy to show that

$$L_N(Y) = \frac{\alpha}{N^{1/\alpha}} x^{-(1+\alpha)} exp(-x^{-\alpha}) \tag{4.42}$$

where $x = \frac{Y}{N^{1/\alpha}}$. The distribution peaks around $Y^* \sim N^{1/\alpha}$, which gives the typical value of $X_{max}$.

## 4.8 Appendix IV C

We start from the expression for the two-point height correlator in the steady state of a $d + 1$ dimensional rough surface, with roughness exponent $\chi$.

$$\mathcal{G}(\mathrm{r}, L) = \int_{k=\frac{2\pi}{L}}^{\frac{\pi}{a}} \frac{d^d\mathrm{k}}{(2\pi)^d} cos(\mathrm{k.r})\Xi(\mathrm{k}) \tag{4.43}$$

Here $a$ is some microscopic length scale, below which the continuum descriptions Eq.4.21 and 4.21 do not apply.

We substitute $\Xi(\mathbf{k}) \sim k^{-(d+2\chi)}$ and $d^d\mathbf{k} \rightarrow k^{d-1}dkd\Omega$, and then carry out the angular integration using the formula[21]

$$\int cos(\mathbf{k}.\mathbf{r})d\Omega = \Gamma(\frac{d}{2})J_{\frac{d}{2}-1}(kr)(kr)^{1-\frac{d}{2}} \tag{4.44}$$

where $J_n(\eta)$ is the $n$-the order Bessel function. The result is

$$\mathcal{G}(r,L) \sim L^{2\chi}\xi^{2\chi}\int_{\xi}^{\frac{\pi r}{a}} \eta^{-(2\chi+\frac{d}{2})}J_{\frac{d}{2}-1}(\eta)d\eta \tag{4.45}$$

where the scaling variable $\xi = 2\pi r/L$. The Bessel function $J_\nu(\eta) \sim \eta^\nu$ near $\eta = 0$[20]. For finite $\xi$ and $\frac{L}{a} \rightarrow \infty$, the integral is dominated by the lower limit if $\chi > 0$. Thus the lattice constant $a$ can be effectively put to zero for $\chi > 0$ in any dimension. For $\chi = 0$ on the other hand, the integral diverges as $\log\frac{L}{a}$ for $a \ll L$, and there is no effective continuum description.

In the remaining part of this section, we evaluate $\mathcal{G}(r,L)$ in $d = 1$ for $0 < \chi < 1$ (The $d = 2$ case for $0 < \chi < 1$ has been treated in the text). We also compute $\mathcal{G}(r,L)$ explicitly for the marginal cases $\chi = 0$ and $\chi = 1$ in general $d$ dimensions.

*d=1*:

We use the relation $J_{-\frac{1}{2}}(\eta) = \sqrt{\frac{2}{\pi\eta}}cos\eta$[20]. After substituting in the above expression and putting the upper limit at infinity, we find for $\xi \ll 1$[22]

$$\mathcal{G}(r,L) \sim \frac{L^{2\chi}}{2\chi}\left[1 - a_\chi\xi^{2\chi} + F(\xi)\right] \tag{4.46}$$

where $a_\chi = \Gamma(1-2\chi)\sin[\frac{\pi}{2}(1-2\chi)]$ if $\chi < \frac{1}{2}$, $\frac{\pi}{2}$ if $\chi = \frac{1}{2}$ and $\frac{1}{2\chi-1}\Gamma(2-2\chi)\cos[\pi(1-\chi)]$ if $\chi > \frac{1}{2}$. $F(\xi) \sim O(\xi)$ for $\chi < \frac{1}{2}$ and $O(\xi^2)$ for $\chi \geq \frac{1}{2}$.

Using similar arguments as in Sec. IV A, we find that in $d = 1$ and $\xi \ll 1$,

$$C(r,L) \sim 1 - a'_\chi\xi^\chi + higher\ \ order\ \ terms \tag{4.47}$$

for $0 < \chi < 1$, where $a'_\chi = \frac{2\sqrt{2}}{\pi}a_\chi$. The cusp exponent for CD spin correlation $\alpha = \chi$ for any Gaussian surface in $d = 1$ also, identical to what we found in two

dimensions.

$\chi = 0$:

The integral can be done for general $d$ dimensions in this case. For finite $\xi$ and $\frac{a}{L} \to 0$, the result is[18]

$$\mathcal{G}(r, L) \sim b_0 ln(\frac{\xi}{2}) - 1 + O(\xi^2) \tag{4.48}$$

where $b_0 = \frac{2}{\psi(1)+\psi(\frac{d}{2})}$ and $\psi(x) = \frac{d}{dx}\ln\Gamma(x)$. To compute $C(r, L)$ from Eq.4.26, we define $\mathcal{G}(0, L) \equiv \lim_{\frac{a}{L}\to 0}\mathcal{G}(a, L)$. In this limit, $\mathcal{G}(0, L) \simeq -b_0 \ln(L/a)$. After substituting in Eq.4.26, we arrive at Eq.4.29 for $\xi \ll 1$.

$\chi = 1$:

A similar calculation as above gives

$$\mathcal{G}(r, L) \sim L^2[1 - c_1\xi^2 ln\xi + O(\xi^4)] \tag{4.49}$$

and

$$C(r, L) \simeq 1 - \frac{2\sqrt{2}}{\pi} c_1 \xi \sqrt{ln\xi} + .... \tag{4.50}$$

for $\ln\frac{L}{r} \gg 1$, where

$$c_1 = \frac{1}{2}\frac{\Gamma(\frac{d}{2})}{\Gamma(\frac{d+1}{2})}.$$

In this case, the Porod law behaviour is recovered, with logarithmic corrections.

## 4.9 Appendix IV D

Consider two coupled stochastic variables $x_1$ and $x_2$, with Gaussian probability distribution of the form

$$P(x_1, x_2) = \frac{1}{2\pi D} exp\left(-\frac{1}{2D}(\alpha x_1^2 + \alpha x_2^2 - 2\beta x_1 x_2)\right) \tag{4.51}$$

where $\alpha = \langle x_1^2 \rangle = \langle x_2^2 \rangle$, $\beta = \langle x_1 x_2 \rangle$ and $D = \alpha^2 - \beta^2 > 0$.

We are interested in finding the correlator $C = \langle X_1 X_2 \rangle$ for the 'clipped' variables $X_1 = sgn(x_1)$ and $X_2 = sgn(x_2)$. Clearly,

$$C = 4\langle \Theta(x_1)\Theta(x_2) \rangle - 1 \tag{4.52}$$

where $\Theta(x)$ is the Heaviside step function.

Let us now introduce the linear transformations

$$\begin{aligned} x_1 &= \sqrt{\frac{D}{2}} \left( \frac{y_1}{\sqrt{\alpha+\beta}} + \frac{y_2}{\sqrt{\alpha-\beta}} \right) \\ x_2 &= \sqrt{\frac{D}{2}} \left( -\frac{y_1}{\sqrt{\alpha+\beta}} + \frac{y_2}{\sqrt{\alpha-\beta}} \right) \end{aligned} \tag{4.53}$$

After substitution, we find

$$\begin{aligned} \langle \Theta(x_1)\Theta(x_2) \rangle = \frac{1}{2\pi} \int dy_1 dy_2 \Theta \left( \frac{y_1}{\sqrt{\alpha+\beta}} + \frac{y_2}{\sqrt{\alpha-\beta}} \right) \times \\ \Theta \left( -\frac{y_1}{\sqrt{\alpha+\beta}} + \frac{y_2}{\sqrt{\alpha-\beta}} \right) exp \left( -\frac{1}{2}(y_1^2 + y_2^2) \right) \end{aligned} \tag{4.54}$$

Since the probability distribution is isotropic in $y$-space, we find after some simplifications that $\langle \Theta(x_1)\Theta(x_2) \rangle = \frac{\theta}{2\pi}$, where $\theta$ is the angle enclosed by the unit vectors

$$\begin{aligned} \mathbf{u}_1 &= \frac{1}{\sqrt{2\alpha}} \left( -\sqrt{\alpha+\beta}, \sqrt{\alpha-\beta} \right) \\ \mathbf{u}_2 &= \frac{1}{\sqrt{2\alpha}} \left( \sqrt{\alpha+\beta}, \sqrt{\alpha-\beta} \right) \end{aligned} \tag{4.55}$$

Clearly, $cos(\theta) = \frac{\mathbf{u}_1 . \mathbf{u}_2}{|\mathbf{u}_1||\mathbf{u}_2|} = -\frac{\beta}{\alpha}$ so that $\theta = cos^{-1}(-\beta/\alpha) = \frac{\pi}{2} + sin^{-1}(\beta/\alpha)$.

After substitution, we arrive at the final result

$$C = \frac{2}{\pi} sin^{-1} \left( \frac{\beta}{\alpha} \right) \tag{4.56}$$

# Bibliography


[1] A-L. Barabasi and H. E. Stanley, *Fractal concepts in surface growth* (Cambridge University Press).

[2] J. M. Kim, A. J. Bray and M. A. Moore, Phys. Rev. A **45**, 8546 (2000).

[3] A. J. Bray, Adv. Phys. **43**, 357 (1994).

[4] D. Das and M. Barma, Phys. Rev. Lett. **85**, 1602 (2000); also D. Das, M. Barma and S. N. Majumdar, cond-mat/0102521.

[5] J. Kondev and G. Huber, cond-mat/0011199.

[6] P. Meakin, *Fractals, Scaling and Growth far from Equilibrium* Cambridge University Press, and references therein.

[7] B. B. Mandelbrot, *The Fractal Geometry of Nature* (W. H. Freeman and Company, San Fransisco) p.260.

[8] M. Matsushita, S. Ouchi and K. Honda, J. Phys. Soc. Japan **60**, 2109 (1991).

[9] Z. Olami and R. Zeitak, Phys. Rev. Lett. **76**, 247 (1996).

[10] J. Kondev, C. L. Henley and D. G. Salinas, Phys. Rev. E **61**, 104(2000).

[11] J. Cardy in *Fluctuating Geometries in Statistical Mechanics and Field Theory*, Les Houches Lectures Session LXII, Elsevier Science (1994).

[12] J. Feder, *Fractals* (Plenum Press, New York, 1988).

[13] S. F. Edwards and D. R. Wilkinson, Proc. R. Soc. London A **381**, 17 (1982).

[14] M. Kardar, G. Parisi and Y-C. Zhang, Phys. Rev. Lett. **56**, 889 (1986).

[15] J. M. Kim, M. A. Moore and A. J. Bray, Phys. Rev. A **44**, 2345(1991).

[16] R. B. Griffiths, Phys. Rev. **152**, 240 (1966).

[17] G. Porod, Z. Kolloid **124**, 83 (1952), Ibid. **125** 51.

[18] Y. L. Luke, *Integrals of Bessel Functions* (McGraw-Hill, 1962).

[19] Y. Oono and S. Puri, Mod. Phys. Lett. B **2**, 861 (1988).

[20] M. Abramovitz and I. A. Stegun (eds) *Handbook of Mathematical Functions*(Dover, New York).

[21] T. Nattermann and L. -H. Tang, Phys. Rev. A **45**, 7156 (1992).

[22] I. S. Gradshteyn and I. M. Ryzhik, *Table of Integrals, Series and Products* (Academic Press, 1965).

# Chapter 5

# Summary

In this thesis, we have studied the interplay between Persistence and coarsening in two different classes of Non-equilibrium systems. In the first part of the thesis covered by Chapters 2 and 3, we studied the scale invariant spatial structure of the persistent region in several coarsening systems in different spatial dimensions. In the second part, we investigated the analogue of phase separation in a fluctuating rough surface, with focus on (2+1) dimensional surfaces.

The first model we studied is the well-known $A+A \to \emptyset$ reaction-diffusion model in $d = 1$, whose dynamics is identical to that of the 1D Ising model with Glauber dynamics. In this model, a set of particles with random initial distribution diffuse all over the lattice, and annihilate each other when two of them meet. Persistent sites at any time $t$ are the sites which remain unvisited by any diffusing particle throughout the time interval $[0 : t]$.

To monitor the growth of spatio-temporal correlations in the distribution of persistent sites, we study the distribution $n(k, t)$ of separations $k$ between consecutive persistent sites. To study this process analytically, we invoked an approximation, where the lengths of adjacent intervals are treated as uncorrelated random variables (The Independent Interval Approximation, or IIA). We constructed a rate equation for the time evolution of $n(k, t)$ based on this approximation, which was solved within a dynamic scaling ansatz. The characteristic length scale was found to diverge with time as $s(t) \sim t^{1/2}$. Over length scales small compared to $s(t)$, the set of persistent

sites has a stationary fractal structure with fractal dimension $d_f = d - 2\theta$. Over larger length scales, the distribution is homogeneous. These results are supported by extensive numerical simulations.

We extended this analysis to the coarsening of $q$-state Potts model in one dimension and found that there are two distinct regimes appearing here. The IIA calculation shows that if $\theta(q) < \frac{1}{2}$, the persistent structure is a fractal over small length scales and homogeneous over large length scales. If $\theta(q) \geq \frac{1}{2}$, the distribution is homogeneous over all length scales. These predictions agreed with recent studies done by other authors.

The study of spatio-temporal correlations associated with persistence was extended to higher dimensions in different models. We did both direct computation of correlations as well as an indirect finite size scaling (FSS) analysis. For a coarsening process in $d$ dimensions characterised by dynamical exponent $z$, we showed that, if $z\theta < d$, the set of persistent sites forms a fractal structure over length scales $\ll t^{1/z}$ and will be randomly distributed beyond this length scale. In this case, persistent fraction for finite lattices has the scaling form $P(t, L) = L^{-z\theta} f\left(\frac{t}{L^z}\right)$ with $f(x) \sim x^{-\theta}$ for $x \ll 1$ and $f(x) \simeq$ constant for $x \gg 1$. This scaling form was verified numerically for a number of coarsening models, like Ising model, TDGL model and the simple diffusion problem.

Recent analytical and numerical studies on Persistence in fluctuating interfaces have discovered that for a large class of interfaces, Persistence follows a power-law decay. For a fluctuating interface characterised by a height field $h(\mathrm{x}, t)$, $P(t)$ is the probability that the height remains above or below its initial height $h(\mathrm{x}, t = 0)$ throughout the time interval $[0, t]$ is defined as the Persistence probability. For an almost flat initial configuration ($h(\mathrm{x}, t = 0) \approx 0$), it has been shown that $P(t) \sim t^{-\theta}$ with a non-trivial exponent $\theta$. The algebraic decay of persistence is very similar to that in coarsening systems, and it is natural to investigate if such an interface 'coarsens' in some way, and if it does, how is it different from usual coarsening systems. For this purpose we defined a discrete spin variable $s(\mathrm{x}, t)$ =sgn$(h(\mathrm{x}, t))$ so that the persistence of interface fluctuations is now identified as the persistence of these spin variables.

We consider surfaces that are rough in the steady state ie., $\langle (h(\mathbf{x},t) - h(\mathbf{x}+\mathbf{r},t))^2 \rangle \sim r^{2\chi}$ for $t \gg L^z$. For Gaussian surfaces in steady state, (eg. the linear Edwards-Wilkinson surface), we showed analytically that the two-point spin correlator in steady state $C(r,L) = \langle s(\mathbf{x})s(\mathbf{x}+\mathbf{r}) \rangle = f(\frac{r}{L})$. This scaling is characteristic of a phase separated system. In conventional phase separated systems, $f(x)$ decays linearly near origin ie., $1 - f(x) \sim x$. In the present case, however, $1 - f(x) \sim x^\chi$ near $x = 0$. The cuspy nature of the correlator near $r = 0$ shows that the ordered phase is not as homogeneous as in more conventional phase segregated systems (eg. binary fluid). While the largest domain is always of size $\sim L^2$, which signifies phase segregation, the smaller clusters have a broad distribution, which is reminiscent of critical systems.

For general non-Gaussian surfaces (eg. the Kardar-Parisi-Zhang surface in $d = 2$), we showed that these conclusions are still valid within the Independent Interval Approximation. We verified these predictions by numerical simulations of the EW and KPZ surfaces, and the results were in very good agreement with the analytical predictions. We also extended the simulations to explore the pre-steady state temporal regime ($t \ll L^z$) We found that the equal time correlator has the same scaling form with $L$ replaced by $\mathcal{L}(t)$, which is typical of a system undergoing domain coarsening. Scaling arguments suggest that $\mathcal{L}(t) \sim t^{1/z}$ where $z$ is the dynamical exponent for the surface fluctuations. For (2+1) dimensional KPZ and EW surfaces, we found that this argument is in excellent agreement with simulations. This result also agrees with a previous work on (1+1) dimensional surfaces.

In conclusion, the study of spatial aspects of the Persistence problem has resulted in the discovery of non-trivial spatial correlations associated with Persistence in coarsening systems. We believe that more studies in this direction will go a long way towards a better understanding of such First passage problems and non-trivial exponents in Non-equilibrium stochastic processes. In particular, it would be very interesting if the proposed fractal structure and dynamical scaling could be verified experimentally, at least for simple processes like diffusion, where the Persistence exponent has already been measured. The intimate connection between Persistence

and coarsening phenomena has also helped us to unearth new features in fluctuating interfaces.